A FEASIBILITY STUDY OF THE OSCILLATORY METHOD FOR THERMAL DIFFUSIVITY MEASUREMENT IN GASES

by

ARNOLD MILTON GOLDSTEIN

A dissertation submitted to the Graduate Faculty in Engineering in partial fulfillment of the requirements for the degree of Doctor of Philosophy, The City University of New York.

1968

This manuscript has been read and accepted for the University Committee in Engineering in satisfaction of the dissertation requirement for the degree of Doctor of Philosophy.

April 25, 1968
date

Robert A. Graff
Chairman of Examining Committee

April 25, 1968
date

Executive Officer

Prof. Clarence B. Anderson
Prof. Robert Pfeffer
Prof. Reuel Shinnar
Prof. Robert A. Graff, Chairman

Supervisory Committee

The City University of New York

To Betty and Laurie

ACKNOWLEDGEMENTS

The aid of the following individuals is gratefully acknowledged:

Professor Robert A. Graff for advice and guidance which assured the successful completion of this dissertation;

Professor Alois X. Schmidt for his continuing interest and for affording me the opportunity to teach on the undergraduate level;

The members of the Supervisory Committee for their valuable suggestions;

The technicians of the Department of Chemical Engineering, in particular, Messrs. J. Bodnaruk, F. Phillips, G. Kousourou, and R. Sperle, for assistance in construction of the experimental apparatus.

The assistance of the following institutions in furnishing financial aid during the course of my graduate study is acknowledged:

The City University of New York for providing a University Research Assistantship covering the period January, 1963 - June, 1964;

The National Science Foundation for providing a Cooperative Fellowship covering the period September, 1964 - September, 1966;

The National Aeronautics and Space Administration for providing a Traineeship covering the period September, 1966 - April, 1968.

This research was supported by a grant from the National Science Foundation and at various times by the City University of New York. Their financial assistance is much appreciated.

TABLE OF CONTENTS

LIST OF FIGURES

LIST OF TABLES

ABSTRACT

The feasibility of the oscillatory method for measuring fluid thermal diffusivities is evaluated experimentally. In this method, a sinusoidal temperature variation is applied to a fluid at one solid boundary. A traveling temperature wave is produced in the fluid and the thermal diffusivity is obtained from the phase difference at two points in the medium.

A diffusivity cell with associated equipment was constructed, and measurements made with air.

The important result of this research is the discovery of laminar convection induced by an oscillatory thermal gradient. There is no information available in the literature about the stability of such thermal systems. This study gives some valuable information on the stability of a semi-infinite medium at a flat surface to an oscillatory surface temperature. Instability occurs in air at amplitudes as low as 0.05 C^{o} and with frequencies as high as 0.2 cps. The apparent thermal diffusivity under convection is 2.3 times the value for air, in agreement with data in the literature for the transition from conduction to laminar convection.

SUMMARY

The objective of this research is to examine the feasibility of the oscillatory method for measuring thermal diffusivity of fluids. In this method, an alternating temperature applied to one surface of a fluid produces a traveling temperature wave. The temperature is measured at two points in the fluid, and the thermal diffusivity is calculated from phase lag, distance between points of measurement, and signal frequency.

In most common methods of thermal conductivity measurement, a constant temperature difference is imposed across a sample of fluid and the conductivity calculated from the resulting heat flux. In these methods, care must be taken to eliminate the possibility of convection and to compensate for end effects. In application to reacting mixtures (where little work has been done), the permanent temperature difference across the medium results in a difference in rate of reaction; a concentration difference develops, giving rise to an additional heat flux.

In principle, the oscillatory method has certain advantages: it is an absolute method and thus preliminary calibration with a fluid of known diffusivity is avoided; calibrated thermocouples are not required, for neither absolute temperature levels nor temperature differences need be measured; an experimental heat balance need not be maintained about the fluid, for the heat flux into the fluid is not measured; the absence of a permanent temperature difference across the medium makes the method attractive for the measurement of the "intrinsic" thermal diffusivity in those

fluid mixtures which are undergoing "slow" reactions relative to the frequency of the temperature oscillations.

The feasibility of the oscillatory method seemed to have been established by Harrison, Boteler and Spurlock (14). They used a cylindrical cell, in vertical position, with oscillating temperature on the lateral surface. Results on nitrogen were reported with a mean deviation of 6.2% from literature values. The frequency range was 0.226 to 0.344 cps. However, no observations of natural convection were reported.

To explore the oscillatory method, an apparatus consisting of a cell, power supply, and recording equipment has been designed and assembled. The temperature signal is supplied by one side of a thermoelectric Peltier battery which forms the top face of a vertical cylindrical cell. Two thermocouples are strung parallel to, and a few millimeters below, the battery face. The Peltier battery is driven by a dual power supply with two sets of controls so that the net heating effects can be adjusted to zero. The recording channels, one for each thermocouple, contain amplifier, filter and strip-chart recorder. Frequency and phase lag are obtained from recordings by averaging over about thirty cycles. The distance between thermocouples, in the direction perpendicular to the battery surface, is measured with a stereomicroscope.

Three groups of determinations on air were made with successive improvements in equipment, mainly in electronic components. In the third group, a calibrated thermocouple was used on the battery surface to obtain the amplitude of the temperature signal. At frequencies above 0.2 cps,

temperature signals were too weak to be adequately recorded, although the Peltier battery received power at the maximum permissible level. The lowest usable temperature amplitude at the battery surface was about 0.05 C^{o}.

The measured thermal diffusivities were always found to be greater than those reported in the literature sometimes by more than a factor of two. The following sources of error were examined and rejected:

1. Impurities. By calculation, the thermal diffusivity of air saturated with water vapor and containing one mole percent CO_2 differs by less than 0.5% from the value for dry air with the normal amount of CO_2.

2. Thermocouple Time Constants. The thermocouple junction is in the form of a bead 0.003 inches in diameter. Using a Nusselt number of two (stagnant fluid), one finds a thermocouple time constant of the order of one-tenth second. This is two orders of magnitude less than the period of the temperature signals.

3. Thermocouple Interference. Because of the disturbance to the temperature field in the gas produced by the presence of a thermocouple, it is possible for one thermocouple to influence the reading of the other. The extent of this interference was estimated by computing the response of an infinite medium initially at uniform temperature to the insertion of a perfectly conducting infinite cylinder initially at another temperature. The response of the medium was never more than two percent at distances corresponding to half the thermocouple separation.

4. Transient Response. If a sinusoidal temperature

disturbance is applied, at time zero, to a semi-infinite medium, the solution contains a transient term and a stationary term. In evaluating thermal diffusivity from a pair of thermocouple traces, stationarity is assumed. By computation, it is found that the transient terms falls to a negligible value after only a few cycles.

5. Harmonics. At the fluid boundary, the temperature signal is assumed to be sinusoidal. The possible effects of higher harmonics were examined by calculating the thermal diffusivity which would be obtained if the signal were triangular (sawtooth). This extreme case would result in only a 10% change in apparent thermal diffusivity, and cannot explain the large observed discrepancies.

6. Vibration. Placing the cell on a vibration damping mount (isolating the apparatus from vibrations over 9 cps) did not alter the observed thermal diffusivities.

7. Insulation. To shield against changes in ambient temperature, the cell was enclosed in an insulated box. The observed diffusivities were not altered.

Since these effects are demonstrably neglibible, it is most likely that the high thermal diffusivities are a manifestation of convection. The following experiments bear on the nature of this convection:

1. Turbulence. When the battery surface in contact with the gas is either heated or cooled, an abrupt and pronounced increase in noise appears when the temperature difference reaches a definite value (approximately 2 to 3 C^{o}). If the heat flow is reversed, the noise abruptly ceases at the same temperature difference.

The same noise is observed with an oscillating wall temperature whenever the signal amplitude exceeds the critical temperature difference. Since in the usual runs temperature amplitudes are kept to a few tenths of a degree, this noise never appears. Taking this noise to indicate turbulent convection, one concludes that the convection of interest here is not turbulent, but laminar.

2. Wall Effect. Removal of the cylinder which formed the inner cylindrical container produced no change in the measured diffusivities. That this drastic change in conditions was without effect, shows that the phenomenon in question is purely local, i.e., convection produced in a semi-infinite medium by temperature oscillation at a horizontal boundary.

3. Temperature and Frequency. Temperature amplitude is found to affect the magnitude of the measured thermal diffusivity much more strongly than frequency. The diffusivities do not extrapolate to the expected value even at zero amplitude. Hence, convection must appear as a step at amplitudes lower than could be reached here.

It is concluded that at frequencies up to 0.2 cps and amplitudes as low as 0.05 C^{o}, laminar convection is induced in the vicinity of a horizontal wall whose temperature is oscillating about the mean in a sinusoidal manner.

The laminar convection hypothesis is supported by the work of Malkus (30). He reported the "effective" thermal diffusivity during laminar convection to exceed that measured during conduction by a factor of 2.1. This finding is in excellent agreement with the data determined in this research.

INTRODUCTION

The aim in undertaking the work described in this dissertation was to study the feasibility of the cyclic heat transfer technique for determining the thermal diffusivity of fluids. This approach is particularly advantageous in the case of reacting mixtures, since the mean temperature is everywhere zero. In addition, the techniques could serve as a source of thermal diffusivity data for single and multi-component systems, providing an independent check on the thermal conductivities which have been obtained by other methods.

The literature survey which follows shows the traditional methods for determining fluid thermal conductivities to be variations on the same basic theme: they all require the imposition of a constant heat flux upon a fluid whose opposing boundaries are at two different temperatures. Such an approach could not be followed for a reactive fluid mixture. Under a constant temperature gradient, a system of this type would rapidly develop a concentration gradient, and hence energy transfer associated with diffusional motion would occur. Failure to avoid this phenomenon would lead to positive errors in the thermal conductivity determination due to the increased heat transmission (4), (5), (16), (39).

The cyclic heat transfer method used in this research project involves imposing a sinusoidal temperature disturbance at the upper end of a long vertical cylinder of test fluid. The phase shift between the response curves obtained at two positions in the fluid is then determined. The thermal diffusivity is simply related to this phase shift,

the frequency of the temperature oscillation, and the distance between the two positions at which the temperatures are monitored.

The absence of a permanent temperature gradient gives this approach great utility, as it can be applied to both reactive and non-reactive fluid systems. Indeed it appears to be the only technique which can be used to measure the "intrinsic" thermal diffusivity of a reactive mixture because of the reduction in mass diffusion induced-energy transmission.

One novel aspect of the method described here is the use of a thermoelectric device, the Peltier battery, to generate the sinusoidal temperature wave. Such a device can be viewed as a reversible "heat pump", causing thermal energy to flow in a direction and quantity which are dependent upon the polarity and magnitude of the electrical current passing through it. With a properly shaped current, such a device can generate a sinusoidal temperature oscillation, and yet add no net heat to the fluid. This feature would be desirable when dealing with reactive mixtures.

The applicability of this approach would seem to be limited to those mixtures for which the reaction rates are "slow" relative to the frequency of the temperature oscillations. In such a situation, the composition of the test fluid would not be affected by the rapidly changing temperature and therefore concentration gradients would not be established. In the absence of these gradients, diffusion would not occur. The transport of additional heat as chemical enthalpy of the diffusing species would be absent and

hence the conduction process is by molecular collisions alone. Thus the experimentally determined thermal diffusivity is that associated with molecular collisions, the "intrinsic" thermal diffusivity. In principle, the use of the reversible Peltier battery would allow such measurements to be made at the ambient temperature, as well as at elevated temperature levels.

When first considered, this approach seemed to offer yet another advantage, a way of getting around the convection problem. On intuitive grounds, it would appear that at sufficiently high frequency convection would not occur since there would be no steady temperature gradient to produce it.

The general feasibility of the cyclic heat transfer technique appeared to already have been established for single component systems, but in different geometry, by Harrison, Boteler and Spurlock (14).

LITERATURE SURVEY

The direct measurement of the thermal diffusivity of fluids is rarely reported in the literature. The major effort in this area has been directed toward the gathering of thermal conductivity data for both single components and non-reactive multi-component mixtures. Required values of thermal diffusivity can then be calculated from this information, in conjunction with density and heat capacity data.

In the main, the "hot wire" or Schleirmacher technique, with its various modifications, has been used to gather what appear to be the best published thermal conductivity values for single gases and non-reactive gaseous mixtures (2), (12), (13), (31); it has been described in detail by Taylor and Johnson (40). A wire, which acts as both an electric heater and a resistance thermometer, is positioned along the axis of a cylindrical tube which confines the test gas. The rise in temperature of the wire, as determined from its increase in electrical resistance, combined with the dissipated electrical power, the wall temperature, and the dimensions of the wire and tube, permits calculation of the thermal conductivity of the test gas. As the thermal conductivity of the wire itself is much greater than that of the gas (by about a factor of 10^4), a correction must be made for the heat conducted longitudinally along the wire. Three methods for compensating for this source of error have been proposed.

The first of these methods is Dickens' (9) compensating hot-wire cell, which utilizes two cells which differ from one another only in length. Thus differential measurements made with this device refer, effectively, to the central portion of the longer cell.

A second approach, the thick-wire-hot-wire cell, was described by Kannuluik and Martin (21), (22). No attempt is made to minimize heat loss through the central wire. Instead a thick wire is used and the ends of the cell are so constructed as to lead to simple boundary problems. In this way the problem of dual heat flow, through wire and through gas, can be mathematically treated without great difficulty.

In the third modification of the hot-wire method, the potential lead cell, extremely fine lead wires are attached to the central wire so as to give the potential drop through the middle segment. Knowledge of the latter leads to the resistance of the wire and thus to the temperature at the center of the cell.

However, regardless of the design of the experimental apparatus, the problems of convective and radiative heat transfer must be considered. There is a classical avenue of approach in each of these areas. The thermal radiation is accounted for by evacuating the cell and then performing the conductivity determination so as to obtain an <u>in vacuo</u> "thermal conductivity" which serves as a radiation correction factor. The convective heat transfer phenomenon poses a different, and in most cases, more serious problem than does radiation, for the former must be completely avoided rather than compensated for. The traditional approach when dealing with the cylindrical type of cell has been to follow closely the experimental research of Kraussold (24) into "Heat Transfer Through Cylindrical Thicknesses by Natural Convection". He established a stability criterion which maintains that convection flow will not occur in an annular space whose axis

is horizontal if the product of the Prandtl and Grashof Numbers for the confined fluid is less than six hundred. With this work as a starting point, the usual tack has been to reduce both the fluid pressure and the physical size of the confining space. However, both of these courses of action have their limitations, for equipment must be sufficiently large to keep relative measurement errors low. In addition, a large reduction in fluid pressure leads to a new complication caused by the uncertain temperature drop at the wall. This so-called "accomodation effect" is also a function of the dimensions and physical nature of the heat transfer surface (9). Hence a proper balance must be struck between apparatus size and operating pressure.

There are alternate techniques which surmount these difficulties in other ways. In the parallel-plate apparatus (32), (20), two horizontal plates, facing each other, are placed at a fixed separation; the upper plate is maintained at a higher temperature than the lower plate. In principle, such a system should be inherently stable in so far as the onset of convective motion is concerned. Knowledge of the magnitude of this temperature difference, the rate of heat input, and the apparatus dimensions are sufficient to calculate the thermal conductivity of the confined fluid.

A newer method, the line source technique, has been presented by Westenberg and de Haas (43). An electrically heated fine wire, serving as a line source of heat, is immersed in a steady, uniform, laminar gas flow and the temperature profile of the gas downstream of the heat source is determined. The gas velocity, the distance from the heat

source, and the relative temperature differences are the only quantities required to calculate the thermal conductivity; corrections for radiation and convection are not required.

Of greater relevance to the present discussion is the work of Harrison, Boteler and Spurlock (14). This research represents one of the few published attempts to determine the feasibility of a cyclic heat transfer method for measuring the thermal diffusivity of gases. Their apparatus consisted, in the main, of a vertical metal tube, which contained the test gas, immersed in a pool of stagnant water. The wall of the tube was electrically heated so as to cause its temperature to oscillate in a sinusoidal manner. Resistance thermometers located near the tube wall and at the tube centerline were used to measure the phase shift between the response curves at these two radial positions. This phase shift data can be combined with the physical dimensions of the system and the frequency of the imposed oscillation to calculate the thermal diffusivity of the test gas. Their results for nitrogen showed a mean deviation of 6.2% between experimentally determined thermal diffusivity values and values computed from the results of other observers for density, heat capacity, and thermal conductivity. Scant attention is paid to the problem of convective instability; they say only that "it is believed that the effects of natural convection were reduced to negligible proportions by proper selection of the frequency range of the temperature fluctuations and by keeping the temperature amplitude low." (12; p. 310). However, the proper magnitude of the wave is not revealed, although their use of fine platinum-resistance thermometers "...permits

the detection of temperature variations of the order of 10^{-4} degree C." (33). The frequency range for the nitrogen measurements between 103.0°F and 169.7°F was published and is given as 0.226-0.344 cps.

The work of Peterson and Bonilla (34) and Lee and Bonilla (25) is also of some interest. Although it is not an absolute method, their frequency response technique did yield excellent results for both nitrogen and helium over a wide range of temperatures. However, the frequency of the temperature oscillation was several orders of magnitude greater than that used in this work (25; Table 1).

While this literature survey is not all inclusive, it does point out the current state-of-the-art. More thorough reviews and compilations of data are presented by Liley (27), (28), Hawkins (15), Lenoir (26), and Bateman (3). The monograph of Tsederberg (41) gives an extensive review of the pertinent work which has been published in the literature of the Soviet Union.

MATHEMATICAL BACKGROUND

Consider a mathematical model in which a sinusoidal temperature fluctuation of frequency f and amplitude T_o is impressed on the boundary of a semi-infinite medium which is initially at the mean temperature T_m. It is assumed that the medium is not in motion and that its density, specific heat, and thermal conductivity are constant. The temperature of this medium T as a function of the distance from the boundary x and time t is given by Jakob (19; p. 294) for large values of t (stationary solution). In modified form, this distribution is:

$$\frac{T-T_m}{T_o} = \exp(-\sqrt{\pi f/\alpha}\, x)\ \sin(2\pi ft - \sqrt{\pi f/\alpha}\, x) \qquad (1)$$

where α is the thermal diffusivity of the medium. From this distribution expression, the temperatures at two points in the medium separated by a distance Δx, will be out of phase with one another by some amount $\Delta\phi$. It follows from equation (1) that α is related to f, $\Delta\phi$, and Δx by:

$$\alpha = \frac{1}{4\pi f}\left(\frac{\Delta x}{\Delta \phi}\right)^2 \qquad (2)$$

When treating experimental data, an average thermal diffusivity $\bar{\alpha}$ is computed. This is obtained from the mean values of the other quantities by the relation:

$$\alpha = \frac{1}{4\pi \bar{f}}\left(\frac{\overline{\Delta x}}{\overline{\Delta \phi}}\right)^2 \qquad (3)$$

A number of circumstances prevent the direct measurement of two of the variables in equation (3), the mean frequency $\bar{f}$ and the mean phase difference $\overline{\Delta\phi}$. However, it is possible to determine two quantities which are dependent upon $\bar{f}$ and $\overline{\Delta\phi}$, respectively. These new variables, the mean wavelength $\bar{\lambda}$, and the mean phase difference $\overline{\Delta\psi}$, are related to the preceding terms by:

$$\bar{f} = C/\bar{\lambda} \quad \text{AND} \quad \overline{\Delta\phi} = \overline{\Delta\psi}/C$$

Both $\bar{\lambda}$ and $\overline{\Delta\psi}$ are determined by making appropriate measurements (to be discussed) from a strip chart recording which had been running at a chart speed C. Thus a relationship which is equivalent to equation (3) is:

$$\bar{\alpha} = \frac{C\bar{\lambda}}{4\pi}\left(\frac{\overline{\Delta x}}{\overline{\Delta\psi}}\right)^2 \qquad (4)$$

EQUIPMENT DESCRIPTION

The experimental apparatus used in this research project consists of the following systems:

1) Thermal Diffusivity Cell
2) Peltier Battery
3) Peltier Battery Power Supply
4) Thermocouple Probes
5) Electronic Apparatus
6) Optical Measurement Instrument
7) Thermal Bath
8) Auxiliary Apparatus

Each of these items will now be discussed.

1) Thermal Diffusivity Cell - The principal function of the Thermal Diffusivity Cell is to confine the test fluid. As originally conceived, the cell is composed of two concentric, Pyrex glass, cylindrical tubes, 1½" O.D. and 6" O.D. (figure 1). The outer cylinder is 6 3/4" long with a 3/16" wall. It is closed at the bottom by a circular aluminum plate into which a circular channel has been cut. The outer cylinder sits in a Teflon gasket which has been placed in the channel. Screwed into tapped holes in this bottom plate are two small valves and two small "Swagelok O-seal" connectors. The valves allow the confined fluid to enter and leave the cell; the function of the connectors will be described shortly. The upper end of the large glass cylinder is sealed by a second circular aluminum plate; it has the same gasket arrangement as the bottom plate. The cell is held together by three long bolts, with spring-loaded heads, which pass between

FIGURE 1 - THERMAL DIFFUSIVITY CELL

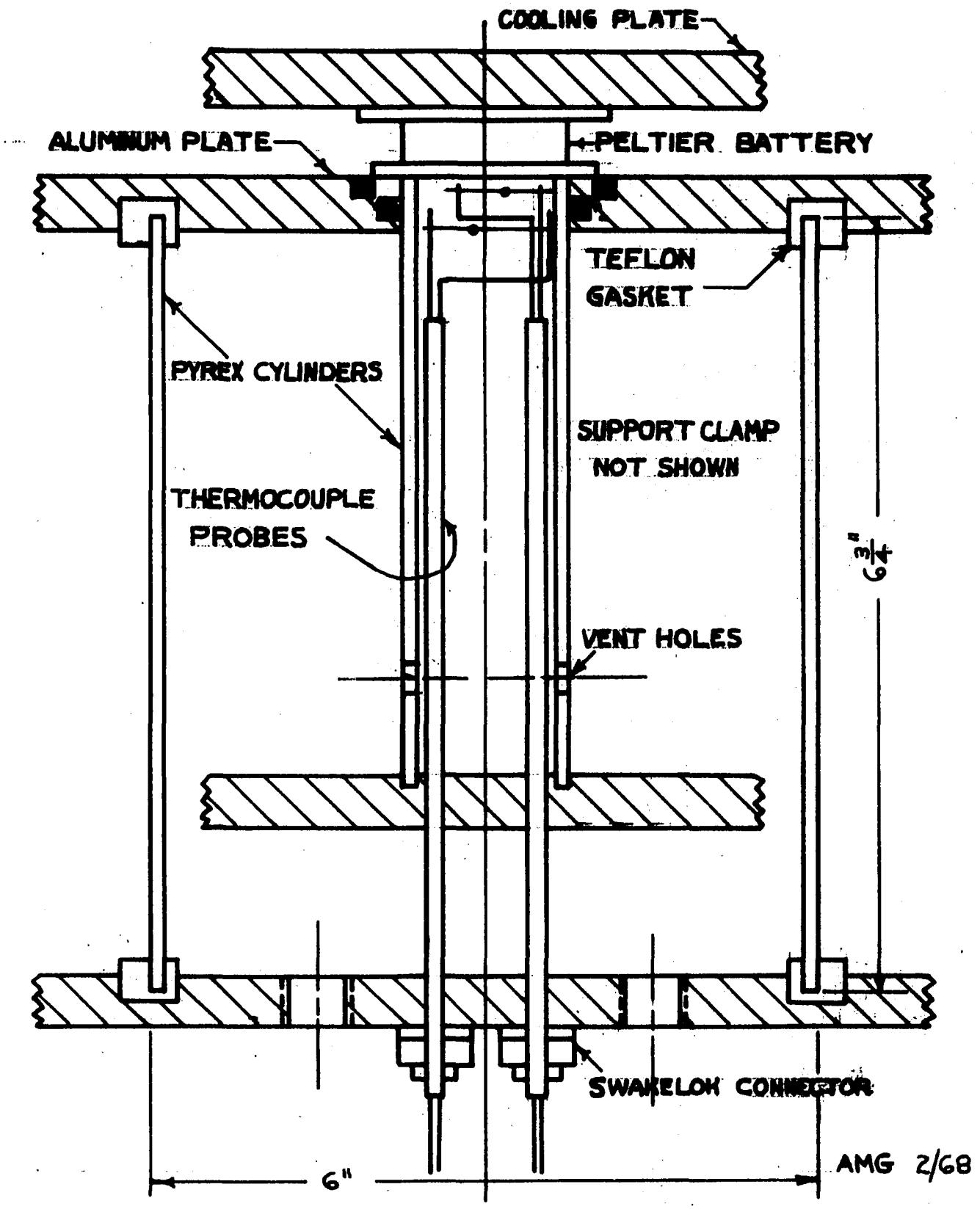

these two large endpieces. These bolts serve yet another function, that of adjustable-length legs upon which the cell sits. This adjustable feature is important, as it enables one to level the cell in conjunction with a bubble level device.

A 1½" diameter hole has been cut through the upper aluminum plate. The inner cylinder, 5½" long with 1/8" wall, passes through this opening and is held at the upper end by a Teflon O-ring. The bottom end of the cylinder is closed by a small aluminum flange. The latter is held in place by bolts which pass through it and are connected to a collar encircling the cylinder. Use of spring-loaded bolt heads furnishes needed elastic elements in the support arrangement. The collar is a split-type which utilizes an O-ring to hold it to the cylinder wall. Such a collar design is used to decrease the possibility of cracking the inner cylinder during assembly of the cell.

At the upper end of the cell is the Peltier battery assembly which consists of a Peltier battery and its cooling plate. A large channel in this plate is filled at all times with flowing water from a constant temperature bath and is covered by one side of the Peltier battery, the so-called "secondary junction". In this manner one side of the battery can be kept at a constant temperature. The other face of the battery, the "primary junction", lies flush against the upper end of the small glass cylinder. It is from this face that the sinusoidal temperature fluctuation emanates. The assembly is held to the cell by three large screws which pass through the cooling plate and into tapped holes in the upper endpiece.

Before a determination is undertaken, the cell is completely filled with test fluid, which passes from the annular space into the inner cylinder through four 1/4" holes drilled through its wall. The thermal diffusivity determination is performed upon the fluid trapped in the inner cylinder. The fluid in the annular space acts as a thermostat medium, and can be circulated through external coils to the same constant temperature bath which supplies water to the Peltier battery cooling plate. Positioned within the inner cylinder are the two thermocouple probes which sense the temperature fluctuations.

The Thermal Diffusivity Cell, as just described, was utilized in performing Runs 1-8, inclusive. For reasons to be described later, a major change was made in the cell configuration at this point. The inner cylinder, its support collar and end flange were removed from the cell. In addition, the upper aluminum plate was reconstructed so that its lower face would be level with the "primary junction" side of the Peltier battery. This cell arrangement was used in performing Runs 9-25, inclusive.

The materials of construction of the cell, Teflon, Pyrex glass, and aluminum alloy 7075, were selected so as to be compatible with a wide range of fluids. In addition, this aluminum alloy possesses good machining characteristics. The cell was designed to be gas-tight, although this feature was never tested.

2) Peltier Battery - The Peltier battery is a thermoelectric device whose major function as a part of this apparatus is the generation of the sinusoidal temperature perturbation. It is

constructed from forty small elements of doped bismuth telluride sandwiched between two copper plates. Each pair of these semi-conductor elements constitutes a single thermoelectric junction. The twenty junctions are arranged so as to be thermally in parallel and electrically in series. Underlying the operation of this device is the "Peltier Effect" (10): the passage of an electrical current through the junction of two dissimilar conductors will cause that junction to emit or absorb thermal energy at a rate proportional to the magnitude of the current. This effect is reversible, i.e., the junction can be changed from a heat sink to a heat source by reversing the direction of the electrical current. Although commercial Peltier batteries are designed as refrigeration units, it is evident that they can be employed as reversible "heat pumps" to generate a temperature wave which oscillates about the ambient condition. However, their application in this manner is complicated by the presence of superimposed Joulean heating. In principle, this irreversible thermoelectric effect can be neutralized through the use of a properly biased electrical voltage.

The Ferroxcube Corporation of America, which markets the Peltier battery model PT 20/20 used in this project, specifies the maximum peak current for this device as thirty amperes during any five second period. In addition, the maximum permissible temperature is given as $90^{o}C$, with the preferred operating level no higher than $55^{o}C$ (11). These specifications place an upper limit on both the mean temperature at which a thermal diffusivity determination can be

made, and the amplitude of the temperature oscillation.

3) Peltier Battery Power Supply - It has been stated that a biased electrical voltage would be required to drive the battery. However, discovery of the exact shape of this voltage through an analytical approach would be a difficult task, complicated by incomplete knowledge of important physical parameters. Even if such an undertaking were successful, generation of the appropriate waveform, in the required twenty ampere, two volt range, would be a formidable problem. It was discovered, by trial, that a biased square-wave voltage would be acceptable. However, a commercial generator of such a voltage, operating in the desired frequency and voltage-current ranges, was not available; thus it was necessary to design and construct such a unit.

The Peltier battery power supply is composed of a frequency selector, a double-pole mercury relay, and two independent, variable D.C. power supplies. The principle of operation is simple: the frequency selector supplies A.C. power to the relay in such a manner as to cause the two D.C. supplies to alternately feed current to the Peltier battery for selected time periods. In this manner both the frequency and bias of the voltage can be regulated (figure 2).

The physical arrangement of the elements comprising the frequency selector is shown in figure 3. An 1800 rpm synchronous motor is stepped down through a variable ratio gear train and drives a custom-machined cam. The rotational velocity of the cam can thus be varied from 3/70 rps to 4 2/7 rps through forty-two different values. The cam drives a roller-actuated switch causing it to pass through a sequence

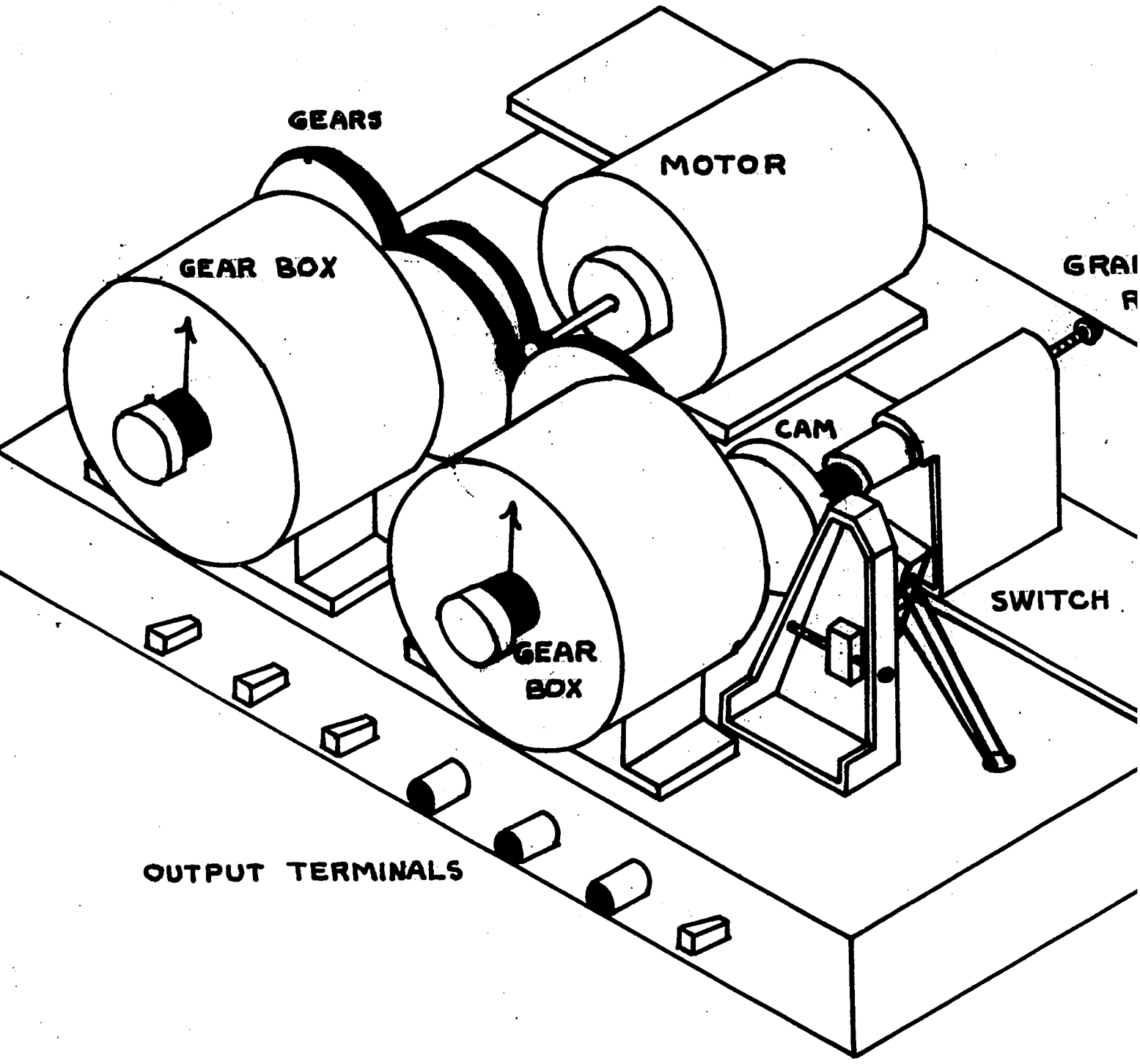

FIGURE 3 - FREQUENCY SELECTOR

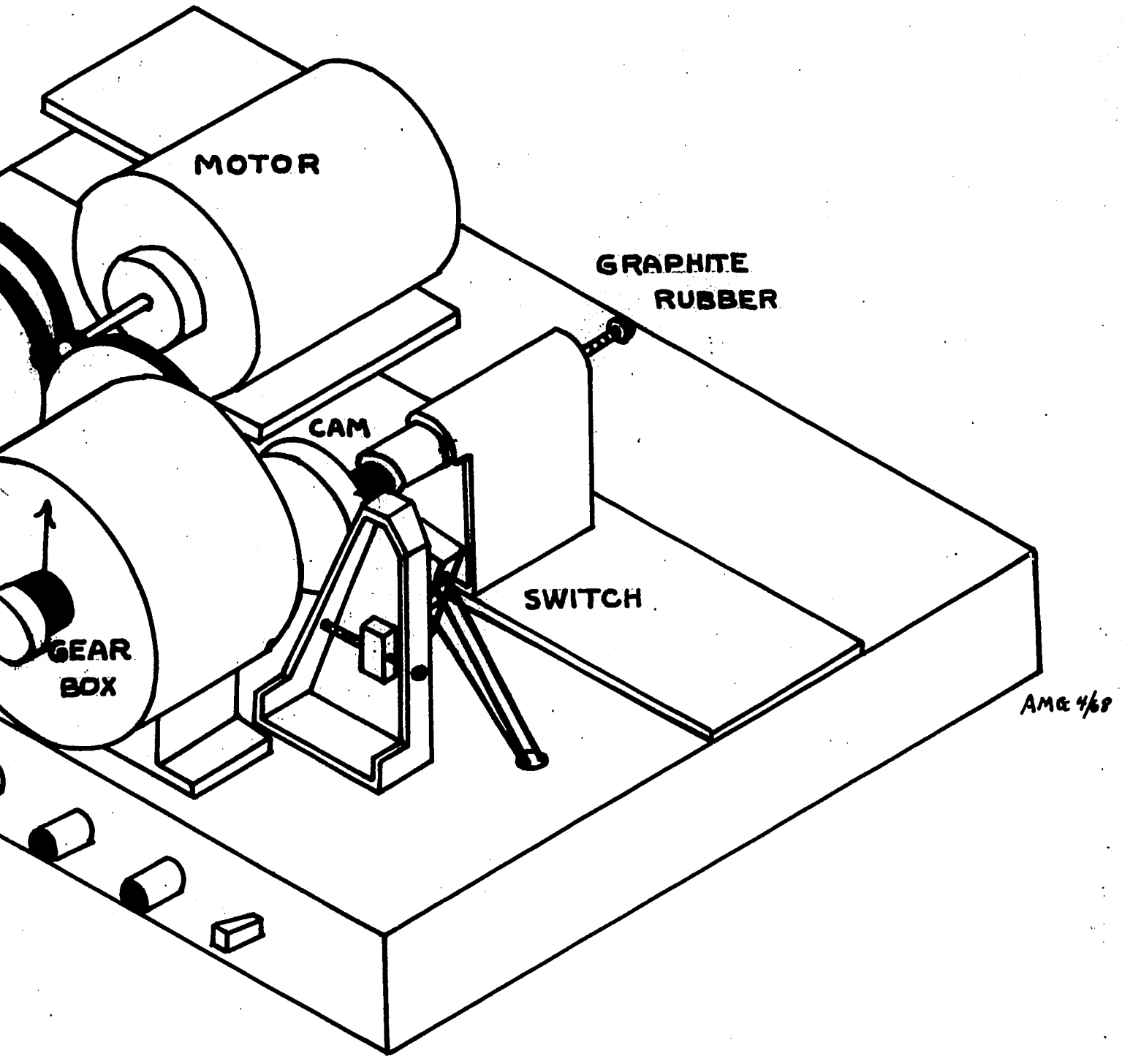

REQUENCY SELECTOR

FIGURE 2- PELTIER BATTERY CIRCUIT

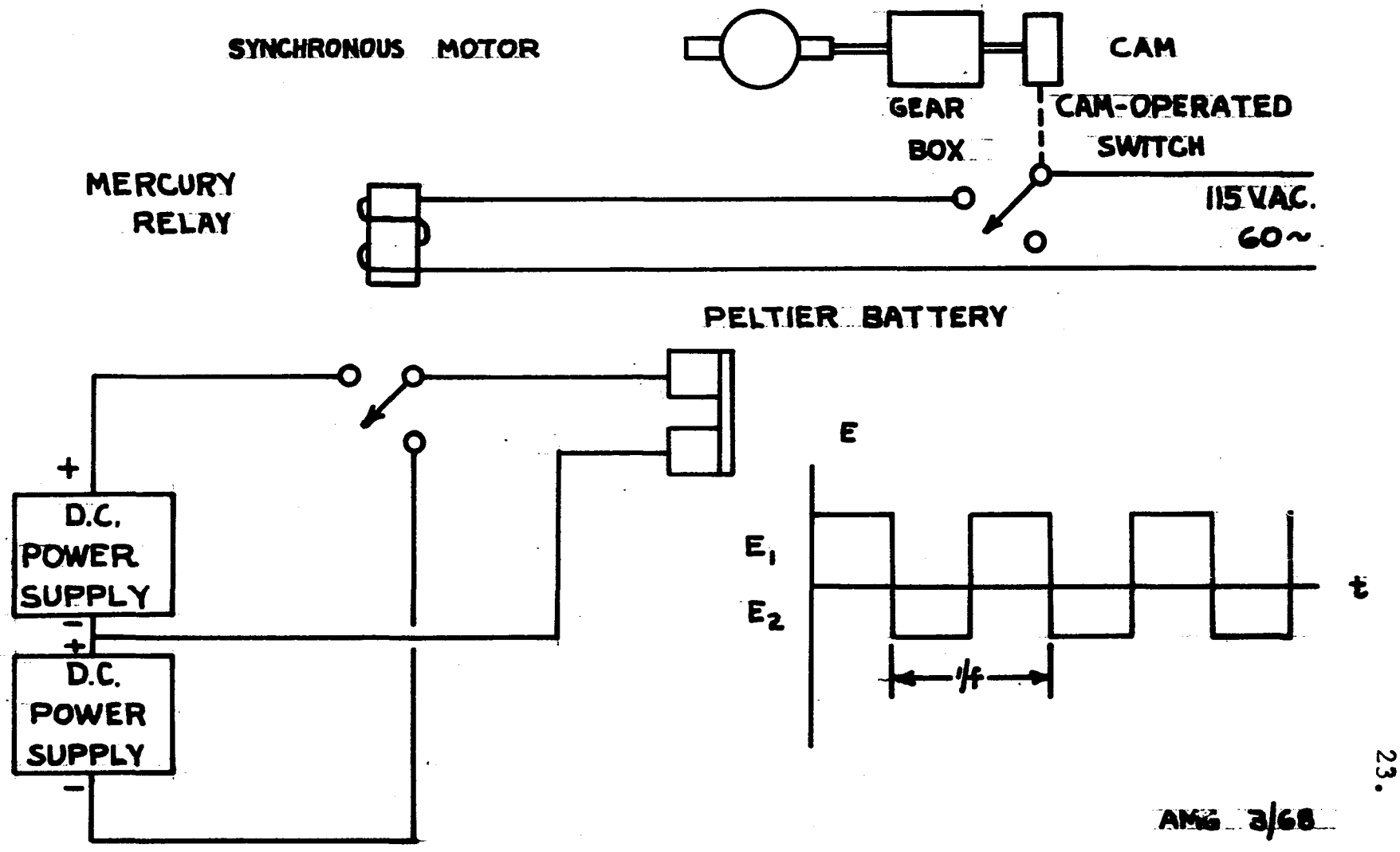

AMG 3/68

FIGURE 4-VOLTAGE INPUT TO PELTIER BATTERY

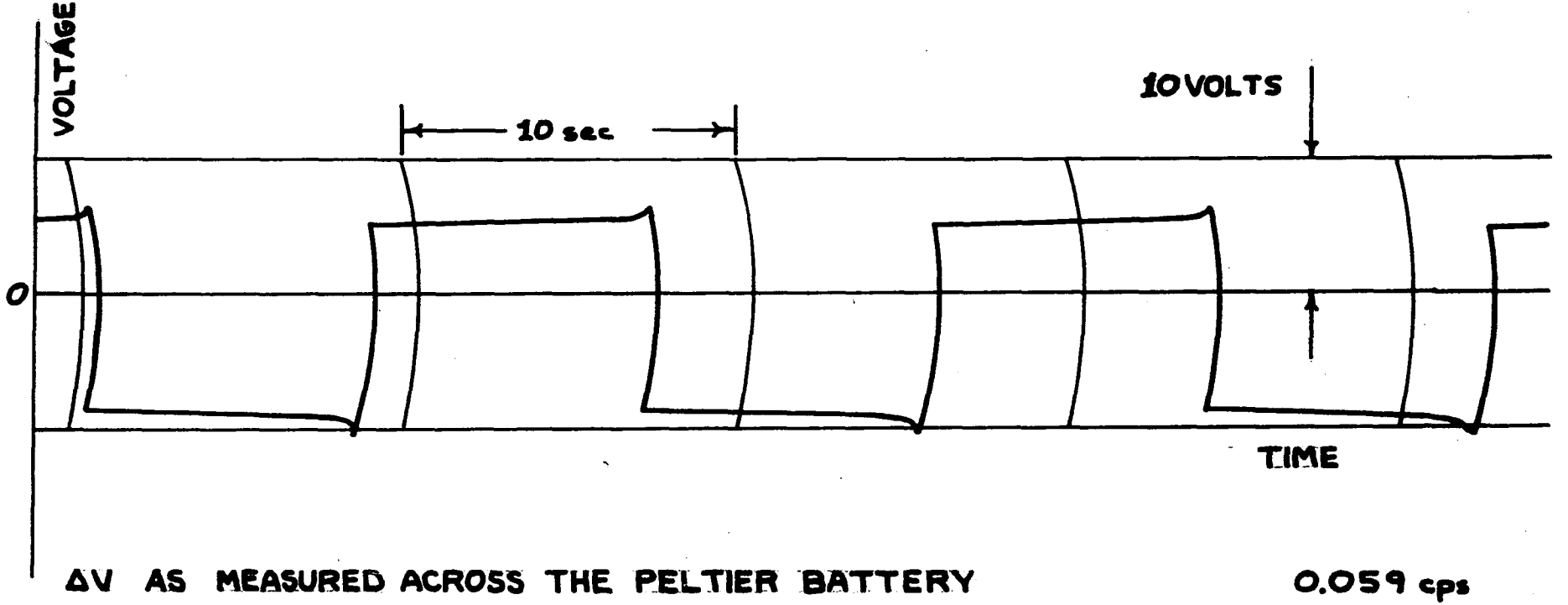

ΔV AS MEASURED ACROSS THE PELTIER BATTERY 0.059 cps

of alternating open and closed positions. Each position is maintained for a time equal to one-half the rotational period of the cam. When it is in the closed position, the switch allows A.C. power to flow to the mercury relay, thus activating it. The relay assumes its deactivated configuration when the switch opens. A spring-loaded graphite "rubber" is compressed against the side of the cam; it acts as a load to compensate for backlash in the gear train.

The two D.C. power supplies are identical in both construction and operation. Each can produce a "flat", well-regulated D.C. voltage in the two volt, twenty ampere range. It was necessary to custom-build the two units because readily available commercial generators could not meet the high current-low voltage specification. Each unit consists of a variable transformer, which controls the output of the source, in series with a full-wave rectifier and an inductance-capacitance (LC) filter. The mercury relay alternately feeds the output of each generator to the Peltier battery.

Thus the Peltier battery is driven by a square-wave voltage whose frequency can be varied, in principle, from 0.043cps to 4.286 cps, through forty-two different values. However, the actual upper bound on the frequency is below this level, a consequence of slippage in the gear train at high rotational velocities. The amplitude of the voltage can also be varied, but in a continuous manner. The output of each source can be independently regulated by adjusting the variable transformer. Alternatively, a variable series resistor can be manipulated to change the amplitude of the wave while maintaining the proportionality between the positive and negative portions of the wave. (figure 4)

4) Thermocouple Probes - Two chromel-alumel thermocouple probes are employed within the cell to detect the fluid temperature fluctuations (figure 1). As can be seen from figure 5, the Probes are fork-like in appearance, with one end of a fine (0.001") chromel-alumel thermocouple wrapped around each prong. These thicker, more rigid wires act as both supports and electrical leads. They pass out of the cell through a ceramic sleeve which insulates the wires and furnishes additional support. The two Probes are identical with the exception of the magnitude of dimension "A". Each probe is locked in position by a "Swagelok" connector, through which it passes. A rubber ferrule within the connector prevents the brittle ceramic sleeve from cracking during assembly of the cell.

In the design shown in figure 5, the second or "cold" junction of the thermocouple probe is located outside the cell. This configuration was modified in an effort to reduce the D.C. output of the probe (to prevent amplifier overloading) by repositioning the "cold" junction within the cell. The re-design was accomplished by grinding away a portion of the ceramic sleeve, thus laying bare a short length of the chromel support wire. The latter was then cut through and the end portion removed from the sleeve. A piece of alumel wire was put in its place and spot welded to the chromel wire. This weld, located within the cell, but far from the Peltier battery, formed the new "cold" junction. By means of this alteration, the difference in mean temperature between the two junctions, and hence the D.C. output of the probe, was reduced.

FIG. 5 - THERMOCOUPLE PROBES

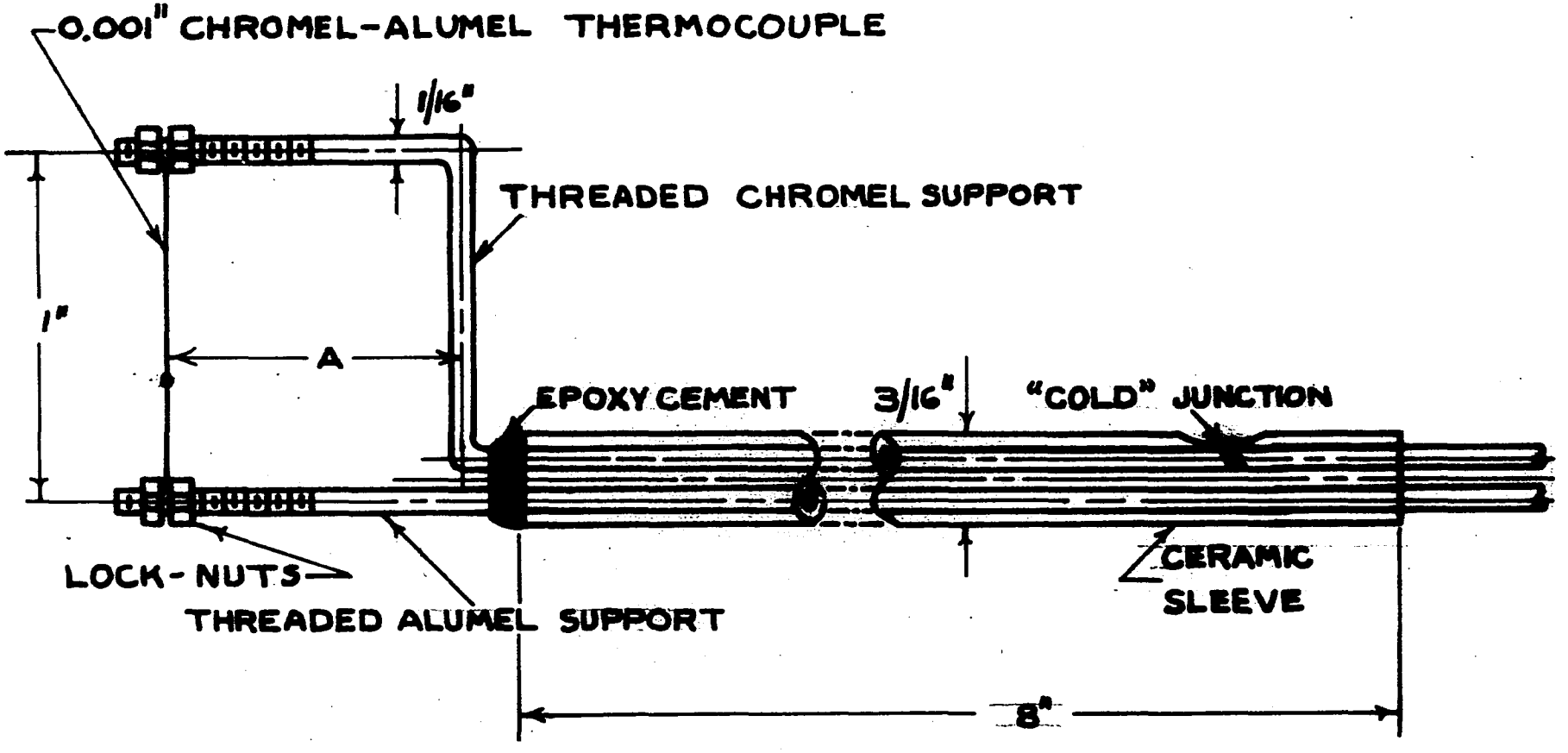

TWO PROBES ARE USED. A=3/4" & A=1"

AMG 1/68

Thermocouples were chosen as the temperature transducers for two reasons: they are readily available in small sizes; their use is not accompanied by the generation of a significant amount of heat. The size specification is essential for it ensures the rapid response of the transducer, a necessary condition when sensing oscillating temperatures. The time constant of the 0.001" thermocouple is estimated to be 0.08 seconds, which is more than two orders of magnitude smaller than the period of a typical temperature wave (Appendix B). Although fine resistance thermometers are capable of rapid response, their use would introduce new sources of heat into the cell, which is undesirable, particularly for reactive fluids. Similarly, thermistors are to be avoided because of their poor transient response. The time constant of a thermistor varies for commercial units between 1 and 200 seconds (29). The choice of chromel-alumel for the thermocouple was dictated by its relatively high sensitivity ($\mu v/^{o}C$), coupled with commercial availability.

5) Electronic Apparatus - The thermocouple probes convert the temperature fluctuations of the test fluid into electrical signals. The purpose of the electronic apparatus is to extract phase difference information from these signals. This task is complicated by a number of factors: signal amplitude, signal frequency and noise level. It was expected that the amplitude of the temperature oscillation would be less than 1 C^{o}. Thus the signal generated at the chromel-alumel junction would be quite small, approximately 30 μv peak-to-peak, at a frequency of about 0.1 cps. In addition,

it was to be expected that the signal would be immersed in a significant level of wide-band noise.

Commercial phase-meters and lock-in amplifiers could not be used because of the low frequency of the information signal. Hence a three step procedure was selected to obtain the required phase difference data. The thermocouple voltage was amplified, filtered, and then displayed on a two-channel strip chart recorder. The phase difference measurements could then be made from these recordings. Although this procedure was utilized for all twenty-five determinations, changes were made at various times in the system components. These modifications widened the range of the operating variables within which it was possible to work and increased the precision of the diffusivity data.

The first six determinations utilized an electronic system whose sole redeeming feature was the availability of the components. This approach was quite acceptable in these early experiments because high precision was not an immediate goal. The amplification stage was fabricated on an Electronic Associates, Inc. TR-10 Analog Computer. The amplified signal then passed through an Allison Low-pass LC model 201 filter set to attenuate at 2 cps and was displayed on a Brush Mark II Recorder. The voltage recordings generated by this apparatus exhibit drift, low frequency A.C. noise and poorly defined extrema, all of which contribute to the poor precision of the thermal diffusivity measurements.

The first improvement was in the area of signal filtration, where a fixed RC bandpass filter was constructed to replace the low pass filter. This new device significantly

reduced signal drift, but was hindered in its ability to remove A.C. noise by a wide pass-band. Passive RC and LC filters are desirable because they generate little noise. Unfortunately it is not practical to construct a passive band-pass filter with variable cutoff which will operate in the desired frequency range. These difficulties were overcome through the purchase of a Krohn-Hite Active Band Pass Filter Model 330BR-4. However, this commercial unit had to be custom modified by the manufacturer in order to meet the required specifications.

The major portion of the difficulty experienced with the original electronic apparatus stemmed from the amplification stage. These obstacles were not unexpected because of the makeshift nature of the unit. The first attempt to ameliorate this situation involved the construction of an amplifying device from commercial operational amplifiers, Nexus type SQ-10 (figure 6). While this new device represented an improvement over the original amplifier, it still exhibited undesirable characteristics, particularly noise and drift. The ultimate solution to the problem was the purchase of a sophisticated amplifier-recorder system from the Brush Instruments Division of the Clevite Corporation. It was composed of a RD 4215-70 Very High Gain DC Preamplifier and a Mark 280 Recorder. In addition, low noise, shielded cable, Belden type 8451 and General Radio type 274, were used to channel the signals between the various components. The circuit diagram is shown in figure 7. With this new equipment it was possible to select from a wide range of chart speeds, sensitivities and filter settings so as to obtain superior outputs,

FIGURE 6 - AMPLIFER

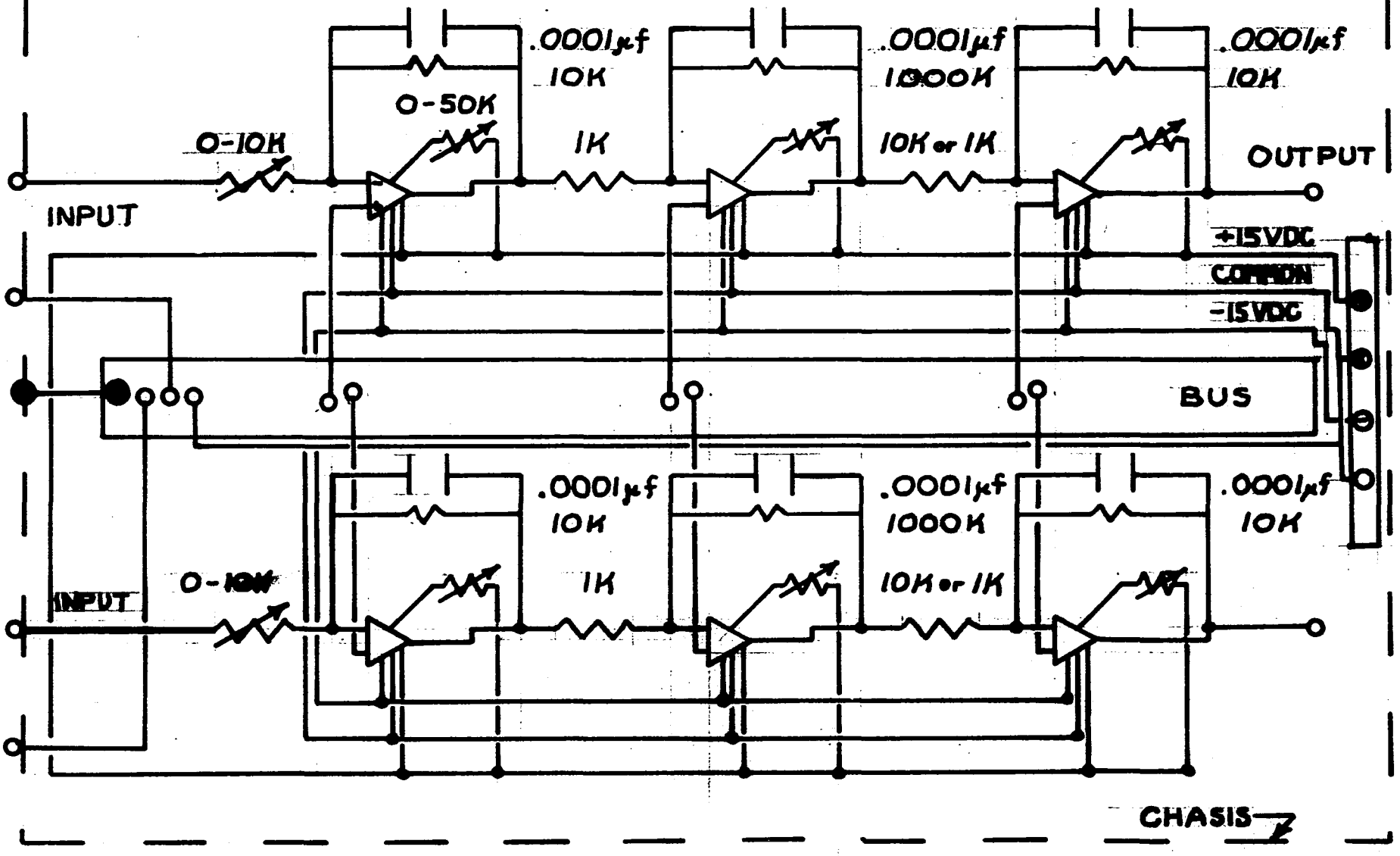

FIGURE 7 - SIGNAL DETECTION AND RECORDING

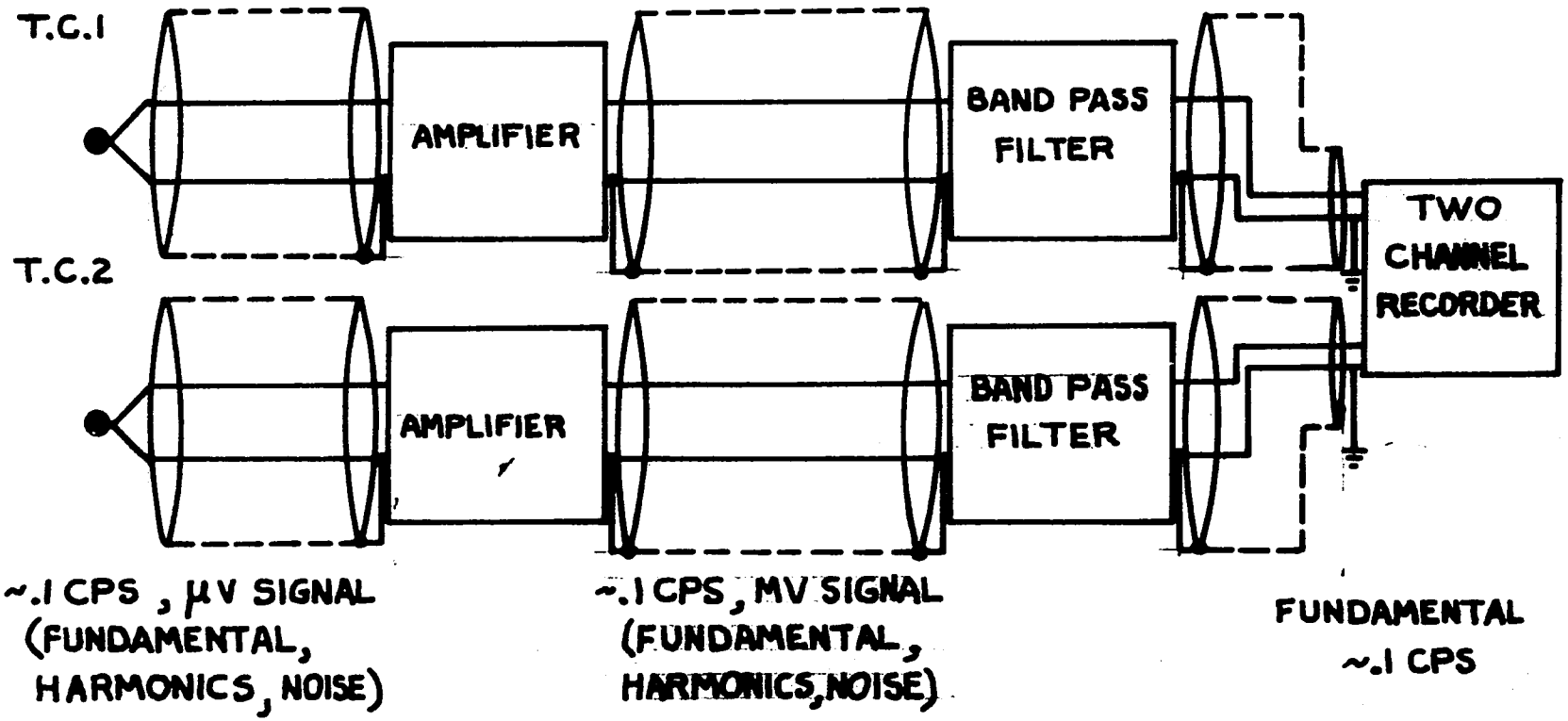

AMG 4/68

and hence more precise thermal diffusivity data. These various changes in equipment and the ensuing improvements in the capability and precision of the electronic apparatus will be examined further in the "Discussion" section of this dissertation.

6) Optical Measurement Instrument - The purpose of the optical measurement instrument is the measurement of the separation between the two thermocouple junctions, i.e., the distance between the two points at which the temperature oscillations are monitored. This function is fulfilled through the use of a modified Bausch and Lomb model ADM-2 Stereo Depth Measuring Microscope, which utilizes an observer's sense of depth perception to make depth measurements. The device is a 20X Stereomicroscope; it uses two identical reticles having concentric dot and ring patterns to cause image fusion at a definite plane in space. Depth measurement is read on a dial indicator, having a range of 1", and a least reading of 0.001". A device is provided by the manufacturer for initial alignment of the microscope.

The thermocouple wires are not visible when the cell is completely assembled. Hence it is necessary to perform the required measurements before the Peltier battery assembly is attached to the remainder of the cell. This operation is carried out by positioning the microscope above the cell, aligning it, and then focusing on each thermocouple junction in turn. The distance moved by the microscope in traveling between the two points of focus is taken to be the distance between the two junctions. Consideration of the accuracy and

precision of this technique will be postponed until a later time.

7) Thermal Bath - As originally conceived, the function of the thermal bath was to maintain the mean temperature of the test fluid and of the Peltier battery "secondary junction" at the same level. For this reason, a coil was placed in the bath to accomodate that portion of the test fluid which filled the annular space within the cell. The idea was to circulate this fluid between the cell and the bath by means of a small blower. However, this procedure was never carried out, as all runs were made at about room conditions. Thus the sole function of the bath was to provide "cooling" water for the Peltier battery.

The thermal bath was of a conventional type with "on-off" heater control. Because of the nature of this controller and the desire to maintain flexibility in the choice of bath temperature, it was necessary to position a flowing tap-water cooling coil within the bath. A small centrifugal pump was used to circulate water from the bath to the Peltier battery cooling plate through flexible rubber hose (figure 8). The latter was used, rather than rigid tubing, to reduce the level of vibrations transmitted to the cell from the pump motor.

8) Auxiliary Apparatus - A number of precautions were taken to protect the cell from environmental effects during a determination. First, the cell was placed on a vibration damping mount, a heavy, low block whose legs are designed for vibration suppression. The supplier, Chemical Rubber Company,

FIGURE 8 - FLUID CIRCULATION SYSTEMS

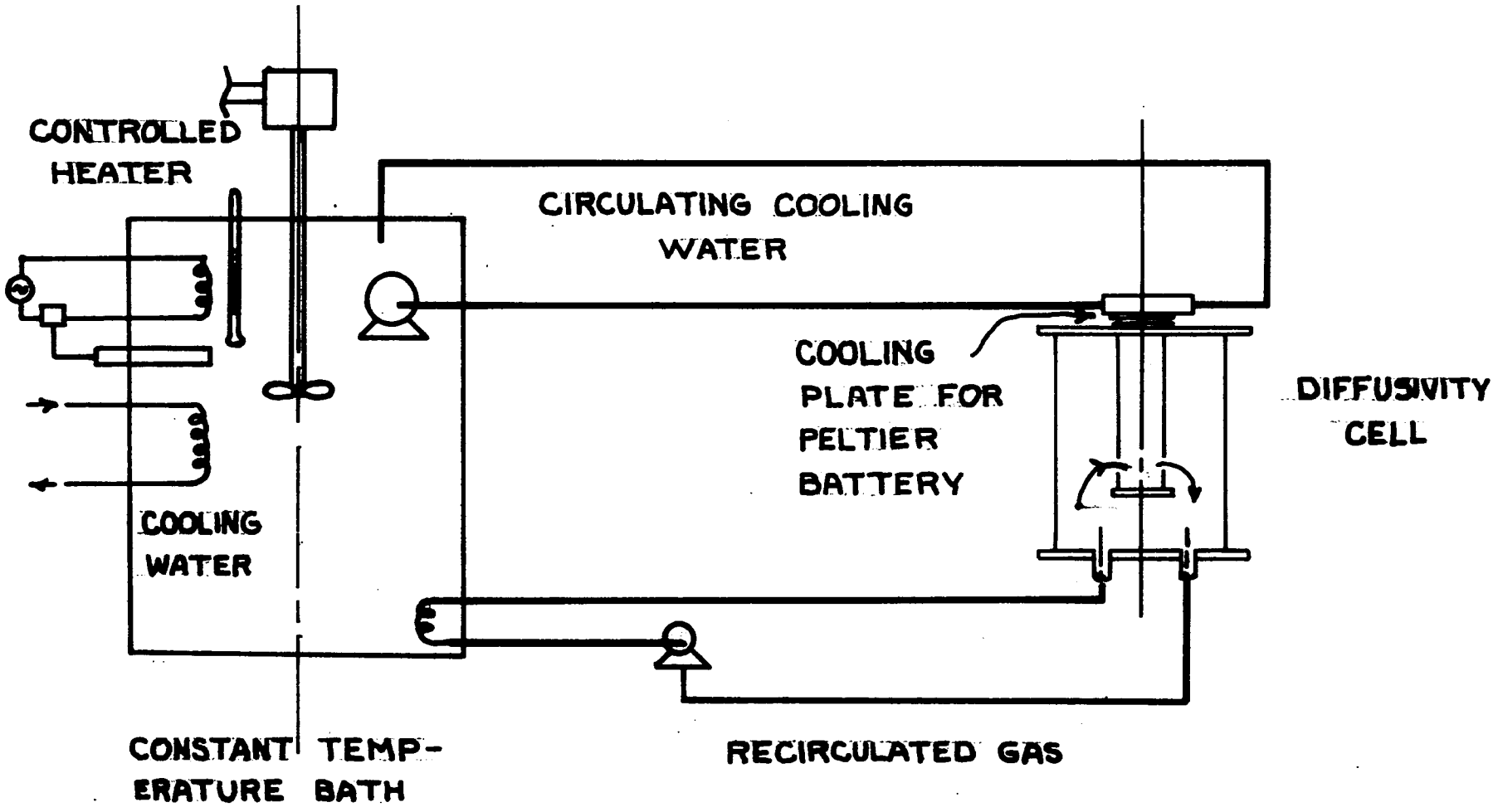

AMG 4/68

claims that this device will absorb vibrations caused by motorized devices, e.g., stirrers and pumps, down to 9 cps. This mount, in turn, rests on a large steel table which is rigidly attached to the concrete floor.

As a second precautionary measure, the cell was enclosed within an insulated box, constructed of wood and "Fiberglas" building insulation. This structure acted to shield the cell from the effect of room air currents.

OPERATING PROCEDURE

The initial step in a determination is the assembly of all major portions of the thermal diffusivity cell, excepting the thermocouple probes, Peltier battery, and cooling plate. These three items are incorporated at a later time. Because of fear of breakage during shipment, the thermocouple probes are provided by the manufacturer without the thermocouple wire in place. The connection of this wire, a task made trying by the size of the wire (0.001"), its tendency to coil and the weakness of the junction, must then be carried out by the experimenter. The relative ease with which the junction separates also makes it a practical impossibility to place the thermocouple wire in tension. If the inner cylinder is not to be used, both probes can be strung outside the cell. If the inner cylinder is to be present, lack of space to maneuver the probes compels one to perform a more difficult operation, that of stringing the probes while they are locked in the cell. In either case, the use of a magnifying lens is most helpful, so as to position the junction approximately midway between the two prongs. The thermocouple wire is fastened to the probe by wrapping an end several times around the threaded portion of each prong, and then tightening down the lock nuts. Considerable caution must be exercised during this step to avoid breaking the junction. In addition, it is imperative to connect the alumel end of the thermocouple to the alumel prong and the chromel end to the chromel prong. If this procedure were not followed, there would be three bimetallic junctions, each capable of generating signals, on every probe.

The probes are introduced into the cell through the opening in the upper aluminum plate. The end of each ceramic sleeve is passed through one of the "Swagelok" connectors, which is then tightened to hold the probe in place. The relative location of the two thermocouple junctions and their distance from the Peltier battery surface can be changed by loosening these connectors and shifting the positions of the probes. A two-wire signal cable is then fastened to the lead wires of each probe, and terminated in a male Cannon audio connector.

With the probes in position, the cell can be placed on the vibration damping mount, which sits in turn, on a rigid steel table bolted to the concrete floor. Once in this location, the cell can be brought to an approximately level position by adjusting the length of the three cell legs in conjunction with a bubble level device lying on the upper aluminum plate. A temporary platform, to hold the Stereomicroscope base is erected alongside the cell. The microscope Power Pod is leveled and then positioned above the opening in the upper aluminum plate so that both junctions would be visible in the same field without moving the microscope laterally. Once the microscope has been properly aligned according to the manufacturer's directions, it is ready to be used to determine the vertical distance between the two thermocouples. This measurement is performed by focusing the device on one junction, setting the dial indicator to zero and then refocusing on the second junction. The required distance can thus be read directly from the dial indicator. In an effort to increase precision, this determination is

made about fifteen times over a period of approximately one hour. Each reading is reported to the nearest 0.0005". The mean value calculated from these data is used to compute $\bar{\alpha}$.

With this measurement completed, the cell can now be sealed by placing the Peltier battery assembly into its position above the upper aluminum plate. Care must be exercised while this is being done to avoid jostling the cell and possibly damaging the fine thermocouple wires. The use of atmospheric air as the test fluid obviates the necessity to purge, refill and pressure test the cell. Of course, determinations run upon other fluids would require the performance of these steps at this point in the operating schedule.

The thermal bath has been allowed to reach the desired temperature during this period. With the Peltier battery in place, the centrifugal pump is activated, thereby circulating cooling water between the bath and the cell. The Stereomicroscope and its support platform are removed from their position near the cell, and the insulated box placed over it. Passing out through small openings in this enclosure are the cooling plate tubing lines and two pairs of electrical leads. One pair of leads connects the Peltier battery with a nearby terminal box and ultimately to the square-wave generator, located some fifteen feet from the cell. This separation is significant as it further isolates the cell from a number of sources of vibrations. The local terminal box includes an ammeter which can be switched into the power line so as to read the current flow through the Peltier battery. To further monitor the performance of the Peltier battery, a

connection is run from this terminal location to the Mark II strip chart recorder. Thus a continuous record of the potential drop across the Peltier battery is made for each run. On the other hand, the current is read intermittently during a run because the ammeter is not a "center-zero" device. When the current polarity changes, the meter presently in use is pushed off scale. A switching arrangement is necessary to protect the meter by reversing its polarity or removing it from the circuit.

An operating frequency can now be selected and the gear boxes set to the proper gear ratios. The frequency selector is then activated so as to allow the synchronous motor to reach its operating temperature. The two D.C. supplies are isolated from the Peltier battery and set to the desired voltage by adjusting the variable transformers built into each supply. Then the power supply circuitry is arranged so that one switch will control the flow of current to the Peltier battery.

While these operations have been going forward, the data recording system is brought to a state of readiness. In the case of the active bandpass filters, the settings are chosen so that the ratio of the high cutoff frequency to the low cutoff frequency is four. This selection insures sharp attentuation outside the pass band, with little reduction in the amplitude of the information signal. Two operations remain before the determination can be started. The power supply circuit is closed for a few minutes causing current to flow to the Peltier battery. The resulting temperature oscillations are recorded in an effort to select for each

channel the proper combination of recorder chart speed and sensitivity which will yield acceptable voltage traces. With these choices made, the circuits are temporarily rearranged so that the output of a single probe is impressed on both channels. In this manner, the phase lag caused by differences in the two recording channels can be determined and thus corrected for at a later time. The circuitry is then returned to its original configuration so that the output of each probe is displayed on a separate channel.

When the effect of these disturbances has vanished, the actual determination can be started. The power supply is activated and thermocouple voltage recordings are collected over a period of many minutes. The recorder output consists of a trace of about one hundred cycles, which must then be analyzed to obtain frequency and phase difference data. The analysis is performed by visually judging the location of the maxima and minima for about thirty to forty of the recorded cycles, and then measuring the distance between corresponding extrema on the two channels with a millimeter scale. The mean value of these data must be corrected for that phase difference, if any, which stems from differences in the two recording channels. This correction factor is particularly significant when the active filters are used, for they are continuously variable and possess a coarsely graduated frequency scale. It is thus difficult to tune both filters to the same pair of cutoff frequencies. The corrected mean phase difference is then used to calculate $\bar{\alpha}$. The voltage recordings can also be used to determine the mean wavelength by averaging the measured distances between successive maxima

or minima. It is in close agreement with that computed from knowledge of the nominal motor speed and the gear ratios; the experimental value is used to calculate $\bar{\alpha}$.

This operating schedule was followed for the twenty-five runs discussed in this work. However, in the last nine runs which constitute Group III, the desire to obtain temperature amplitude data necessitated the addition of a number of new steps to the aforementioned procedure. A thirty gage calibrated copper-constantan (Appendix K) thermocouple was placed in a rectangular channel which had been machined in the "primary junction" plate of the Peltier battery. The "hot" thermocouple junction was positioned at the center of this plate, with the insulated lead wires extended down its long axis. The "cold" junction was placed within the cell, though far from the Peltier battery. The lead wires were terminated in a female audio Cannon connector, which was coupled in turn, to a shielded two-wire cable.

It would have been preferable to simultaneously record the voltages generated by this differential surface thermocouple and the two fork-like probes. Unfortunately, the availability of but two high gain channels meant that this design could not be implemented. The problem was circumvented by first recording the signal of the differential thermocouple, rearranging the electronic apparatus, and then simultaneously recording the output of the two probes. In the case of the differential surface thermocouple, it was necessary to guard against both spurious signals and unsuspected attenuation of the desired signal, so as to maintain the reliability of the thermocouple calibration. For example,

it was found that the surface thermocouple received an undesired low-frequency signal from the square-wave generator itself. This occurrence was not unexpected, for the copper plate upon which the thermocouple lies is insulated from current-carrying thermoelectric elements by a finite resistance. Although proper grounding attenuated this signal by an appreciable amount, the residual portion was still significant. Hence it was necessary to correct the final voltage readings to account for its presence.

In summary, the normal procedure as concerns these "surface" waves is to read their magnitude from the recorder chart to the nearest whole division, apply the proper correction, and then express the amplitude of the surface temperature oscillation in Centigrade degrees.

EXPERIMENTAL RESULTS

The experimental research performed in this project is divided into four groups: three series of thermal diffusivity determinations and a qualitative study of turbulent convection. Although the cell was designed for use with any fluid compatible with the materials of construction, the simplest approach was to use air at ambient conditions as the test fluid. Physical property data for air, of course, is readily available and its use averts possible difficulties with gas-tight seals.

A. Group I - Preliminary Thermal Diffusivity Determinations

The aim in performing the first six determinations, which constitute Group I, was to test out both the method and the various systems which form the experimental apparatus. The experimental data for the Group I determinations are shown in Table 1, along with values of thermal diffusivity computed from these quantities. These thermal diffusivities are the least precise values obtained.

An expression was derived which allows one to calculate the statistical estimate of the variance of the $\bar{\alpha}$ values, $S^2(\alpha)$, from the statistical estimates of the variances of the measured quantities, $S^2(\lambda)$, $S^2(\Delta x)$ and $S^2(\Delta\psi)$. (Appendix A). These values are also contained in Table 1. They show that the standard deviation of $\bar{\alpha}$ ranges from $\pm$ 45% to $\pm$ 65% of the value itself. The variance expression is:

$$\frac{S^2(\alpha)}{(\bar{\alpha})^2} = \frac{S^2(\lambda)}{(\bar{\lambda})^2} + 4\,\frac{S^2(\Delta X)}{(\overline{\Delta X})^2} + 4\,\frac{S^2(\Delta\psi)}{(\overline{\Delta\psi})^2} \qquad (5)$$

TABLE 1 - GROUP I DATA SUMMARY

RUN NUMBER	1	2	3	4	5	6
Nominal Frequency, cps	0.043	0.054	0.060	0.067	0.077	0.087
Aver. Wavelength, $\bar{\lambda}$, mm	116.8	93.8	84.2	75.0	65.7	57.6
s^2, (λ), mm^2	1.4	0.6	1.4	1.1	1.4	1.2
Aver. Phase Diff., $\overline{\Delta\psi}$, mm	3.3	3.4	3.6	4.5	4.2	3.8
$s^2(\Delta\psi)$, mm^2	1.4	1.2	1.0	1.0	0.8	1.4
Aver. Distance Between Probes, $\overline{\Delta X}$, mm	5.79	5.79	5.79	5.79	5.79	5.79
$s^2(\Delta x)$, mm^2	0.06	0.06	0.06	0.06	0.06	0.06
$\overline{\Delta\phi}$, sec	0.66	0.68	0.72	0.90	0.84	0.76
$\bar{f}$, cps	0.043	0.053	0.059	0.067	0.076	0.087
$\bar{\alpha}$, mm^2/sec	143	109	87	49	50	53
$S(\alpha)$, mm^2/sec	±83	±71	±49	±22	±29	±33
$[S(\alpha)/\bar{\alpha}]100$	±58%	±65%	±56%	±45%	±58%	±62%
$[S(\lambda)/\bar{\lambda}]100$	±1.0%	±0.8%	±1.4%	±1.4%	±1.8%	±1.9%
$[S(\Delta x)/\overline{\Delta x}]100$	±4%	±4%	±4%	±4%	±4%	±4%
$[S(\Delta\psi)/\overline{\Delta\psi}]100$	±36%	±32%	±28%	±22%	±21%	±31%
$(\bar{\alpha}_{exper.} - 21)x100/21$	+581%	+419%	+314%	+133%	+138%	+152%
Was Inner Cell Present	Yes	Yes	Yes	Yes	Yes	Yes
Filter Type	LOW PASS ALLISON LC FILTER					
Preamplifier Type	ANALOG COMPUTER					
Recorder Type	BRUSH MARK II					

FIGURE 9 - AMPLIFIED, FILTERED THERMOCOUPLE OUTPUT AT 0.077 cps

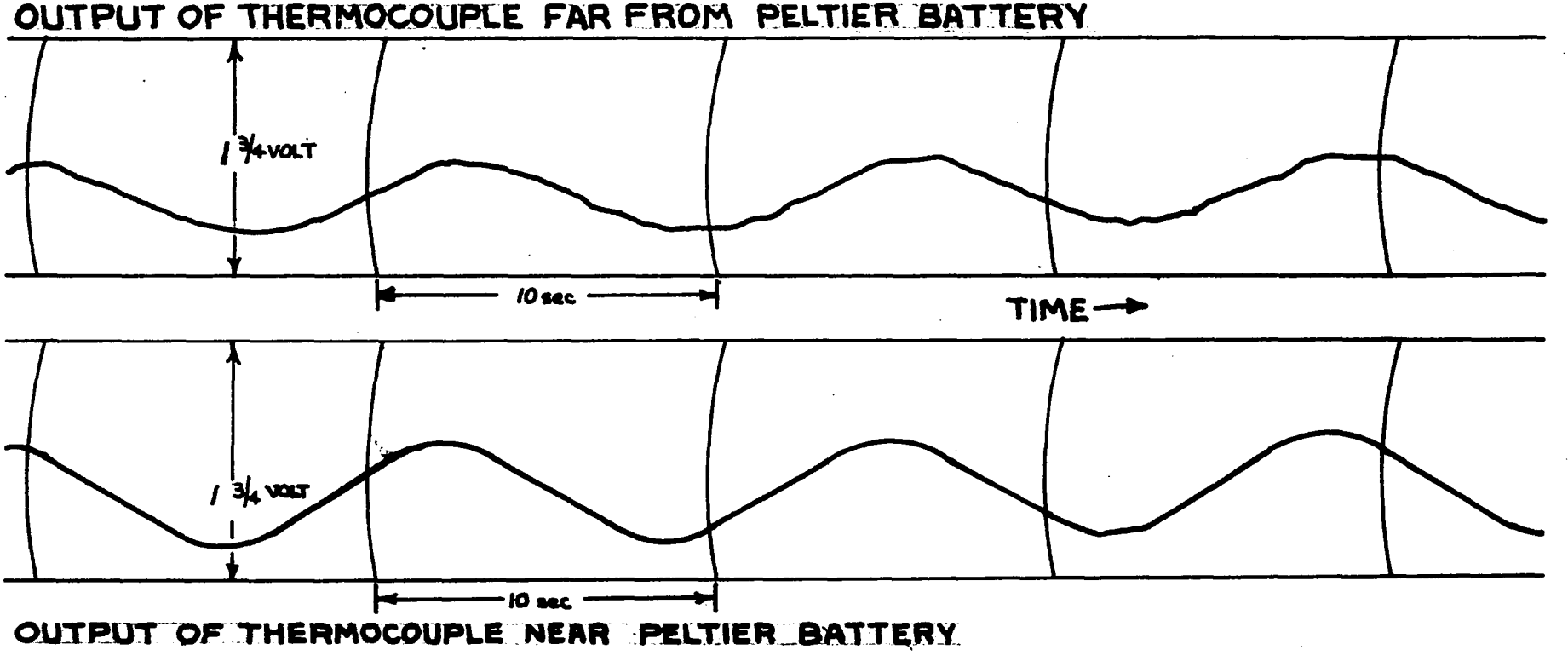

AMG 4/68

FIGURE 10 - AMPLIFIED, FILTERED THERMOCOUPLE OUTPUT AT 0.102 cps

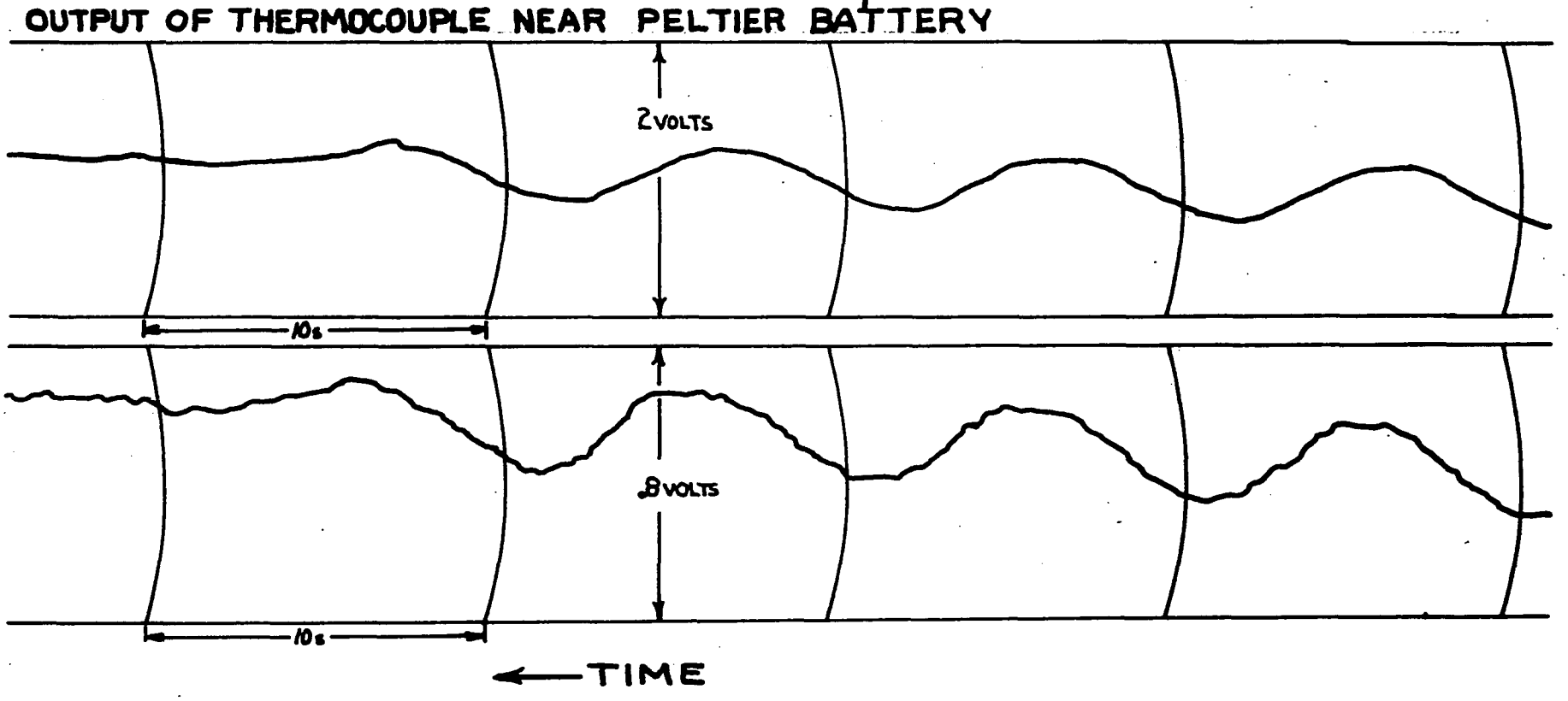

AMG 4/68

For a typical determination:

$$\frac{S^2(\lambda)}{(\bar{\lambda})^2} = .103\text{x}10^{-3},\quad 4\frac{S^2(\Delta x)}{(\overline{\Delta x})^2} = 7.15\text{x}10^{-3},\quad 4\frac{S^2(\Delta\psi)}{(\overline{\Delta\psi})^2} = 515.\text{x}10^{-3}$$

Hence, the major contribution to the overall imprecision is the uncertainty in the mean phase difference. Examination of a typical recording (figures 9, 10) shows the extrema to be poorly defined with the waves exhibiting both low frequency noise and drift. The difficulty in locating the extrema can be readily seen. Hence any attempt to improve the precision of the data must start with an upgrading of the thermocouple waves. These attempts will be outlined later.

Of greater concern, however, is the gross inaccuracy of the $\bar{\alpha}$ values. The accepted value for the thermal diffusivity of air at ambient conditions is approximately 21 mm^2/sec. Thus the experimental values of $\bar{\alpha}$ differ from those presented in the literature by + 133% to + 581%. It is possible to postulate many different reasons for this difficulty. A number of these will be discussed later.

B. Group II - Thermal Diffusivity Determinations With Improved Apparatus

The aim in performing the ten experiments which constitute Group II was to improve the accuracy and precision of the $\bar{\alpha}$ values by certain major modifications in the experimental apparatus. These data points are shown in Table 2. Each of these changes will now be discussed.

As previously mentioned, the major contribution to the imprecision of the thermal diffusivity values was the poor quality of the thermocouple output recordings. This condition made location of the extrema difficult, and manifested itself in large values of $(S(\Delta\psi)/\overline{\Delta\psi})$. Several steps were taken to improve this situation. The amplifier network used in the Group I determinations had been wired on a TR-10 Analog computer. The circuit diagram is shown in figure 11. This amplifier exhibited serious shortcomings in the areas of noise, drift and gain. However, these undesirable features were not unexpected owing to the makeshift character of the equipment. After amplification the thermocouple voltages passed to a passive LC filter. The latter attenuated noise above 2 cps, but could do nothing about low frequency noise and drift. The amplified, filtered signal was then displayed on a Brush Mark II strip chart recorder. This instrument has two rather narrow (40 mm-wide) channels and chart speeds of 1, 5, 25 and 125 mm/sec. The poor quality of the recordings stemmed directly from the shortcomings of this electronic system (figure 9,10). Low frequency noise and drift arising in both the amplifier network and external sources could not be removed. In addition, efforts to accentuate wave extrema were limited by the gain of the amplifier and the chart width and speed of the recorder. The use of such a system to obtain Group I data was justified by the availability of the various components and the desire to evaluate the gross characteristics of the experimental apparatus.

FIGURE 11 - AMPLIFIER CIRCUIT WIRED ON TR-10 COMPUTER

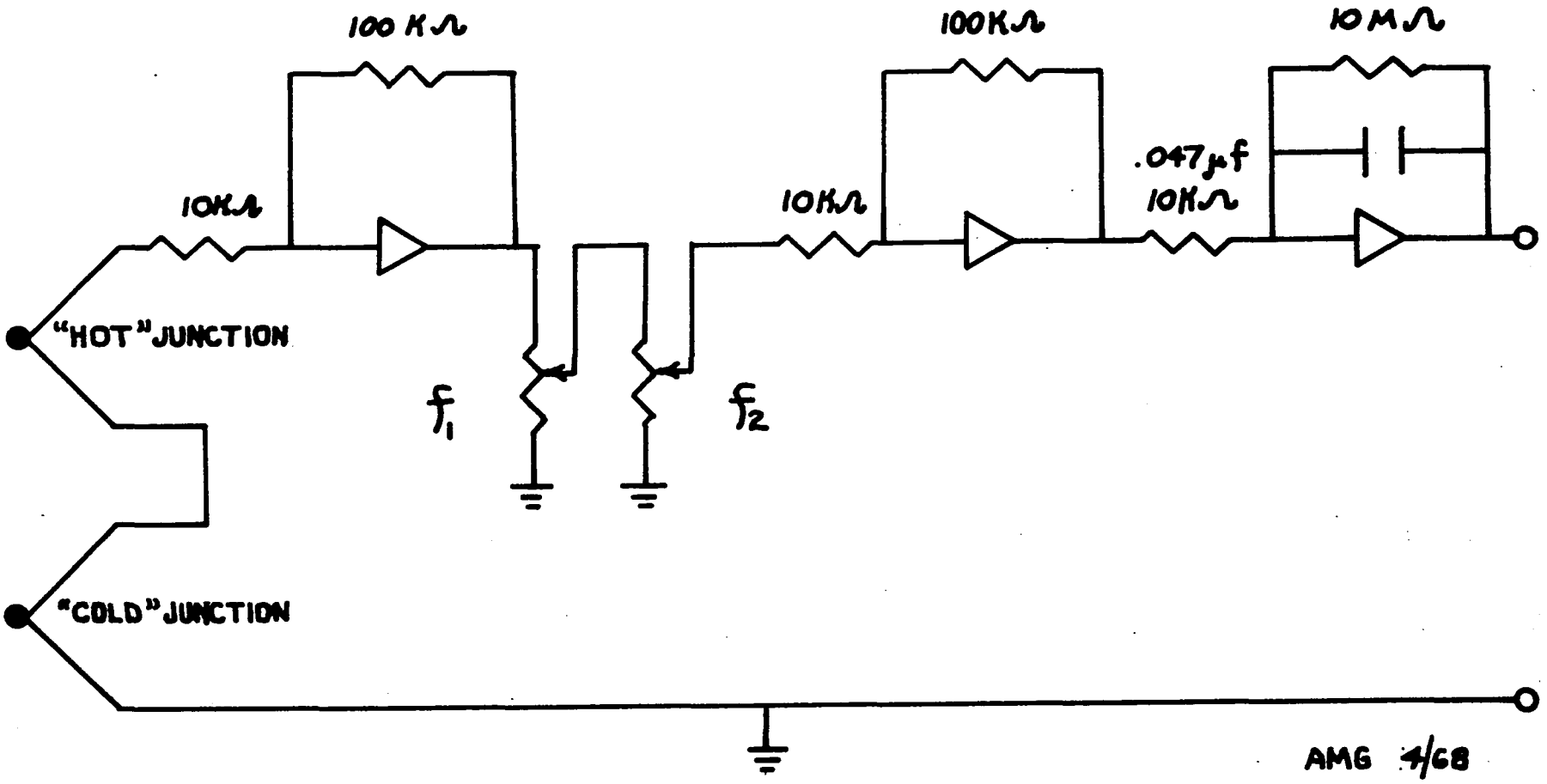

TABLE 2 - GROUP II DATA SUMMARY

RUN NUMBER	7	8	9	10	11	12	13	14	15	16
Nominal Frequency - cps	0.060	0.102	0.060	0.102	0.204	0.102	0.204	0.204	0.102	0.476
Aver. Wave Length, $\bar{\lambda}$, mm	84.1	99.8	83.5	49.1	49.8	101.4	103.1	103.4	103.4	47.0
$S^2(\lambda)$, mm^2	4.7	0.7	0.17	0.08	0.02	0.4	0.4	0.2	0.3	1.1
Aver. Phase Diff., $\Delta\psi$, mm	1.4	3.5	1.5	3.3	4.3	7.3	12.3	12.0	6.6	8.4
$S^2(\Delta\psi)$, mm^2	0.21	0.19	0.33	0.11	0.13	0.38	0.30	0.34	0.54	2.48
Aver. Distance Between probes, Δx mm	1.4	1.4	5.1	5.1	5.1	5.3	5.3	5.3	5.3	5.3
$S^2(\Delta x)$, mm^2	0.03	0.03	0.01	0.01	0.01	0.02	0.02	0.02	0.02	0.02
$\Delta\phi$, sec.	0.28	0.35	0.30	0.66	0.43	0.73	0.62	0.60	0.66	0.42
$\bar{f}$, cps	0.059	0.100	0.060	0.102	0.201	0.099	0.194	0.193	0.097	0.426
$\bar{\alpha}$, mm^2/sec	34	13	384	47	56	43	31	32	53	30
$S(\alpha)$, mm^2/sec	±24	±5	±295	±10	±10	±8	±3	±4	±12	±11
$[S(\alpha)/\bar{\alpha}]100$	±71%	±38%	±77%	±21%	±18%	±19%	±10%	±12%	±23%	±37%
$[S(\lambda)/\bar{\lambda}]100$	±2.6%	±0.8%	±0.5%	±0.6%	±0.3%	±0.6%	±0.6%	±0.4%	±0.5%	±2%
$[S(\Delta x)/\overline{\Delta X}]100$	±12%	±12%	±2%	±2%	±2%	±3%	±3%	±3%	±3%	±3%
$[S(\Delta\psi)/\overline{\Delta\psi}]100$	±33%	±12%	±38%	±10%	±8%	±8%	±4%	±5%	±11%	±19%
$(\bar{\alpha}$ exper.$-21)$ x 100/21	62%	-38%	1720%	124%	166%	105%	48%	52%	152%	43%
Was Inner Cell Present	Yes	Yes	No	No	No	No	No	No	No	No
Filter Type	RC BANDPASS								KROHN-HITE	
Preamplifier Type	BRUSH RD4215-70									
Recorder Type	BRUSH MARK 280									

The first improvement in the apparatus was the acquisition of two high gain, low noise Brush RD 4215-70 preamplifiers and a wide-channel Brush Mark 280 recorder. This step was taken after efforts to fabricate an acceptable amplifier network from commercial operational amplifiers were unsuccessful. Noise and drift emanating from the new preamplifier were low, and when the preamplifier was coupled to the recorder, a wide range of sensitivities were available. The new recorder channel width was twice the size of that for the Mark II, and many more chart speeds could be selected. It was thus possible to find combinations of chart speed and sensitivity which led to highly readable traces with more clearly defined extrema. In all aspects the new system was a significant improvement over that previously used.

The need to improve the filtering operation performed on the thermocouple voltages was also recognized. As a first step, two single-stage, passive, band-pass filters of the fixed RC type were designed and constructed (figure 12). The use of this device led to a reduction in signal drift, but its performance as concerned low-frequency noise left something to be desired. A wide frequency pass band, common with such a filter, was the difficulty. It was overcome by the acquisition of an active low-frequency band-pass filter; custom modification of the unit was required to adapt it to the specific needs of this project.

The success of these efforts to upgrade the thermocouple voltage recordings (figures 10 and 13) is shown in the values of $(S(\Delta\psi)/\overline{\Delta\psi})$ 100 in Tables 1 and 2. The Group I data exhibit an average value of $\pm$ 28% for $(S(\Delta\psi)/\overline{\Delta\psi})$ 100, with 21%

FIGURE 12 - CHARACTERISTIC FOR RC FILTER

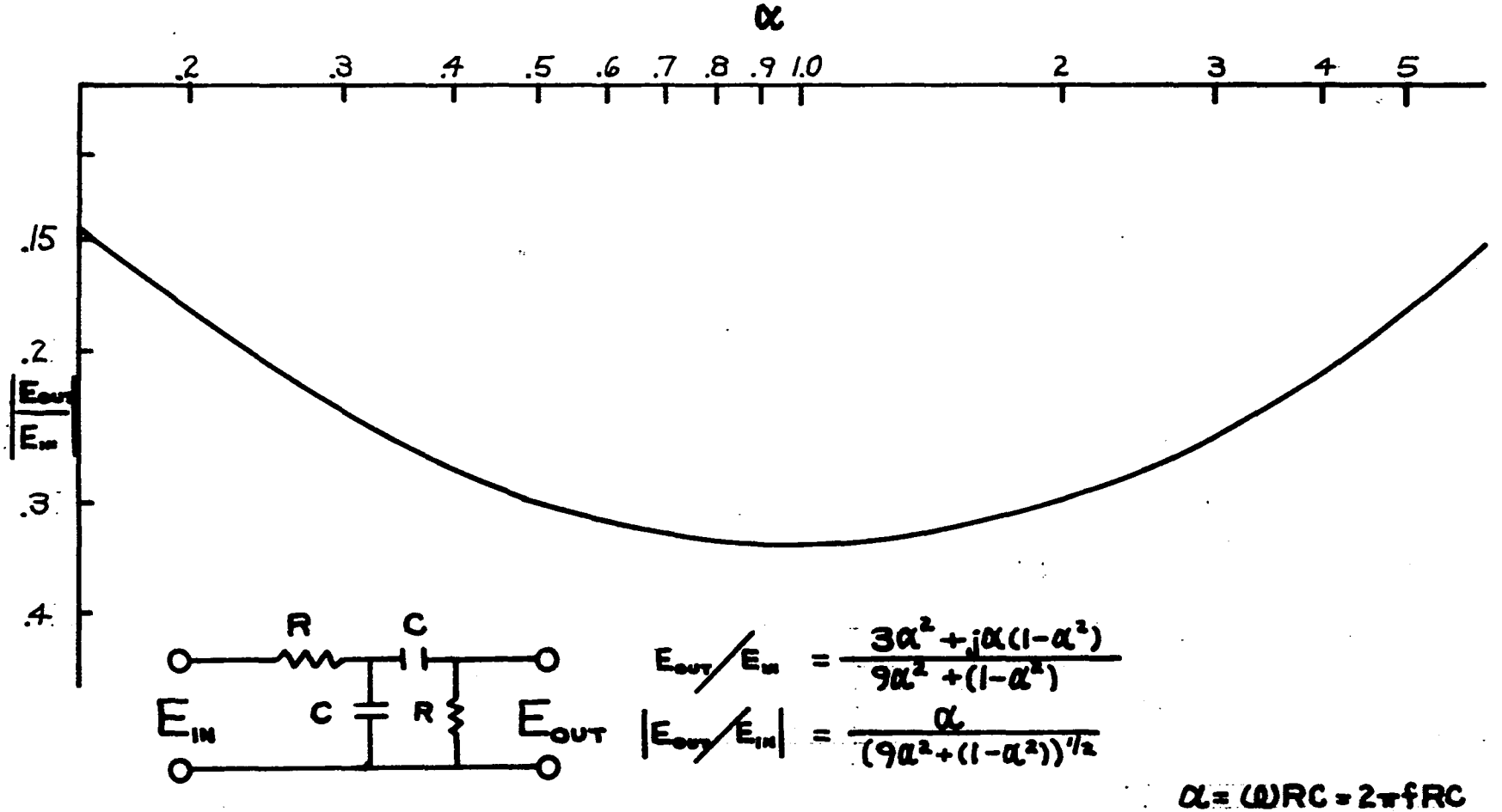

AMG 4/68

being the lowest value for the six runs. The Group II data exhibit an average value of ± 15% for this quantity, with eight of the ten runs below the ± 21% Group I minimum. It can be concluded that a meaningful improvement has been made in the ability to locate extrema and hence in the precision of the phase difference measurements.

Unfortunately, there is no straight-forward manner by which the accuracy of the phase-difference measurement can be evaluated. In general, the accuracy of a measurement technique can be verified by one of two means: use upon a known standard or use in conjunction with a technique of known accuracy upon a known or unknown value. In this instance, however, neither approach is practical. Neither calibrated phase meters nor calibrated sources of out-of-phase sinusoidal signals which operate in the required low-frequency range are commercially available. The best that can be done is an evaluation of the average phase difference caused by the electronic apparatus and a correction of the final value by this amount.

It is possible, however, to make statements about both the accuracy and precision of the distance and wavelength measurements. The distance measurements were made with a stereomicroscope for both Groups I and II, and showed consistently good precision; the average value of $(S(\Delta x)/\overline{\Delta x})$ 100 was about ± 4% for these sixteen runs. The accuracy of this technique was established by measuring the height of a number of small steps which had been cut in a brass block. The average value of the optical measurements for a given step agreed with the micrometer measurement to within about - 1%. Hence an accuracy of about - 1% is claimed for this technique.

FIGURE 13 - SAMPLE OF THERMOCOUPLE OUTPUT FOR RUN 22

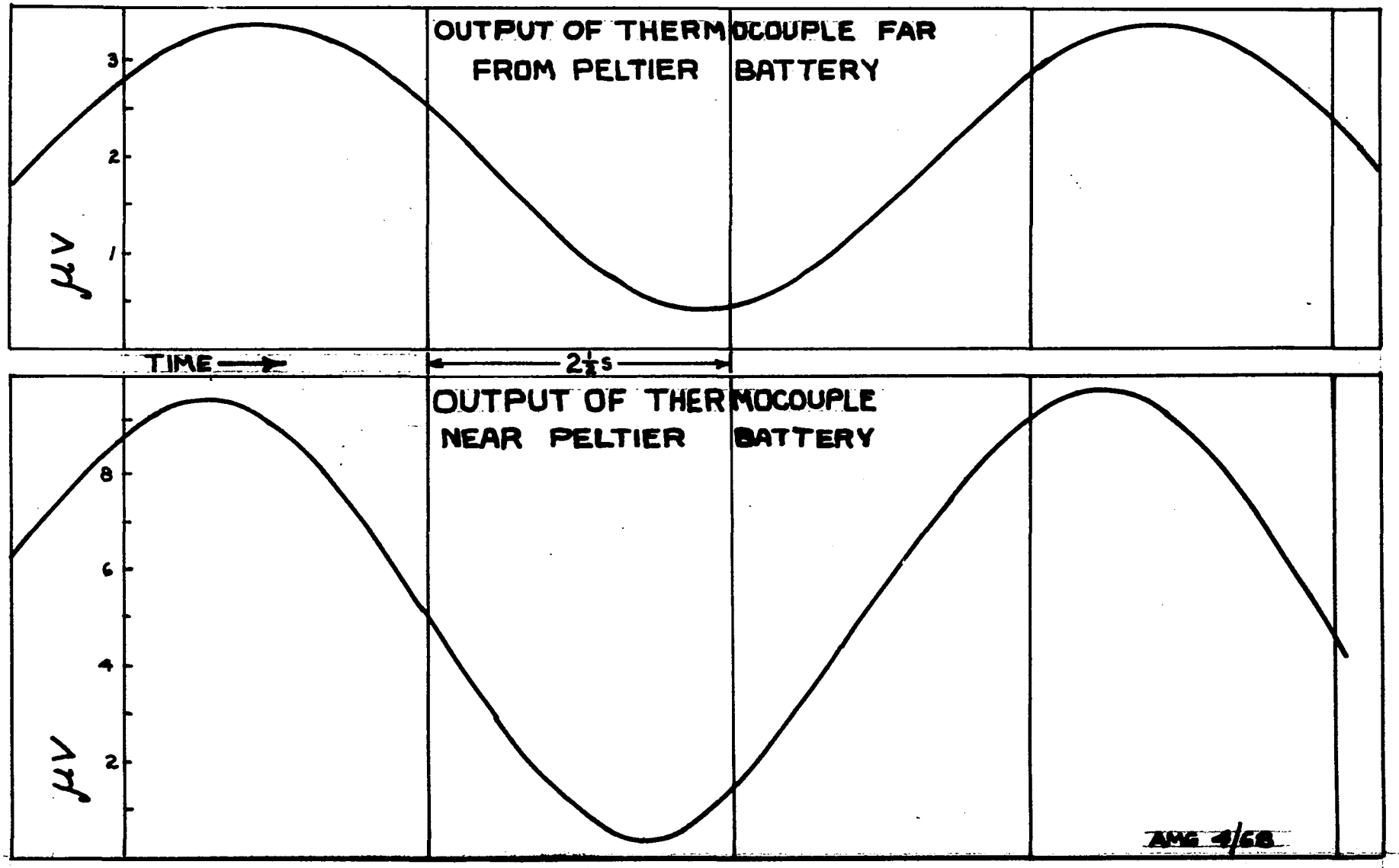

The wavelength measurements also exhibited good precision. For the sixteen runs under discussion, no value of $(S(\lambda)/\bar{\lambda})$ 100 exceeded $\pm$ 3% with the average value of this quantity being $\pm$ 1.1%. In addition, the average frequency computed from $\bar{\lambda}$ agreed with the nominal frequency, i.e., that frequency computed from knowledge of the gear ratios and motor speed of the generating device, to better than -5% for fifteen of the sixteen runs. The average value of this quantity is -2.4%, which is taken as the accuracy of this measurement.

The chart speed of the recorder, although not a measured quantity, must also be considered. For both of the recorders used in this work, the manufacturer guarantees a chart speed accuracy of ¼%.

On the basis of the preceding discussion it can be concluded that the described equipment modifications were responsible for a significant improvement in the precision of the $\bar{\alpha}$ measurements. For the six Group I determinations, the average value of $(S(\alpha)/\bar{\alpha})$ 100 was $\pm$ 57%. For the ten Group II determinations the average value of this quantity was $\pm$ 33%. It should also be mentioned that the use of this new apparatus led to an additional benefit, the ability to operate at higher frequencies than before. The smaller amplitudes associated with this high frequency level could be detected by the more sensitive electronic apparatus used in gathering the Group II data. Thus determinations at 0.1 cps and above became possible.

It was previously mentioned that the Group II experiments were also performed to gain further insight into the possible

possible causes of the gross inaccuracies in the $\bar{\alpha}$ values. On the basis of what has just been discussed, it seems probable that measurement inaccuracies are not the source of the difficulty being experienced. The estimated accuracy for both the frequency and distance measurements is quite good. Unfortunately, this quantity cannot be evaluated for the phase difference measurement. It seems unlikely, however, that this value would be off by the approximately 100% which would be required to explain the $\bar{\alpha}$ inaccuracies as due to instrument problems alone.

The modifications just discussed were aimed primarily at improving the measurement precision. Other changes were also made whose purpose was the improvement of the system's accuracy.

One of the assumptions which was made in the derivation of equation 1 was of an infinite medium in the y and z directions. It was later felt that the presence of the small cylinder within the thermal diffusivity cell might invalidate this simple, one dimensional conduction model, and hence the equation to calculate $\bar{\alpha}$. In addition, it was also possible that temperature gradients existing between the cylinder walls and the gas would give rise to convective waves. To properly examine these conditions in an analytical manner would be a formidable task. An alternate approach was to redesign the cell to allow for removal of the inner cylinder and to then perform further thermal diffusivity measurements. If no improvement in the accuracy of the data was observed, one would be able to conclude that wall effects, if they did exist, were of negligible importance.

Two other alterations were also made. A vibration damping mount designed to isolate apparatus from vibration frequencies down to 9 cps was purchased; the thermal diffusivity cell was placed on this base for all of the Group II determinations. The base was to serve as an impediment to the possible vibration of the thermocouple wires and hence to stirring of the gas in their vicinity. The second step was the construction of an insulated box which surrounded the cell and gave it some protection from environmental changes.

Examination of Tables 1 and 2 and figures 17 and 18, gives some insight into the effect of these changes. The six runs of Group I (numbers 1-6 of figure 15) and the first two runs of Group II (at 0.059 cps, run 7 and at 0.100 cps, run 8) were performed with the inner cylinder present. The last eight runs of Group II (runs 9-16 of figure 15) were performed after the inner cylinder had been removed. Only at one frequency (0.060 cps) are there values for both situations (runs 3,7, and 9), a consequence of the different capabilities of the electronic apparatus used in the Group I and II determinations. The seven data points from 0.067 cps to 0.102 cps inclusive are the most informative (figure 15). Of this collection of points, four were for the case of the inner cylinder present (numbers 4,5,6,8) and the other three for the case of the inner cylinder removed (numbers 10,12,15). For the first group (inner cylinder present), the mean value of $\bar{\alpha}$ was 41 mm^2/sec; for the second group (inner cylinder removed), the value of this quantity was 48 mm^2/sec. The first value exhibits a +95% error, whereas the second value exceeds the accepted level by 129%. It is thus impossible

FIGURE 14 - THERMAL DIFFUSIVITY AS A FUNCTION OF OPERATING FREQUENCY - GROUP II VALUES

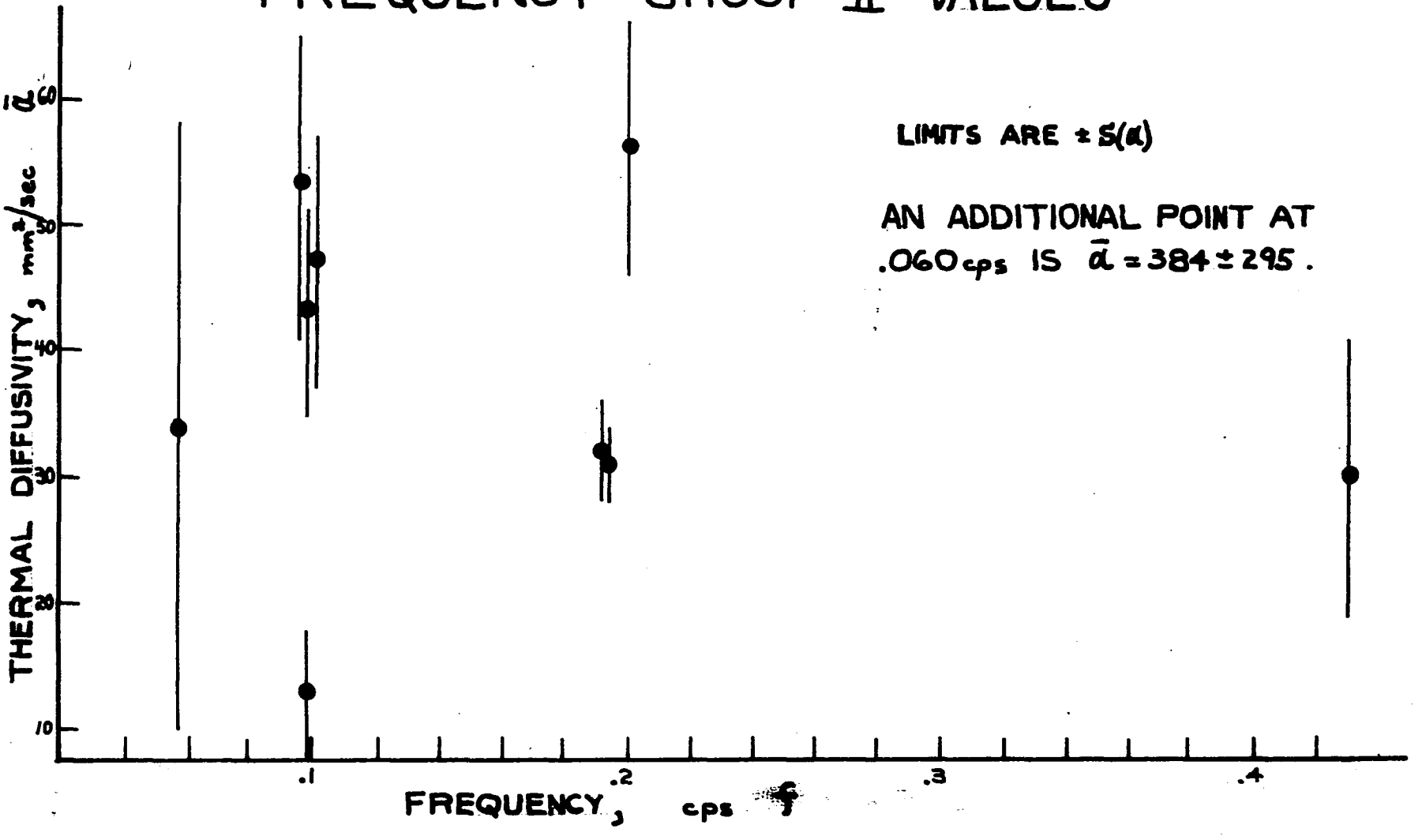

FIGURE 15-THERMAL DIFFUSIVITY AS A FUNCTION OF OPERATING FREQUENCY - GROUPS I, II

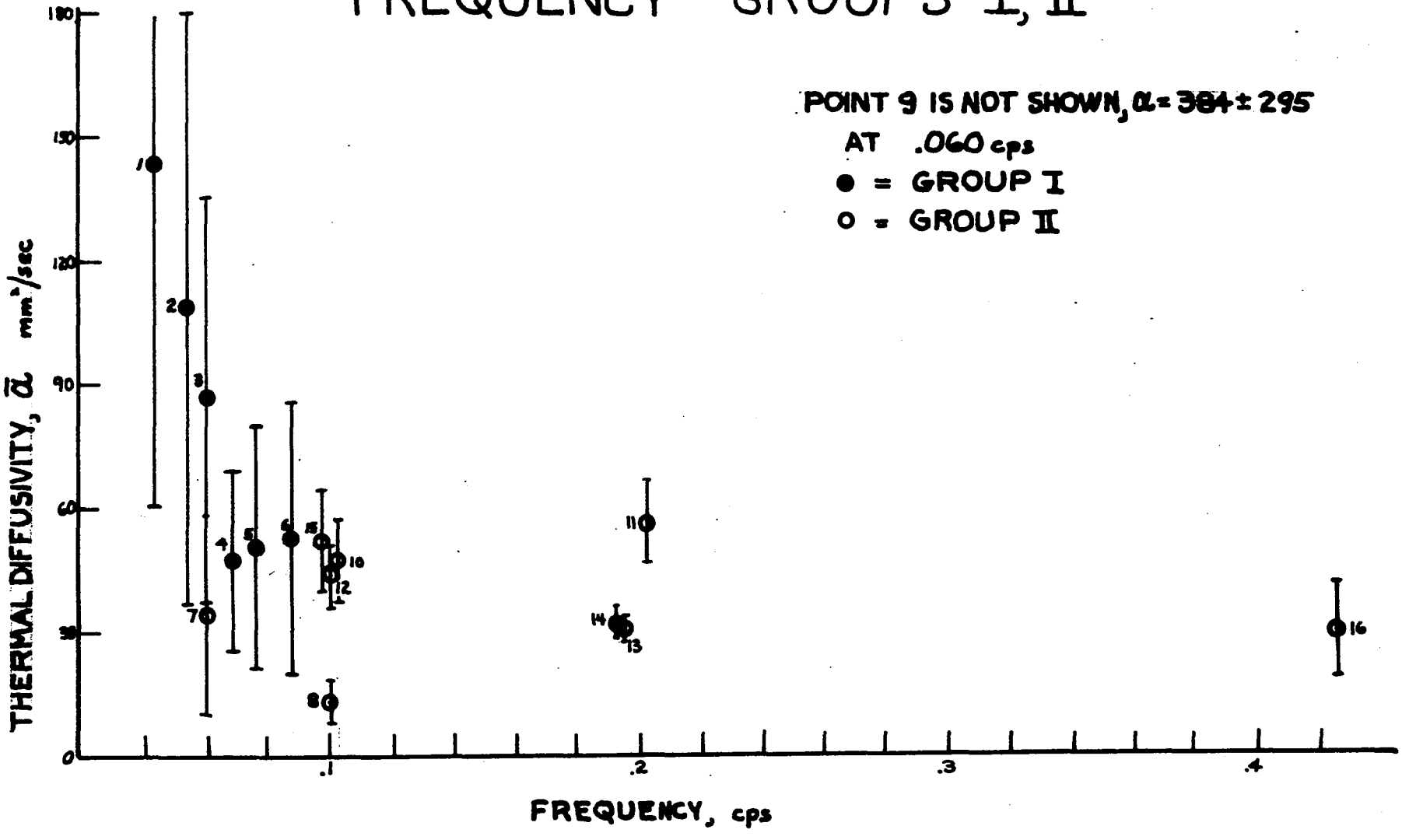

to attribute any beneficial effect to the removal of the inner cylinder on the basis of this data. Indeed it is apparent that these seven $\bar{\alpha}$ data points are indistinguishable from one another within the range of present precision, and that none of the described apparatus changes caused an improvement in the accuracy of the data.

C. Qualitative Study of Turbulent Convection

The preceding experiments had not diminished the possibility that convective flow was occurring within the cell. Indeed the elimination of other possible factors after their proper consideration gave some support to the convection hypothesis. A study was undertaken to examine this phenomenon more closely. The investigation utilized the thermal diffusivity cell in its original, two-cylinder configuration, and was composed of six separate experiments. In each experiment the output of a single thermocouple probe was examined. The signal was properly conditioned so that both the complete wave and its magnified oscillatory component could be displayed simultaneously on a two-channel strip chart recorder. In four of these experiments the aim was to determine the effect of a non-oscillatory temperature difference on the thermocouple output. To generate such an exciting function, a constant electrical current was supplied to the Peltier battery; the polarity was adjusted so as to cause net heating in two runs and net cooling in two runs. The thermocouples exhibited strikingly similar responses in each instance (figure 16). A short time after power was applied to the Peltier battery the thermocouple voltage signal began to deviate from the initial level in an almost linear manner. During this

FIGURE 16-ONSET OF OSCILLATIONS WITH HEATING

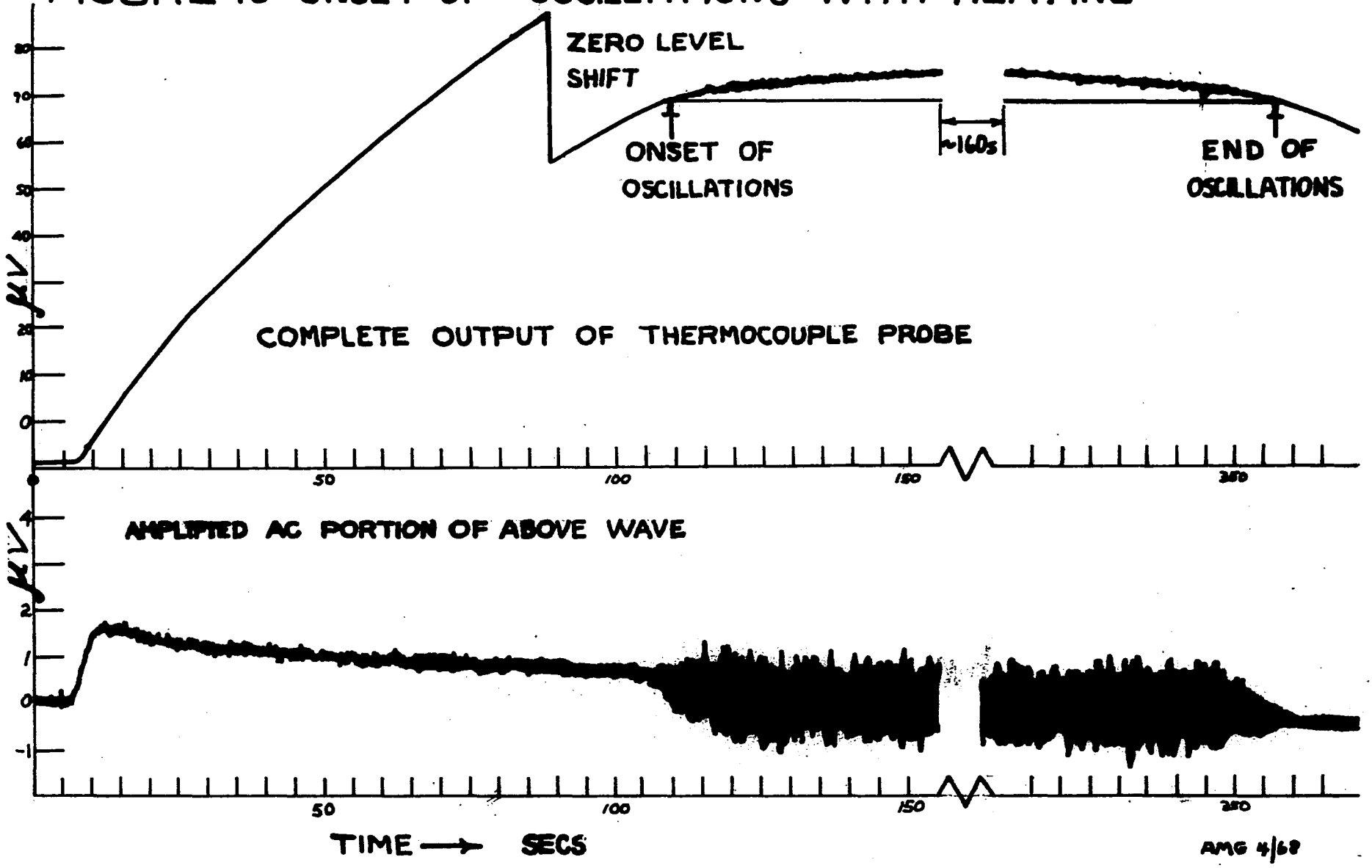

period, however, the AC component exhibited only slight change and was little different from the output before the application of power to the Peltier battery. Within a short time, however, significant changes became apparent. Once the complete wave had passed a given voltage level, a sudden decrease in the slope of the curve was observed. Indeed the output seemed to be approaching some steady value. In addition, a pronounced oscillatory component, similar to electrical noise in appearance, was evident at about the same time. These conditions persisted even after the Peltier battery current had ceased. However, once the complete wave had passed below the level at which these two phenomena had begun, marked changes were again apparent. The noise-like oscillatory component vanished at this time and the output again exhibited a sudden change in slope. Examination of the magnified oscillatory component showed its amplitude, during the period of interest, to be three to four times greater than that of the background noise. This amplitude ratio is but an estimate, however, because of the necessary presence of a low-pass filter set at 16 cps. Its use also makes a discussion of the signal's frequency spectrum meaningless.

As previously mentioned, this interesting behavior occurred for all four experiments in which a constant voltage difference was impressed upon the Peltier battery. Indeed the excess thermocouple voltage level at which these changes begin and end is approximately the same for each of these runs, and is estimated to be equivalent to about 2-3 C^{o}.

In the last two experiments of this series, square-wave voltages of various amplitudes were impressed on the

Peltier battery, As before, the output of one thermocouple probe was monitored; both the complete wave and the magnified AC component were recorded. At low power levels the thermocouple voltage exhibited an oscillatory component of the expected sinusoidal type which was superimposed upon a mean level. The output rose from the initial value and in a short time attained a quasi-steady state condition in which the wave oscillated about a constant value. However, at higher power levels, this quasi-steady state was not reached. The sinusoidal component, although initially of proper shape, became badly distorted when the thermocouple output exceeded a given level. Examination of the magnified AC component revealed the presence of high-frequency noise similar to that previously detected for constant heating or cooling. Indeed the voltage level (temperature excess) at which the distortion began corresponded closely to the levels previously observed. A short time after the onset of this distortion the entire sinusoidal component was obliterated, with the output then composed almost completely of high frequency noise (figure 17).

D. Group III - Thermal Diffusivity Determinations as a Function of Frequency and Temperature Amplitude

The aim of the last principal piece of experimental work was to investigate the suspected convective heat flow in a quantitative manner. The usual approach in free convection studies is to correlate results in terms of the Grashof and Prandtl numbers, or, alternatively, in terms of their product, the Rayleigh number. Indeed a Rayleigh number

FIGURE 17-ONSET OF OSCILLATIONS WITH CYCLING

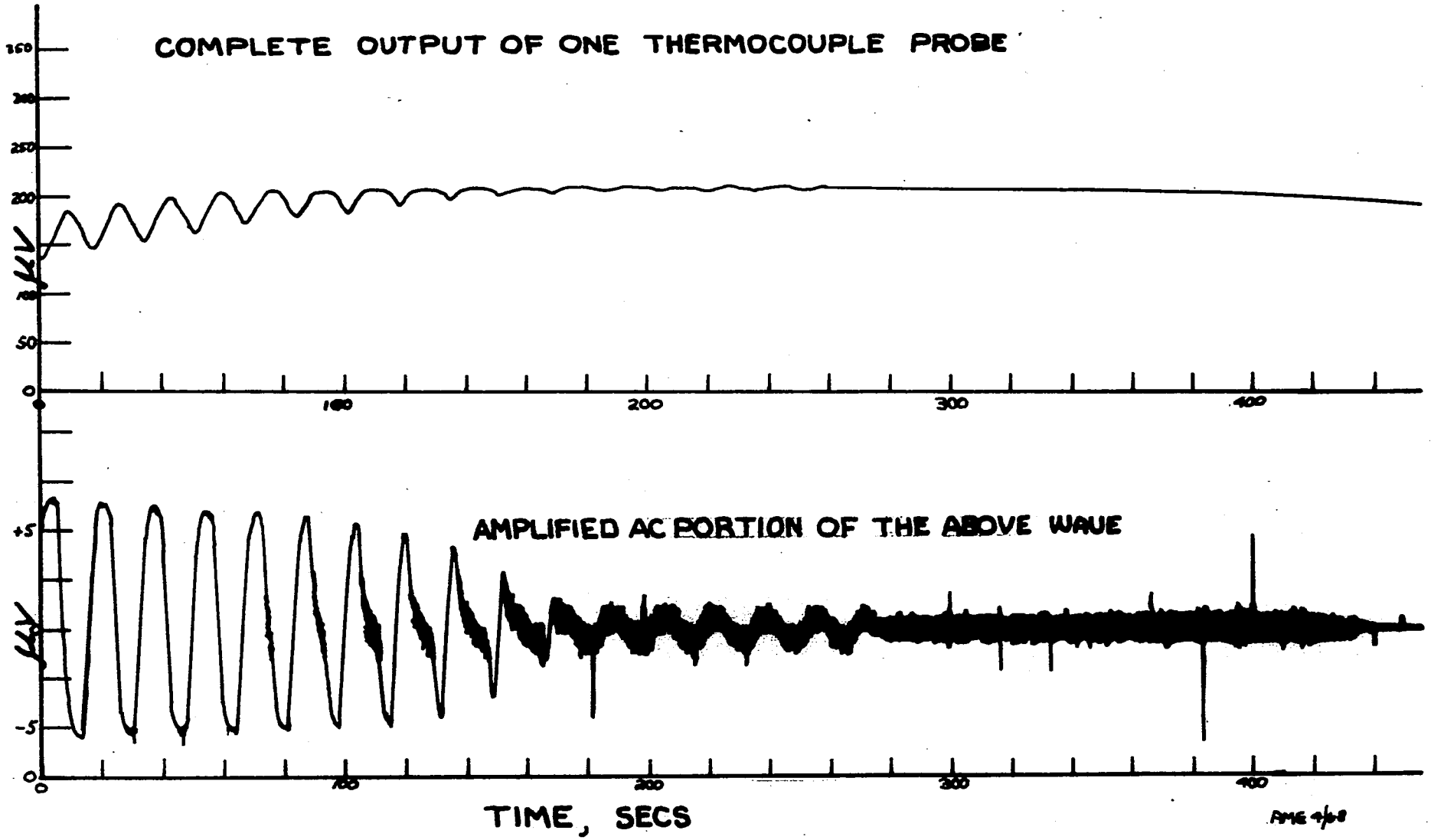

criterion for the onset of convective instability has been presented in the literature for a number of different geometries. However, the quest for such a stability criterion by analytical means would be a formidable task for the system used here. Hence the experimental approach was necessary.

It will be shown later that the operating frequency f and the temperature amplitude at the Peltier battery surface T_o are the significant parameters in such a correlation for a single gas at a given temperature and pressure. The experimental values of the mean thermal diffusivity which had already been determined could not be correlated in this manner because of the use of uncalibrated thermocouple probes, and hence the absence of T_o data. To overcome this difficulty a copper-constantan differential thermocouple was calibrated so as to accurately sense small temperature differences (Appendix K). The output of the thermocouple passed through a network composed of a preamplifier, and a low-pass LC filter; it was recorded on the two-channel Mark 280 recorder. The calibration procedure used here allowed for calibration of the entire system.

One junction of the thermocouple was then placed in a channel which had been cut in the surface of the Peltier battery which faces the test gas. The second junction was located in the bulk gas, far from the Peltier battery. Thermal diffusivity measurements were then made, but with one exception. After a number of cycles had passed, the output of the calibrated surface thermocouple was recorded for a short time. Then the two "fork-like" probes were connected

FIGURE 18 - THERMAL DIFFUSIVITY $\bar{\alpha}$ AS A FUNCTION OF TEMPERATURE AMPLITUDE AT PELTIER BATTERY WALL T_o - GROUP III

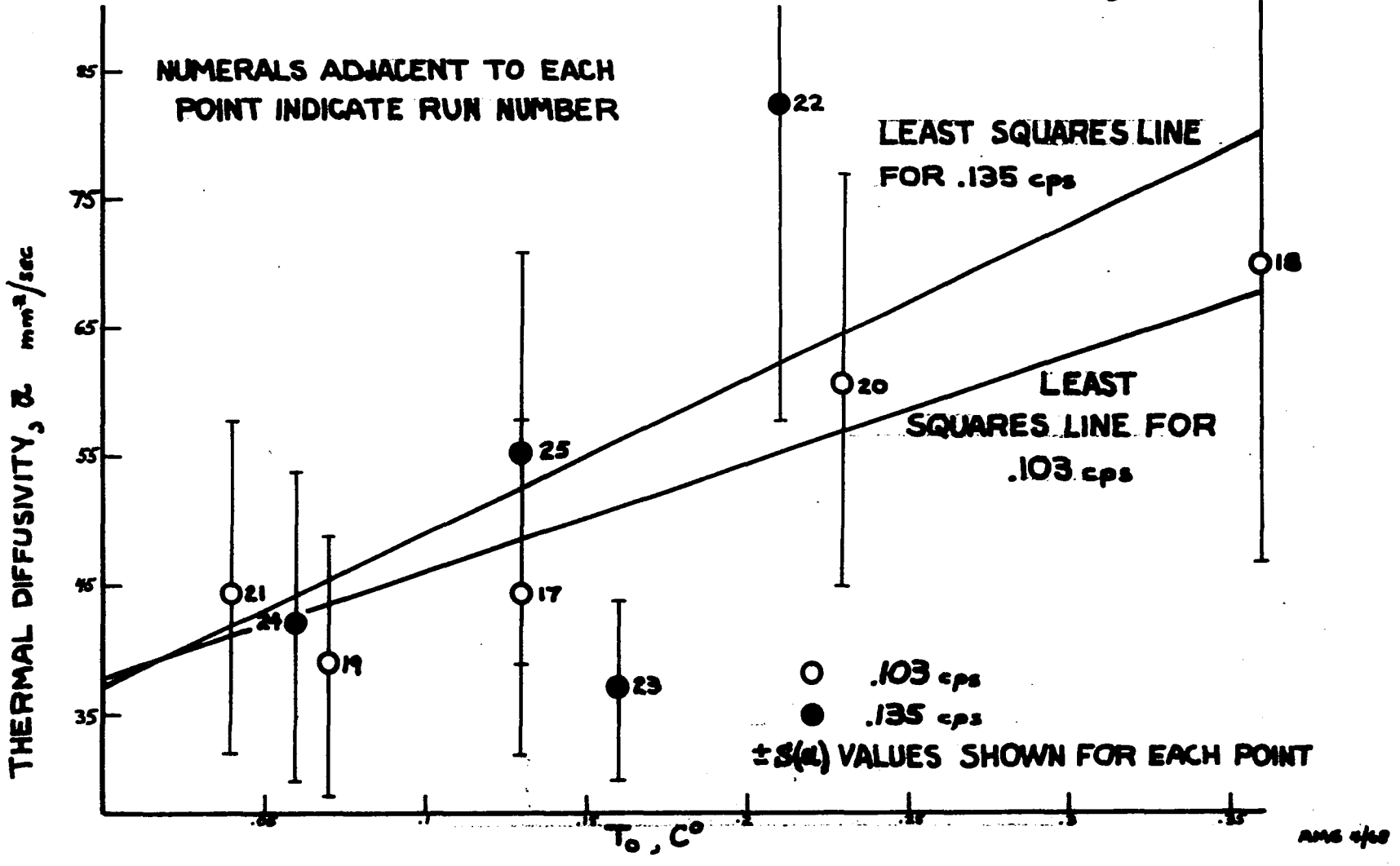

TABLE 3 - GROUP III DATA SUMMARY

RUN NUMBER	17	18	19	20	21	22	23	24	25
Nominal Frequency, cps	0.102	0.102	0.102	0.102	0.102	0.134	0.134	0.134	0.134
Aver. Wavelength $\bar{\lambda}$, mm	97.5	97.2	97.3	97.2	97.3	148.5	147.7	148.6	148.1
$S^2(\lambda)$, mm^2	0.9	0.3	0.7	0.2	0.5	0.7	1.1	1.8	1.6
Aver. Phase Diff. $\overline{\Delta\psi}$, mm	7.0	5.6	7.5	6.0	7.0	9.0	13.3	12.6	11.1
$S^2(\Delta\psi)$, mm^2	1.02	0.84	0.81	0.62	1.00	1.73	1.31	3.15	2.67
Aver. Distance Between Probes $\overline{\Delta X}$, mm	5.3	5.3	5.3	5.3	5.3	5.3	5.3	5.3	5.3
$S^2(\Delta X)$, mm^2	0.02	0.02	0.02	0.02	0.02	0.02	0.02	0.02	0.02
$\overline{\Delta\emptyset}$, sec.	0.70	0.56	0.75	0.60	0.70	0.45	0.67	0.63	0.55
$\bar{f}$, cps	0.103	0.103	0.103	0.103	0.103	0.135	0.135	0.135	0.135
$\bar{\alpha}$, mm^2/sec	45	70	39	61	45	83	37	42	55
$S(\alpha)$, mm^2/sec	±13	±23	±10	±16	±13	±25	±7	±12	±16
$[S(\alpha)/\bar{\alpha}]100$	±29%	±33%	±25%	±27%	±29%	±30%	±18%	±29%	±30%
$[S(\lambda)/\bar{\lambda}]100$	±1.0%	±0.6%	±0.9%	±0.5%	±0.7%	±0.6%	±0.7%	±0.9%	±0.9%
$[S(\Delta X)/\overline{\Delta X}]100$	±3%	±3%	±3%	±3%	±3%	±3%	±3%	±3%	±3%
$[S(\Delta\psi)/\overline{\Delta\psi}]100$	±14%	±16%	±12%	±13%	±14%	±15%	±9%	±14%	±15%
$(\alpha_{exper.}-21)x100/21$	114%	233%	86%	190%	114%	295%	76%	100%	162%
Was Inner Cell Present	No	No	No	No	No	No	No	No	No
Filter Type	KROHN-HITE ACTIVE BAND PASS								
Preamplifier Type	BRUSH RD-4215-70								
Recorder Type	BRUSH MARK 280								

to the electrical circuitry and the usual waves were recorded. Values of $\bar{\alpha}$ and of T_o, the amplitude of the wave at the Peltier battery surface, were obtained from these experiments, which are designated "Group III".

The $\bar{\alpha}$ data obtained in this series of experiments are presented in figure 18 and Table 3. It is not unexpected that these new data points exhibit approximately the same accuracy and precision as the data of Group II, for no effort was made to improve either of these factors. For the nine runs which constitute Group III, the average value of $(S(\alpha)/\bar{\alpha})$ 100 was $\pm$28%; the average departure from the accepted value was +153%.

DISCUSSION

For twenty-four of the twenty-five thermal diffusivity determinations reported in the preceding section, the discrepancy between the experimental value and the accepted value ranged from +43% to +1720% with a median value of +135%. The purpose of this discussion is to examine possible causes of this inaccuracy.

1. Impurities - The experimental data was compared to the accepted value of 21 mm^2/sec for the thermal diffusivity of pure air at ambient conditions. However, the fluid used as the test medium was air contaminated by additional quantities of water vapor and CO_2. It can be shown (Appendix E) that failure to account for these substances does not significantly affect the value of α which is being used as the standard for this work. Indeed for the extreme case of air saturated with water vapor and containing one mole percent of CO_2, the calculated value of α differs by only 0.5% from that for dry air with the normal CO_2 composition.

It was conjectured that the thermocouple probes were contributing in a number of possible ways to the observed discrepancies. Each of these claims will be considered in turn.

2. Thermocouple Time Constants - The fine thermocouple wires (0.001") used in this work were chosen so that the probes would be sensitive to the low-frequency temperature oscillations of the fluid. The calculated time constant of the thermocouple junction was shown to be at least

two orders of magnitude smaller than the period of the oscillations generated by the Peltier battery (Appendix B). Thus one can conclude that thermocouple response time was not a problem.

3. Thermocouple Interference - The thermocouple probes were designed so that both junctions were located within the cell. The aim was to keep them at the same mean temperature so as to minimize the D.C. output of the probe. However, had both junctions been exposed to the temperature oscillations, the output of each probe would have been the sum of two voltages, each of different amplitude and phase. Under such circumstances it would not have been possible to obtain meaningful values of $\Delta \psi$. Therefore an effort was made to locate the "cold" junction far from the Peltier battery to take advantage of the exponential decay of the temperature wave. A calculation substantiated this tactic, for it showed that the wave was of negligible amplitude at the "cold" junction (Appendix C). Hence the recorded oscillations could be used to determine phase differences.

However, this exponential decay of the temperature wave could give rise to a complication. In order for them to sense the rapidly decreasing temperature oscillations, the probes must be positioned close to the Peltier battery surface, and hence near to one another. The possibility exists, therefore, that each probe would affect the other's output. This problem is amenable to analysis if one considers the following simple model: at time $t = 0$, a perfectly conducting cylinder of radius $r = a$ and temperature T_1 is placed in perfect thermal contact with a poorly conducting semi-infinite medium whose

temperature is zero. Carslaw and Jaeger (6; p. 341-2) give the temperature distribution, T, for the region $r \geq a$. In modified form, it is:

$$T/T_1 = (2/\pi) \int_0^\infty e^{-\tau u^2} \frac{(J_o(ru/a)\ \phi - Y_o(ru/a)\ \psi)}{\phi^2 + \psi^2} du \qquad (6)$$

where: $\phi = uY_o(u) - \eta Y_1(u)$

$\psi = uJ_o(u) - \eta J_1(u)$

$\tau = \alpha t/a^2$

$\eta = 2 \pi a^2 \rho c/S$

S = heat capacity per unit length for cylinder

ρ = density of the semi-infinite medium

c = heat capacity of the semi-infinite medium

Values of T/T_1 as a function of dimensionless time τ and dimensionless position r/a have been published (18), but only for the case $\eta = 2$. These numerical results are not applicable to the thermocouple problem, for here $\eta = .0007$. Thus it is necessary to evaluate the above expression by a numerical integration scheme (Appendix D).

Results of a general nature are shown in figure 19. Of greater relevance to the present problem is figure 20, which presents the temperature distribution at the surface r/a = 212. It is evident from these results that the temperature at this position never exceeds two percent of the perturbation temperature T_1. In the real case, this value of r/a would correspond to the position

approximately midway between the two thermocouples. Hence it seems reasonable to conclude that the two thermocouples do not interact with one another to any significant degree. The thermocouple probes are thus rejected as the source of the large deviations noted in the experimental values of $\bar{\alpha}$.

4. Transient Response - The derivation of equation (1) by Jakob (19; p. 294) is valid for large values of time. The solution for all time, $t \geq 0$, is presented by Carslaw and Jaeger (7; p. 334) and is:

$$\frac{T-T_m}{T_o} = \exp(-\sqrt{\pi f/\alpha}\, x)\, \sin(2\pi ft - \sqrt{\pi f/\alpha}\, x) + 2f \int_o^\infty (\exp(-\rho t)\, \sin \sqrt{\rho/\alpha}\, x)/(\rho^2 + (2\pi f)^2)\, d\rho \quad (7)$$

The term on the far right in equation (7) is the transient portion of the solution. This integral was evaluated numerically (using a digital computer). The results for one set of typical conditions are shown in figure 21. They illustrate the fact that after the passage of only a few periods, the transient portion of the distribution is negligible when compared to the quasi-steady term. Hence equation (4) would be invalid for only the first few periods; they were omitted when computing $\bar{\lambda}$ and $\overline{\Delta \psi}$. One can conclude therefore that omission of the transient term does not lead to the large positive errors which have been observed.

Two other possible sources of difficulty involve the nature of the thermocouple voltage recordings and the manner in which they are used.

FIGURE 19 - TEMPERATURE DISTRIBUTION IN AN IMPERFECT CONDUCTOR ($r>a$) SURROUNDING A PERFECTLY CONDUCTING CYLINDER ($r=a$) FOR THE CASE $T(r\leq a, t=0) = T_i$

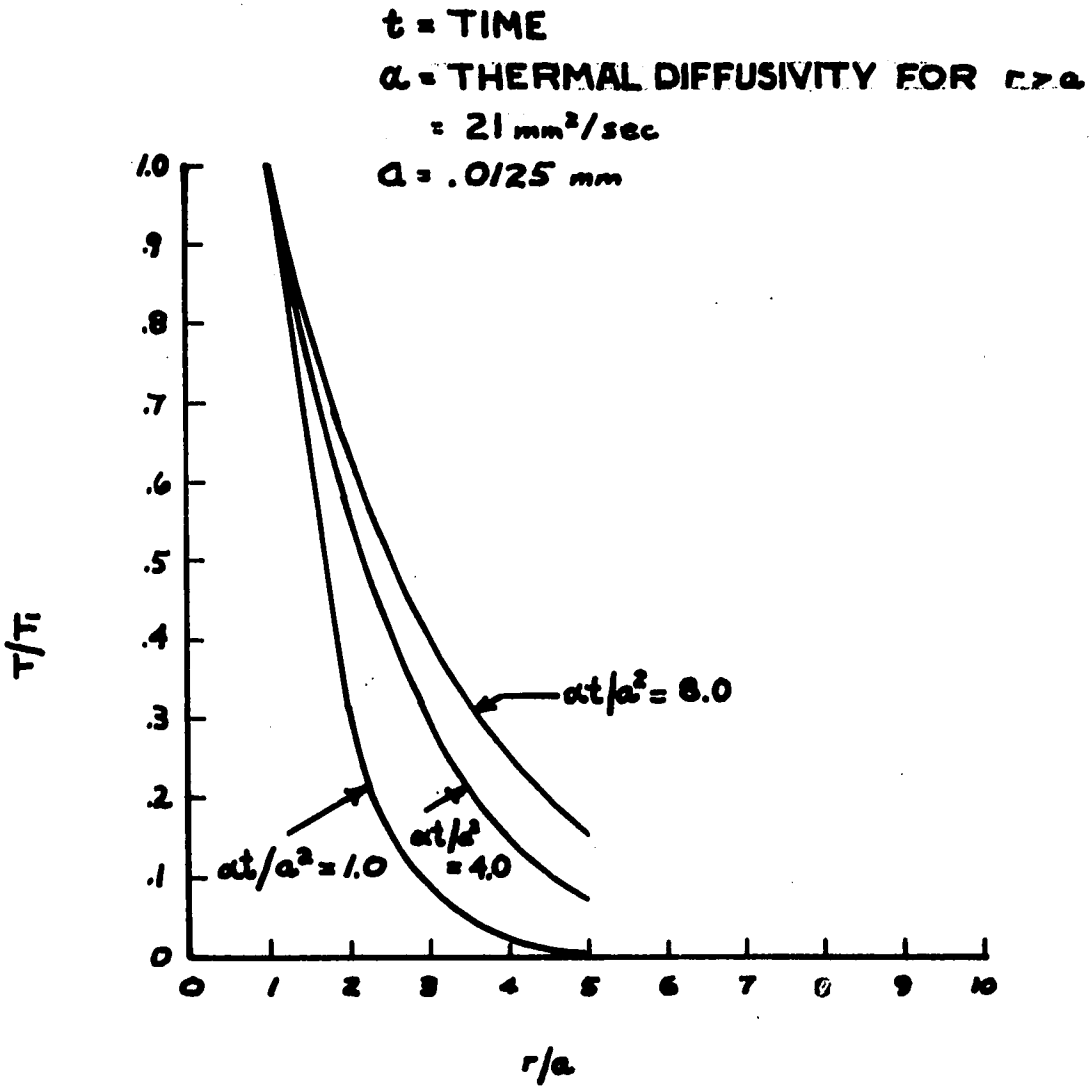

FIGURE 20-TEMPERATURE DISTRIBUTION IN AN IMPERFECT CONDUCTOR AT $\frac{r}{a}=212$ SURROUNDING A PERFECTLY CONDUCTING CYLINDER ($r=a=.0125$ mm) FOR THE CASE $T(r \leq a, t=0)=T_1$

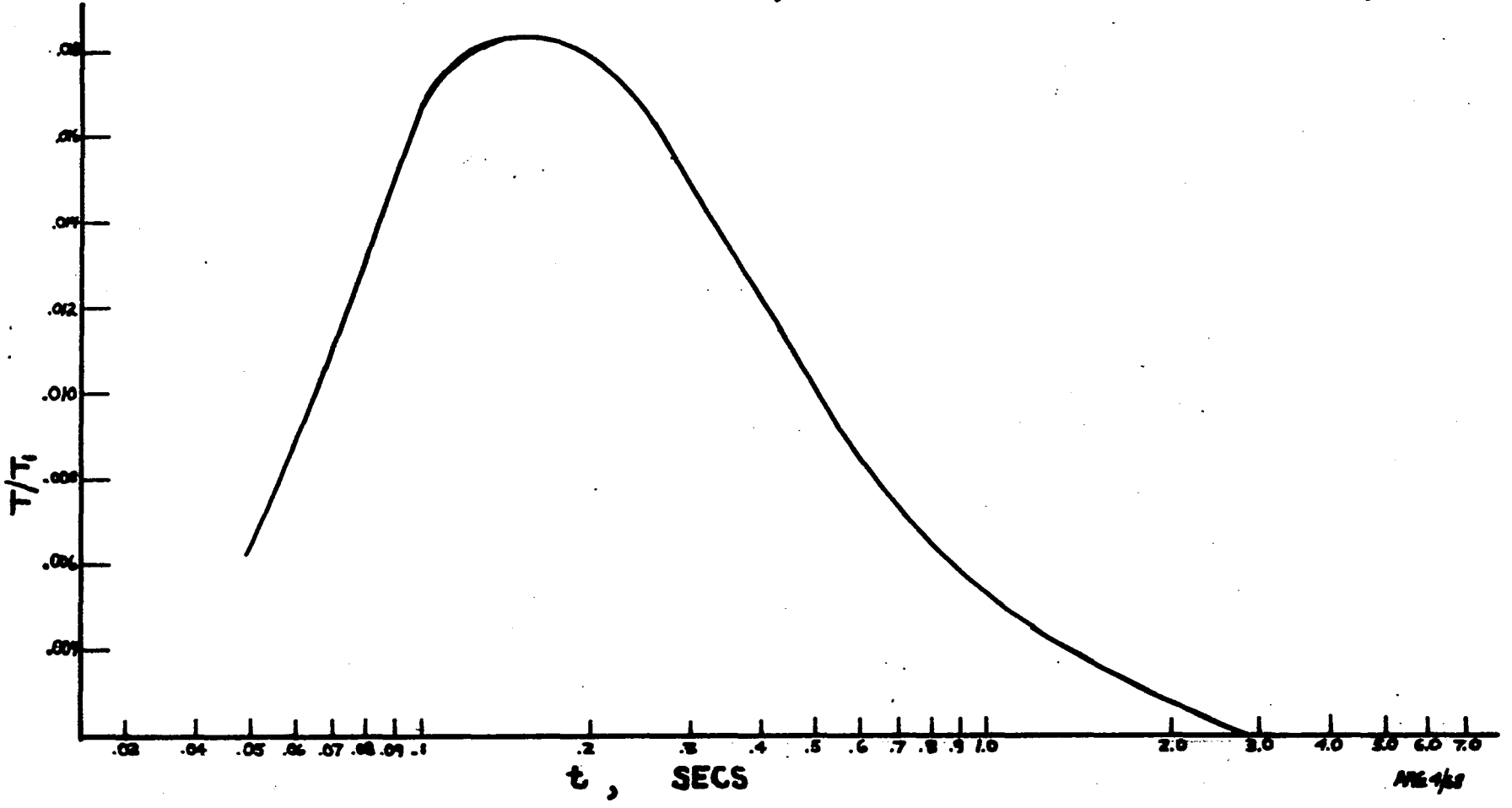

FIGURE 21- SOLUTION TO THE UNSTEADY CONDUCTION PROBLEM FOR $t \geq 0$

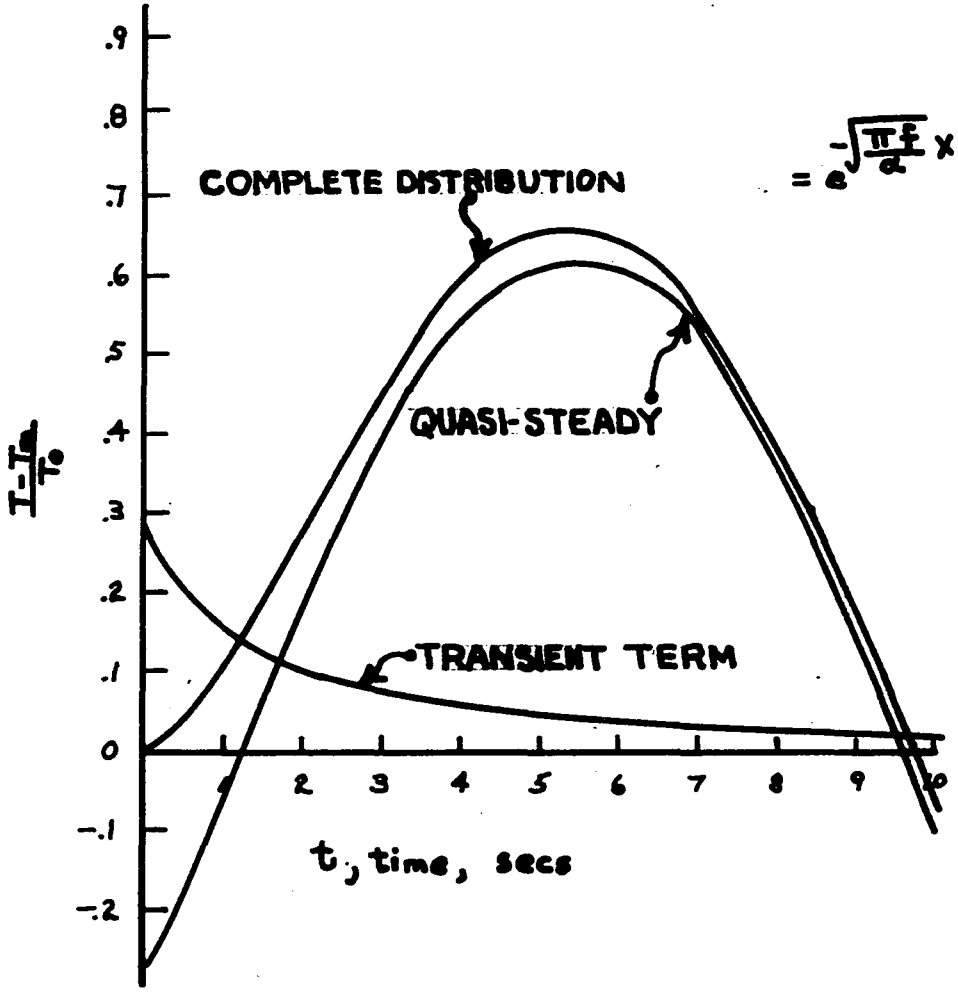

$$= e^{-\sqrt{\frac{\pi f}{\alpha}}x} \sin\left(2\pi f t - \sqrt{\frac{\pi f}{\alpha}}x\right) +$$

$$2f\int_0^\infty \frac{e^{-\rho t}\sin\sqrt{\rho/\alpha}\,x}{\rho^2+(2\pi f)^2}\,d\rho = \frac{T-T_\infty}{T_0}$$

$\alpha = 21\ mm^2/sec$

$f = .060\ cps$

$X = 5\ mm$

Ans: 4/5

5. HARMONICS -

These recordings appear to be sinusoidal in nature when subjected to visual inspection. However, a Fourier analysis was not performed. It is thus possible that the wave generated by the Peltier Battery, and hence these recordings, may contain some harmonics and thus not be true sine waves of the expected frequency. A calculation was performed to estimate the effect upon $\bar{\alpha}$ of such a non-sinusoidal wave being analyzed as though it were sinusoidal, i.e., using equation (4) which was derived for a sine input. A "sawtooth" input was chosen as a "worst case" (Appendix F). It was shown that the presence of higher harmonics would tend to cause the computed value of $\bar{\alpha}$ to differ from that computed from equation (4). However, this effect would be small, even for this "worst case", about 10%, rather than the large errors whose source is being sought.

6. The $\bar{\alpha}$ Expression -

The other point concerning the thermocouple recordings also involves equation (4):

$$\bar{\alpha} = (C\,\bar{\lambda}/4\,\pi)\left(\overline{\Delta x}/\overline{\Delta \psi}\right)^2 \qquad (4)$$

It was mentioned previously that average values of λ, Δx, and $\Delta\psi$ were used in an effort to decrease relative errors. Intuitively, the grouping on the right of equation (4) was designated the "average thermal diffusivity". It was suggested, however, that this form was not a valid expression for $\bar{\alpha}$, and that the difficulties which were being encountered stemmed from its use. Statistical analysis refuted this contention. Equation (4) was shown to be a good approximation to the actual expression for the average themal diffusivity; the

use of this approximation introduced little error, about 7%. (Appendix G).

6. Vibration - The cell was placed on a vibration damping mount designed to attenuate mechanical vibrations down to 9 cps for the determinations of Group II and III. The equipment change was one of several steps taken to reduce the amplitude of the vibrations reaching the cell. The aim was to prevent the thermocouple wire, whose natural frequency has been calculated to be about 80 cps (Appendix J), from vibrating and hence mixing the fluid. It was found that use of the damping mount did not change the accuracy of the experimental data.

7. Insulation - Prior to the Group II and III determinations, the cell was enclosed within an insulated box to protect it from environmental temperature changes. This added precaution did not affect the accuracy of the experimental data.

The preceding factors lend themselves to analysis in a straight-forward manner. On the basis of these studies, it can be concluded that they do not significantly contribute to the large inaccuracies noted in the experimental values of $\bar{\alpha}$.

The Group I thermal diffusivity values as plotted in figure 22 exhibit an interesting frequency effect. From this dependence of $\bar{\alpha}$ upon f suggests that convective flow is the cause of the observed inaccuracies. Intuitively, it seems reasonable that a system's stability as concerns the onset of convection should decrease with decreasing frequency of the exciting function. If convective flow did

FIGURE 22 - THERMAL DIFFUSIVITY AS A FUNCTION OF OPERATING FREQUENCY - GROUP I VALUES

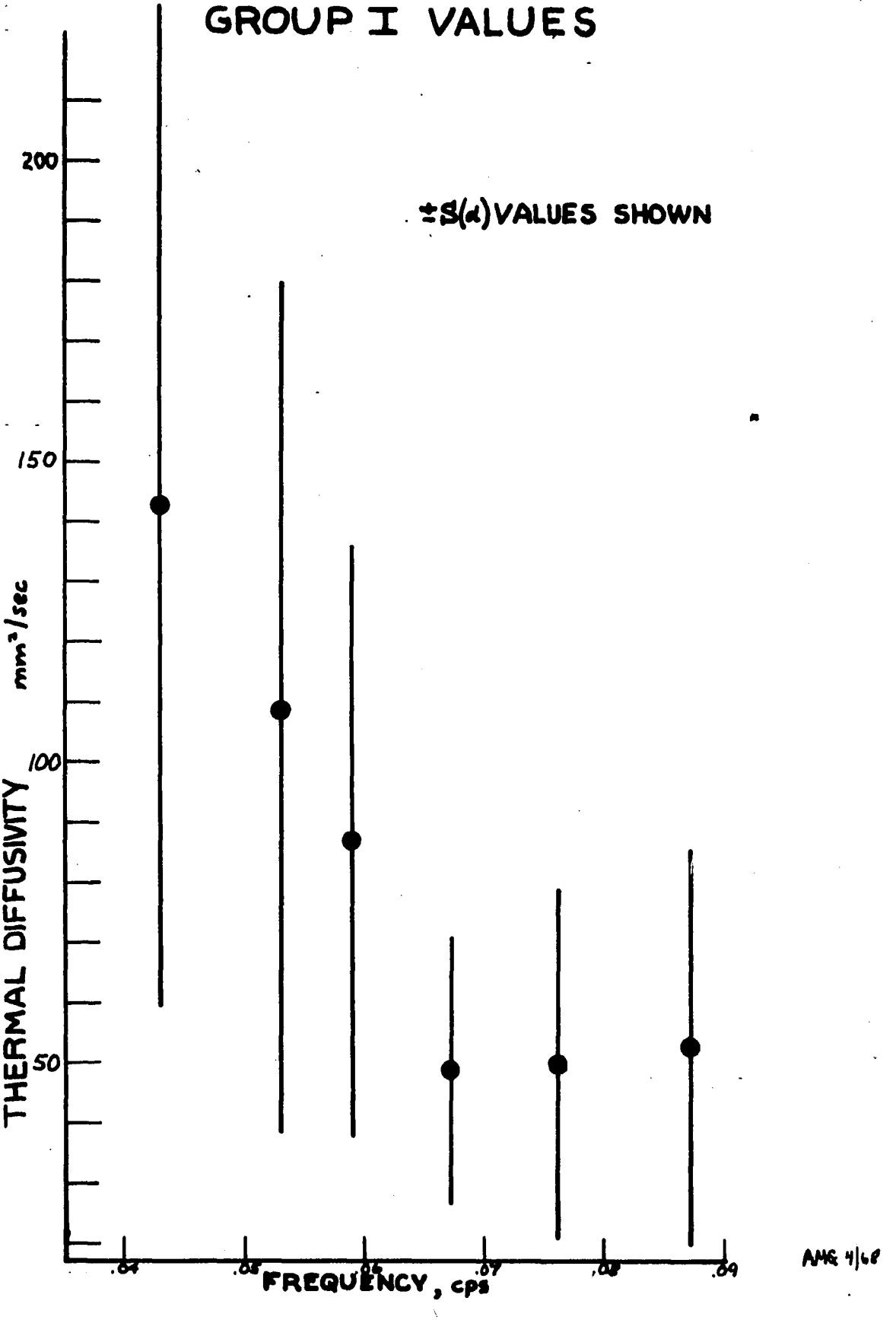

occur, one would also expect greater heat transfer, i.e., higher values of the apparent thermal diffusivity. Both of these conclusions based on the convection hypothesis seem to be supported by the Group I data. It should be mentioned, however, that the figure 22 plot of $\bar{\alpha}$ versus f may conceal the effect of yet another factor, temperature wave amplitude. It seems reasonable that the convective stability of the fluid should also be dependent upon the amplitude of the temperature oscillations, decreasing as the amplitude rises. Unfortunately, wave amplitude is dependent upon two factors - the magnitude of the electrical current supplied to the Peltier battery and the frequency of the oscillations. For a constant current flow, the lower the frequency, the higher the wave amplitude. Thus figure 22 may indicate an effect dependent upon frequency, amplitude or some combination of these two factors. One can conclude from the data of Group I that the measured values of thermal diffusivity are imprecise and inaccurate, with convective flow a probable cause of the latter. A three part experimental study was undertaken to investigate this situation more clearly.

8. Turbulence - The aim in performing these experiments was to examine the response of the system to different temperature perturbations. In four of the experiments the effect of a non-oscillatory temperature difference was investigated. As was previously described, both constant heating and constant cooling produced the same response, a high-frequency, high-amplitude noise. This signal was encountered in the thermocouple output when the system's temperature departed by 2-3 C^{o} from the original level. The onset of this noise was accompanied by a marked decrease in the slope of the thermocouple output. It was

found that both effects disappeared when the temperature again passed below the critical level.

One explanation for these occurrences is the onset of turbulent convection, which manifests itself in the appearance of the high-amplitude, noise-like oscillatory component. This turbulence would cause a rapid improvement in the rate of heat transfer, which could be viewed, in a simple manner, as an increase in the effective thermal conductivity of the heat transfer medium. Examination of the temperature distribution for constant heating of a semi-infinite body (Appendix H) shows that a decrease in $\partial T / \partial t$ is a natural consequence of a rise in thermal conductivity. Hence the observed sudden change in slope of the thermocouple signal is also explained by the convection hypothesis.

In the last two experiments of this series, an oscillatory temperature was used to perturb the system. At high amplitude levels, the normal sinusoidal output of the thermocouple probe became badly distorted. Again, the presence of a superimposed high frequency noise signal was uncovered. Shortly after the onset of this noise, the sinusoidal component was obliterated.

It is felt that both these phenomena and those just discussed are manifestations of turbulent convection. It is apparent that convective instability is predictable for the cases in which the Peltier battery is maintained at a temperature below that of the bulk gas. However, its appearance under the other conditions is unexpected, for the presence of a heated horizontal plate above a column

of fluid is a stable configuration. It is likely that the presence of the inner cylinder is the causative agent in these situations with radial temperature gradients between the walls and the bulk gas giving rise to the convective motion. It is postulated that in each case, the same critical temperature difference is exceeded and hence turbulent convection occurs. However, in each instance, the onset of this turbulence has been observed to coincide with the attainment of a particular temperature level by the gas close to the Peltier battery. This situation can be explained by a simple analysis (Appendix I) which shows the maximum horizontal temperature difference to be about the same over a wide range of heating rates.

On the basis of the preceding discussion it is possible to conclude that turbulent convection can occur during a diffusivity determination under the proper conditions - inner cell present and large power input to the Peltier battery. (The absence of the turbulent convection during the Group I runs when the inner cylinder was present is attributable to the very low power input.) However, it has also been clearly shown that turbulent convection cannot be the cause of the inaccurate $\bar{\alpha}$ values, for the presence of this phenomenon rapidly obliterates the sinusoidal component, thus making the determination of $\bar{\alpha}$ impossible.

9. Wall Effect - It was postulated that the concentric cylinder cell arrangement used to gather the Group I data was responsible in a number of possible ways for the erroneous thermal diffusivity data. It was conceivable that the presence of the inner cylinder invalidated the simple,

one-dimensional conduction model used to derive equation (4). In addition, temperature gradients existing between the cylinder walls and the gas could give rise to convective waves. As previously described, these possible wall effects were experimentally examined by redesigning the cell to allow for removal of the inner cylinder. Thermal diffusivity determinations were then performed with the cell in this configuration. As presented in figure 18, the seven data points from 0.067 cps to 0.102 cps, inclusive, are the most informative. Four of these points were for the case of the inner cylinder present (numbers 4,5,6,8) and the other three for the case of the inner cylinder removed (numbers 10, 12, 15). It is apparent from figure 18 that these seven data points are indistinguishable from one another within the range of the present precision. Hence one can conclude that wall effects, if they did exist, were of negligible importance.

10. Temperature and Frequency - On the basis of the preceding discussion it seems reasonable that laminar convection is the cause of the inaccurate thermal diffusivity values, and that this phenomenon is a direct consequence of the oscillatory nature of the temperature which is impressed upon the fluid by the horizontal Peltier battery. This behavior is clearly unexpected.

Stability criteria in terms of the Rayleigh number ($N_{Ra} = N_{Gr} \cdot N_{Pr} = T_o g \beta \rho^2 L^3 c_p / \mu k$, with L defined as a significant length) have been published for the onset of laminar convection when the body force and the temperature gradient are parallel, i.e., the "heated-from-below" problem.

For example, Chandrasekhar (8) gives critical Rayleigh number values above which convective motion will occur for three different conditions. If both confining surfaces are rigid, a value of 1707.762 is predicted; for the case in which slip can occur at both surfaces, i.e., two free surfaces, the value is 657.511; for one rigid and one free surface the value is 1100.65. However, "all of these stability predictions have been based on the assumption that the fluid is of infinite expanse, that both boundaries are thermally conducting, and that the vertical temperature gradient is a constant." (38) These conditions are not met in the experimental apparatus used in this work. Thus these criteria are not rigorously applicable to the present case. However, they can be used to obtain a rough approximation to the critical Rayleigh number, if certain terms are reinterpreted. Under these new interpretations, the significant length L is one-half the wave-length of the damped sinusoidal oscillation, equation (1); T_o is the temperature amplitude as measured between the Peltier battery surface and the bulk gas. It can be shown (16) that $\lambda/2 = (\alpha\,\pi/f)^{\frac{1}{2}}$. Hence, $L = (\alpha\,\pi/f)^{\frac{1}{2}}$ and

$$Ra' = \frac{\pi^{3/2}\, T_o g \rho^{\frac{1}{2}} K^{\frac{1}{2}} \beta}{\mu f^{3/2} c_p^{\frac{1}{2}}} \quad .$$

For the Group III data, this quantity varies from 52.5 to 475. (Table 4) For a cylinder of length L = 25.7 mm (= $\lambda/2$ at 0.1 cps for air) and 5.625" I.D. (the inner diameter of the large cylinder), the diameter to length ratio is 5.55.

TABLE 4 - GROUP III RAYLEIGH NUMBER DATA

RUN NO.		17	18	19	20	21	22	23	24	25
NOMINAL FREQ.	cps	.102	.102	.102	.102	.102	.134	.134	.134	.134
$\bar{f}$	cps	.103	.103	.103	.103	.103	.135	.135	.135	.135
To	C^{o}	.13	.36	.07	.23	.04	.21	.16	.06	.13
$\bar{\alpha}$	mm^2/sec	45	70	39	61	45	83	37	42	55
N_{Pr}		.708	.708	.708	.708	.708	.708	.708	.708	.708
N'_{Ra}		172.5	475.0	92.7	305.0	53.1	184.2	140.6	52.5	114.0

PHYSICAL PROPERTIES FOR AIR AT $25^{o}C$ & 1 ATM.

$$N'_{Ra} = \frac{T_o \, g\beta\pi^{3/2} \, \alpha^{\frac{1}{2}}}{\nu \, f \, 3/2}$$

86.

The Ra_c = 1100.65 criterion, although derived for the case of a fluid of infinite horizontal expanse, can be applied to this case as an approximation. (The stability criterion of Sherman and Ostrach (37) would be more relevant because it considers a fluid which is bounded, rather than infinite in the horizontal direction. Unfortunately, this work furnishes only a lower bound to the critical Rayleigh number for a vertical cylinder of the required length to diameter ratio.) The fact that the Ra' values for the Group III data lie below 1707.762 points out the difficulty of predicting the onset of instability for this situation. The need for a proper stability criterion in terms of an appropriate Rayleigh number is evident from this discussion.

The Group III data are also presented in figure 18. The beneficial effect of decreasing the amplitude of the temperature wave is clearly shown. However, extrapolation of the linear regression line $T_o = 0$ yields an intercept of about 34 mm^2/sec, i.e., almost 62% above the expected value. Because of this, it seems reasonable to conclude that a discontinuity exists in the relationship between $\bar{\alpha}$ and T_o. The value of T_o at which this discontinuity occurs should correspond to the critical Rayleigh number above which laminar convective flow will occur.

Although the influence of T_o on the experimental values of $\bar{\alpha}$ has been demonstrated, the effect of the wave frequency is less apparent. Failure to uncover a frequency effect may be due to the imprecision of the data, or the range of the parameters investigated here, for the influence of f on $\bar{\alpha}$ is expected. Thus, although it was possible

to correlate $\bar{\alpha}$ against a function of the form $T_o^a f^b$, the confidence range on the two exponents were quite broad. This was particularly true for the exponent of the frequency term. Efforts to improve the reliability of this correlation would be hampered by the nature of the apparatus itself, which places an upper bound on the choice of operating frequency value. There are two reasons for this situation: the thermal capacitance of the Peltier battery and the switching characteristics of its power supply system. It is possible to estimate the time constant of the Peltier battery at about 2 seconds. Hence the frequency response of this device is judged to be approximately ½ cps (Appendix L). This calculation tends to explain the difficulty encountered in generating waves in the frequency range above 0.5 cps. An additional complication at higher frequencies is that the rise time of the square-wave voltage which powers the Peltier battery is no longer negligible in comparison to the "half-period" of the wave. In addition, the gear train of the present frequency selector device exhibits excessive slippage when forced to operate at the high rotational velocities which are required to generate these frequencies.

Further evidence can be drawn from the technical literature to support the laminar convection hypothesis. Malkus (30) experimentally investigated the transitions in heat transfer mode which occur in a Benard cell as the temperature of the lower plate is raised to progressively higher levels. Experiments were performed for both distilled water and for acetone. The fluid layer thickness varied from 0.05" to 8.00". The thermal diffusivity of the fluid

was obtained by measuring the heat flux through the fluid and the temperature difference across it. Malkus observed the first transition in the mode of heat transfer, from conduction to laminar convection, at a Rayleigh number of 1700 $\pm$ 80; this value agrees well with the theoretical value of 1708 for a fluid bounded by two rigid planes. Of greater interest is the finding that the ratio of α_{EFF} to α changes at this point from 1 to 2.1 $\pm$ .1; α_{EFF} is a measure of the heat transferred by both conduction and convection, i.e., the experimentally determined "effective" thermal diffusivity.

The median thermal diffusivity determined in this research for air was about 49 mm^2/sec. This value is 135% in excess of the expected value, i.e., the ratio of the experimentally determined value to that expected for pure conduction is about 2.3. This observation is in agreement with that of Malkus and lends added support to the laminar convection hypothesis.

The apparatus used by Harrison, Boteler and Spurlock (14) has been described previously. The principal differences from the method used here (other than the technique for heat flux generation) are in geometry and in temperature measurement. A vertical tube of approximately one inch internal diameter was used to contain the test gas with the heat flux supplied on the lateral surface. Temperature measurements were made with platinum resistance thermometers having sensitivities of the order of $10^{-4}C^{o}$. The frequency range is essentially the same as in the work reported here.

Since Harrison, et. al. did not explore the problem of convective instability, it is necessary to speculate on its apparent absence under their experimental conditions. The answer is not to be sought through geometric considerations: the tube is of large diameter, and temperature gradients perpendicular to the body force have far lower convective stability than those parallel to the body force. Although they did not report the amplitude of their temperature waves, their use of platinum resistance thermometers, rather than thermocouples, allows one to speculate about the magnitude of this quantity. It is generally accepted that such thermometers can detect temperature variations of the order 10^{-4} C^{o}. The smallest amplitude employed in this work was .05 C^{o} (thermocouple sensitivity being the limiting factor). Hence their temperature signals may have been two orders of magnitude lower in amplitude than those used here. If this is the case, it is quite possible that these authors were able to work below the limit for convective instability.

CONCLUSIONS

Natural convection appears as the limitation on the oscillatory method for the measurement of thermal diffusivity in fluids. This convection is induced by temperature waves generated in the vicinity of a horizontal surface subjected to an oscillatory temperature. With air as the medium, convection occurs at frequencies as high as 0.2 cps and temperature amplitudes as low as 0.05 C^{o}. The apparent thermal diffusivities are about double the value for the fluid.

RECOMMENDATIONS

Laminar convection induced by an oscillatory temperature at a horizontal wall has never been explored. Investigation is warranted because of its appearance in the oscillatory method of thermal diffusivity measurement and because of the enhanced heat transfer which arises.

An analytical study should be undertaken to establish stability criteria. This would determine the region of frequency and temperature amplitude in which thermal diffusivity measurements are possible.

Once the range of interest has been established, it should be possible to design a system in which the phenomenon can be observed directly. Observations of flow patterns would require either smoke injection or an optical technique such as interferometry. The experimental work would serve to check the analytical approach and establish the convection patterns which arise from oscillations in wall temperature.

NOMENCLATURE

a, radius of cylinder

a, unspecified exponent

A, surface area

A_n, Wassiljewa constant

b, unspecified exponent

c, heat capacity of semi-infinite medium (equation 6 only)

c_p, heat capacity

C, recorder chart speed

C, capacitance (figure 12)

E, modulus of elasticity

f_N, natural frequency of vibration

f, frequency

f, potentiometer setting (figure 11 only)

$\bar{f}$, average frequency

g, gravitational acceleration

h, heat transfer coefficient

$J_o(u)$, zero order Bessel function of the first kind

$J_1(u)$, first order Bessel function of the first kind

k, thermal conductivity

L, a significant length

N_{Fo}, Fourier number

N_{Gr}, Grashof number

N_{Pr}, Prandtl number

N_{Ra}, Rayleigh number = $T_o g \beta c_p \rho^2 L^3/\mu k$

$N_{Ra'}$, modified Rayleigh number = $\pi^{3/2} T_o g \beta \rho^{\frac{1}{2}} k^{\frac{1}{2}}/\mu f^{3/2} c_p^{\frac{1}{2}}$

Q, thermal flux per unit area

r, radial position

R, electrical resistance

S, statistical estimate of the standard deviation

S, heat capacity per unit length for cylinder (equation 6)

S^2, statistical estimate of the variance

t, time

T, temperature

T_m, mean temperature

T_o, temperature amplitude

u, dummy variable of integration (equation 6)

V, volume

x, distance from Peltier battery

$Y_o(u)$, zero order Bessel function of the second kind

$Y_1(u)$, first order Bessel function of the second kind

α, thermal diffusivity

$\bar{\alpha}$, experimentally determined average thermal diffusivity

α, = $2\pi fRC$ (figure 12)

β, coefficient of fluid thermal expansion

δ, plate thickness

Δx, distance between thermocouple junctions

$\overline{\Delta x}$, average distance between thermocouple junctions

$\Delta \phi$, phase difference in real time

$\overline{\Delta \phi}$, average phase difference in real time

$\overline{\Delta \psi}$, average phase difference as measured on recorder chart

η, = $2a^2 \rho \pi c/S$ (equation 6)

θ, temperature difference

λ, wavelength

$\bar{\lambda}$, average wavelength as measured on recorder chart

μ, viscosity

μ, mean value

ρ, density

ρ, dummy variable of integration (equation 7)

σ^2, variance

τ, $= \alpha\, t/a^2$ (equation 6)

τ, time constant

ϕ, $= uY_o(u) - \eta\, Y_1(u)$ (equation 6)

ψ, $= uJ_o(u) - \eta J_1(u)$ (equation 6)

APPENDIX A

Standard Deviation Expression for the $\bar{\alpha}$ Relation

It has been mentioned that $\bar{\alpha}$ is computed from the equation:

$$\bar{\alpha} = (C\ \bar{\lambda}/4\ \pi)\ (\overline{\Delta x}/\overline{\Delta \psi})^2 \qquad \text{(A-1)}$$

Following the scheme set forth in Volk (42), an expression for the variance of such an equation can be derived as follows: if $X = f(x_1, x_2, \ldots)$ then

(A-2)

$$\sigma^2(X) = (\partial X/\partial x_1)^2_{\substack{x_i \\ i \neq 1}}\ \sigma^2(x_1) + (\partial X/\partial x_2)^2_{\substack{x_i \\ i \neq 1}}\ \sigma^2(x_2) + \ldots$$

Let $w = axy^2z^{-2}$, then

$$\sigma^2(w) = a^2\ \mu_y^4\ \mu_z^{-4}\ \sigma^2(x) + 4\ a^2\ \mu_x^2\ \mu_y^2\ \mu_z^{-4}\ \sigma^2(y) + 4\ a^2\ \mu_x^2\ \mu_y^4\ \mu_z^{-6}\ \sigma^2(z) \qquad \text{(A-3)}$$

$$\sigma^2(w)/\mu_w^2 = \sigma^2(x)/\mu_x^2 + 4\ \sigma^2(y)/\mu_y^2 + 4\ \sigma^2(z)/\mu_z^2 \qquad \text{(A-4)}$$

Now replacing x by $\bar{\lambda}$, y by $\overline{\Delta x}$, and z by $\overline{\Delta \psi}$ and using statistical estimators in place of the mean and variance:

$$S^2(\alpha)/\bar{\alpha}^2 = S^2(\lambda)/\bar{\lambda}^2 + 4\ S^2(\Delta x)/(\overline{\Delta x})^2 + 4\ S^2(\Delta \psi)/(\overline{\Delta \psi})^2$$

(A-5)

APPENDIX B

Time Constant for Thermocouple Bead

The manufacturer states that the junction of the 0.001" chromel-alumel thermocouple is a spherical bead of 0.003" diameter. The time constant for such a body can be shown to be:

$$\tau = c_p \, V \, \rho/h \, A$$

For a sphere the ratio of the volume V to the surface area A is equal to one-third of the sphere radius. To evaluate the heat transfer coefficient h we assume the junction to be surrounded by a stagnant fluid and use $hD/k = 2$. Hence

$$\tau = c_p \, \rho \, r^2/3 \, k$$

DATA: $k = 5.6 \times 10^{-5}$ cal/sec cm $^{\circ}$C (for air at atmospheric)

For the thermocouple junction:

$r = 3.8 \times 10^{-3}$ cm

$c_p = .105$ cal/gm $^{\circ}$C

$\rho = 8.90$ gm/cm^3

Therefore $\tau = 0.081$ seconds

At f = .1 cps, $\lambda = 10$ seconds. Thus the wavelength is more than two orders of magnitude greater then the thermocouple time constant.

APPENDIX C

The Rapid Decay of the Temperature Wave

The cold junction of each Thermocouple Probe is located about 90 mm from the surface of the Peltier Battery. From the temperature distribution expression, equation (1), it can be shown that:

$$\frac{(T - T_m)_{x=x_i}}{(T - T_m)_{x=x_j}} = \exp(-\sqrt{\pi f/\alpha}(x_i - x_j)). \qquad \text{(C-1)}$$

In a typical determination, the two "hot" junctions are located 4.0 mm and 9.4 mm, respectively from the Peltier Battery wall. Substituting into equation (C-1) at f=.060 cps and α = 21 mm^2/sec, we get

$$\frac{(T - T_m)_{x=90\ mm}}{(T - T_m)_{x=4.0\ mm}} = \exp(-8.14) = .0003$$

and

$$\frac{(T - T_m)_{x=90\ mm}}{(T - T_m)_{x=9.4\ mm}} = \exp(-7.74) = .00044.$$

It is possible to conclude, therefore, that the wave is of negligible amplitude at the "cold" junction.

APPENDIX D

Disturbance in Temperature Field Caused by Thermocouple

As previously discussed, it is necessary to numerically evaluate the expression:

$$\frac{T}{T_1} = (2/\pi) \int_0^\infty \exp(-\tau u^2) \frac{\left[J_o(ru/a)\ (\phi) - Y_o(ru/a)\ (\psi) \right]}{\phi^2 + \psi^2} du$$

where $\phi = uY_o(u) - \eta Y_1(u)$ $\qquad \tau = \alpha t/a^2$

$\psi = uJ_o(u) - \eta J_1(u)$ $\qquad \eta = 2\pi a^2 \rho\ c/S$

S = heat capacity per unit length for cylinder

ρ = density of the semi-infinite medium

c = heat capacity of the semi-infinite medium

a = radius of the cylinder

r = radial position measured from cylinder center

t = time

u = dummy variable of integration

T = temperature of semi-infinite medium

T_1 = initial temperature of the cylinder

The integration was performed by dividing the region beneath the curve into a number of sections of pre-determined width, and evaluating the area of each section by a Simpson's Rule scheme. For each of these sections, the area is evaluated at least twice, using a grid of decreasing size. The idea was to have the final value for the area of a section agree to 0.01% with the magnitude calculated using a grid of twice the width. Because of the nature of the upper limit, it was necessary to terminate the integration at some arbitrary point. Thus the integration beneath

the curve was continued until the total area changed by no more than 0.01%.

The program was written in Fortran IV; it required 6.5 minutes to compile on the IBM 7040, and approximately 5 minutes to generate one data point. The accuracy of the results obtained from this program was determined by computing values of T/T_1 for the case: $\alpha = 6.4$ mm^2/sec, $\eta = 2.0$, $r/a = 1$, and comparing them with the results presented graphically by Jaeger (18). The discrepancies ranged from -4% to +3% for three values of T/T_1. This accuracy was sufficient for the purpose at hand. Results are shown in figure 19.

APPENDIX E

The Effect of Small Amounts of CO_2 and Water Vapor on the Thermal Diffusivities of Air

Consider an extreme case: air at 60°F, 1 atm, 100% relative humidity and, say, 0.01 mole CO_2 per mole of dry gas.

COMPONENT	MOLE FRACTION	THERMAL CONDUCTIVITY (26) BTU/hr ft °F	HEAT CAPACITY (35; p. 229) BTU/lb °F	DENSITY (35; p. 176) lb/ft^3
Air	.9727	.0146	.24	.0765
CO_2	.0098	.0091	.20	.1169
H_2O	.0175 p. 101 (17)	.0098	.43	.0477 (35; p.75

c_p(mixture of gases) = (.9727) (.24) + (.0098) (.20) + (.0175) (.43) = .24 BTU/lb °F

ρ (mixture of gases) = (.9727) (.0765) + (.0098) (.1169) + (.0175) (.0477) = .0764 lb/ft^3

k (mixture of gases). Using the method of Wassiljewa (26):

Wassiljewa Constants

Air in CO_2 1.20 CO_2 in air 0.95 H_2O in air 0.73
in H_2O 0.87 in H_2O 0.78 in CO_2 0.99

$$A_n(1 - y_n) = y_1A_{n-1} + y_2A_{n-2} + y_3A_{n-3} + \ldots$$

$$A_1(1 - y_1) = .0098\ (1.20) + .0175(.87) = .0098$$

$$A_2(1 - y_2) = .9727\ (.95) + .0175\ (.78) = .9377$$

$$A_3(1 - y_3) = .9727\ (.73) + .0098\ (.99) = .7198$$

$$k_m = k_1/(1 + (A_1(1-y_1)/y_1)) + k_2/(1 + (A_2(1-y_2)/y_2)) + k_3/(1 + (A_3(1-y_3)/y_3))$$

$$k_m = .0146/(1 + (.0270/.9727)) + .0091/(1 + (.9377/.0098)) + .0098/(1 + (.7198/.0175)) = .0145 \text{ BTU/hr ft } ^{o}F$$

$$\alpha \text{ mixture} = k_{mixture}/\rho_{mixture}\, c_{p_{mixture}} = 20.4 \text{ mm}^2/\text{sec}$$

$$\alpha \text{ air} = k_{air}/\rho_{air}\, c_{p_{air}} = 20.5 \text{ mm}^2/\text{sec}$$

Therefore:

$$\frac{\alpha_{air} - \alpha_{mixture}}{\alpha_{air}} \; 100 = .5\%$$

APPENDIX F

The Effect of Higher Harmonics on $\bar{\alpha}$

For a sinusoidal input of the form $(T-T_m)/T_o = \sin 2\pi ft$, the temperature distribution has been shown to be:

$$(T-T_m)/T_o = \exp(-\sqrt{\pi f/\alpha}\, x)\ \sin(2\pi ft - \sqrt{\pi f/\alpha}\, x)$$ from which $\alpha = (1/4\pi f)\ (\Delta x/\Delta \phi)^2$ was derived. Now consider a "saw-tooth" function which is represented by the equation:

(F-1)

$$(T-T_m)/T_o = \frac{8}{\pi^2}\left\{\sin 2\pi ft - \frac{1}{9}\sin 6\pi ft + \frac{1}{25}\sin 10\pi ft\right\}$$

For an input voltage of this form, the temperature distribution should be:

(F-2)

$$(T-T_m)/T_o = \frac{8}{\pi^2}\left\{\exp(-\sqrt{\pi f/\alpha}\, x)\ \sin(2\pi ft-\sqrt{\pi f/\alpha}\, x) - (1/9)\exp(-\sqrt{3\pi f/\alpha}\, x)\ \sin(6\pi ft-\sqrt{3\pi f/\alpha}\, x) + (1/25)\exp(-\sqrt{5\pi f/\alpha}\, x)\ \sin(10\pi ft-\sqrt{5\pi f/\alpha}\, x)\right\}$$

Now consider the following experimental conditions:

f, oscillation frequency, = 0.060 cps

x_1, distance of first thermocouple to Peltier Battery, = 5.6 mm

x_2, distance of second thermocouple to Peltier Battery, = 11.4 mm

In a hypothetical case, the output of the first thermocouple has a zero at t_1 = 1.47 sec. The output of the second thermocouple has a zero at t_2 = 3.00 sec. Now we compute α :

1) Sinusoidal Input assumption: $\alpha = \left(\frac{1}{4\pi(.060)}\right)\ \left(\frac{11.4-5.6}{3.00-1.47}\right)^2 =$

$19.1\ \frac{mm}{sec}^2$

2) "Sawtooth" Input assumption: One must use a "trial and error" approach with equation (F-2) to solve for α when $(T-T_m)/T_o = 0$. Assuming $\alpha = 21\ mm^2/sec$ we can satisfy (F-2) at $t_1 = 1.47$ sec.

$\exp(-\sqrt{\pi f/\alpha}\ x_1) = \exp(-.53) = .588$ $\qquad 2\pi f t_1 = 0.554$

$\exp(-\sqrt{3\pi f/\alpha}\ x_1) = \exp(-.92) = .390$ $\qquad 6\pi f t_1 = 1.663$

$\exp(-\sqrt{5\pi f/\alpha}\ x_1) = \exp(-1.885) = .306$ $\qquad 10\pi f t_1 = 2.771$

$$0 \stackrel{?}{=} .588 \sin(.024) - (.390/9) \sin(.740) + (.306/25) \sin(1.586)$$

$$0 \approx 0$$

Therefore, the unsuspected presence of higher harmonics would lead to erroneous $\bar{\alpha}$ values, but the error would be small, about 10 %.

APPENDIX G

The Validity of the $\bar{\alpha}$ Expression Is Shown

Let $Y = Y(x_1, \ldots, x_N)$. It can be shown that:

$$\mu_Y \cong Y(\mu_1, \ldots, \mu_N) + \tfrac{1}{2} \sum_i \sigma_i^2 \frac{\partial^2 Y(\mu_1, \ldots, \mu_N)}{\partial x_i^2} + \tag{G-1}$$

$$\sum_{i \neq j} \sum \rho_{ij} \sigma_i \sigma_j \frac{\partial^2 Y(\mu_1, \ldots, \mu_N)}{\partial x_i \, \partial x_j}$$

where the approximation is due to the termination of the Taylor Series.

Let $Y = x_1 x_2^2 x_3^{-2}$ (G-2)

From (G-1), it follows that:

$$\mu_Y \cong \mu_1 \mu_2^2 \mu_3^{-2} + \mu_1 \mu_3^{-2} \sigma_2^2 + 3\mu_1 \mu_2^2 \mu_3^{-4} \sigma_3^2 + 2\mu_2 \mu_3^{-2} \rho_{12} \sigma_1 \sigma_2 - \tag{G-3}$$

$$2\mu_2^2 \mu_3^{-3} \rho_{13} \sigma_1 \sigma_3 - 4\mu_1 \mu_2 \mu_3^{-3} \rho_{23} \sigma_2 \sigma_3$$

Replacing terms in equation (G-3) by their statistical estimators yields:

$$\bar{Y} \cong \bar{x}_1 \bar{x}_2^2 \bar{x}_3^{-2} + \bar{x}_1 \bar{x}_3^{-2} S_2^2 + 3\bar{x}_1 \bar{x}_2 \bar{x}_3^{-4} S_3^2 + 2\bar{x}_2 \bar{x}_3^{-2} r_{12} S_1 S_2 \tag{G-4}$$

$$-2\bar{x}_2^2 \bar{x}_3^{-3} r_{13} S_1 S_3 - 4\bar{x}_1 \bar{x}_2 \bar{x}_3^{-3} r_{23} S_2 S_3$$

and if x_1, x_2, x_3 are independent of one another:

$$r_{12} = r_{13} = r_{23} = 0$$

$$\bar{Y} \cong \bar{x}_1\bar{x}_2^2\bar{x}_3^{-2} + \bar{x}_1\bar{x}_3^{-2}S_2^2 + 3\bar{x}_1\bar{x}_2\bar{x}_3^{-4}S_3^2 \qquad \text{(G-5)}$$

Now the equation which was derived to compute the thermal diffusivity was $\alpha = (1/4\pi f)\ (\Delta x/\Delta\emptyset)^2 = (C\lambda/4\pi)\ (\Delta x/\Delta\psi)^2$

Rewriting the last form of this equation gives:

$\alpha 4\pi/C = \lambda(\Delta x)^2(\Delta\psi)^{-2}$. This form is similar to that of equation (G-2). Thus from equation (G-5), it follows that:

$$\bar{\alpha} = (C\bar{\lambda}/4\pi)\ (\overline{\Delta x}/\overline{\Delta\psi})^2 + (C\bar{\lambda}/4\pi)\ (S^2_{\Delta x}/(\overline{\Delta\psi})^2) + (3C\bar{\lambda}/4\pi)\frac{(\overline{\Delta x})^2 S^2_{\Delta\psi}}{(\overline{\Delta\psi})^4} \qquad \text{(G-6)}$$

Typical values for Group I Data:

C = 5 mm/sec

$\bar{\lambda}$ = 116.8 mm $\qquad S^2_{\lambda} = 1.4\ mm^2$

$\overline{\Delta x}$ = 5.79 mm $\qquad S^2_{\Delta x} = .06\ mm^2$

$\overline{\Delta\psi}$ = 3.3 mm $\qquad S^2_{\Delta\psi} = 1.4\ mm^2$

$\alpha = 143 + 0.3 + 9.5 = 143 + 9.8 = 153\ mm^2/sec$

Error = (9.8/143) 100 = 7%

APPENDIX H

The Observed Decrease in $\partial T/\partial t$ is Explained as a Consequence of the Onset of Convection

A rigorous approach would involve solutions for the time-dependent temperature distribution in both the conductive and convective regimes, and a comparison of $\partial T/\partial t$ obtained from these two expressions. This formidable task is avoided by consideration of a simple conduction model in which the onset of convection is viewed as pure conduction heat transfer through a medium of increased thermal conductivity.

Consider a semi-infinite medium of thermal conductivity k, thermal diffusivity α, heat capacity c_p, and density ρ, which is initially at a temperature T_i. At time t=0, a constant flux per unit area Q is impressed on the boundary of this body. Obtain the temperature distribution, T, as a function of time ($t \geq 0$) and position, as measured from the boundary ($x \geq 0$).

$$\partial\theta/\partial t = \alpha\, \partial^2\theta/\partial x^2 \text{ where } \theta = T - T_i \qquad \text{(H-1)}$$

I.C. $\quad \theta(x=x, t=0) = 0$

B.C.1 $\quad -k\, \partial\theta/\partial x \Big|_{\substack{x=0 \\ t=t}} = Q$

B.C.2 $\quad \theta(x\to\infty, t\geq 0) = \text{well-behaved}$

Application of the LaPlace Transform to this problem yields:

$$\bar{\theta}(s,x) = (Q\alpha^{\frac{1}{2}}/ks^{3/2}) \exp(-x\sqrt{s/\alpha}) \qquad \text{(H-2)}$$

The inverse of this transform is (1):

(H-3)

$$\theta(t,x) = (Q\alpha^{\frac{1}{2}}/k)\left[(2t^{\frac{1}{2}}/\pi^{\frac{1}{2}})\ \exp(-x^2/4\alpha t) - (x/\alpha^{\frac{1}{2}})\ \operatorname{erfc}(x/2\alpha^{\frac{1}{2}}t^{\frac{1}{2}})\right],$$

$$\therefore\ \partial\theta/\partial t\Big|_{\substack{t=t\\x=x}} = (Q^2/\pi tk\rho c_p)^{\frac{1}{2}}\ \exp\ (x^2\rho c_p/4kt) \qquad \text{(H-4)}$$

Let subscript 1 = pure conductive regime

Let subscript 2 = pseudo-conductive regime during which convection is occurring

(H-5)

$$(\partial\theta/\partial t)_{k_1}/(\partial\theta/\partial t)_{k_2} = \phi^{\frac{1}{2}}\ \exp\left[(-x^2\rho c_p/4tk_1)\ (\phi-1)\ (1/\phi)\right]$$

where $\phi = k_2/k_1$

From the experimental curve of thermocouple voltage versus time (figure 19), we estimate that:

$$(\partial\theta/\partial t)_{k_1}/(\partial\theta/\partial t)_{k_2} = \frac{\text{5 divisions}/14\frac{1}{2}\ \text{seconds}}{\text{1 division}/40\ \text{seconds}} = 13.8$$

The break in the experimental curve occurred at $t\approx100$ seconds; x is estimated at 7mm. The data for air at 25°C are:

$\rho = .074\ \text{lb/ft}^3$, $c_p = .25$ BTU/lb °F, $k_1 = .014$ BTU/hr ft °F

Substitution os these values into equation (H-5) gives:

$$13.8 = \phi^{\frac{1}{2}}\ \exp\ (-.0063(\phi-1)\ (1/\phi)) \qquad \text{(H-6)}$$

Solution of equation (H-6) yields $\phi\approx190 = k_2/k_1$

∴ (convective regime "thermal conductivity") >

(Pure conduction thermal conductivity)

Thus it has been shown that a decrease in the slope of the temperature-time curve can be viewed as a consequence of the onset of convection if the latter is assumed to manifest itself by an increase in thermal conductivity.

APPENDIX I

The Cause of the Turbulent Convection Observed During the Steady Heating of the Gas

The occurrence of turbulent convection when the Peltier battery is being heated has been explained as a consequence of the horizontal temperature gradient between the inner cylinder walls and the gas. It is postulated that in each case, the same critical temperature difference is exceeded and hence turbulent convection occurs. However, in each instance, the onset of this turbulence has been observed to coincide with the attainment of a particular temperature level by the gas close to the Peltier battery. This situation can be explained by the following analysis.

The gas and glass are considered to be non-interacting, semi-infinite mediums. The temperature at the surface x=0 increases linearly, i.e.,

$$T(x=0, t\geq 0) = kt.$$

For such a system, Carslaw and Jaeger (6) give the temperature distribution T as a function of position x and time t as:

$$T = kt\left((1+x^2/2\alpha t)\ \mathrm{erfc}\left(x/2(\alpha t)^{\frac{1}{2}}\right) - x\left(\exp(-x^2/4\alpha t)\right)/(\pi\alpha t)^{\frac{1}{2}}\right)$$

$$= 4kt\ i^2\mathrm{erfc}\left(x/2(\alpha t)^{\frac{1}{2}}\right)$$

where α is the thermal diffusivity of the medium.

Let $\Delta T = T_{gas} - T_{glass}$

$$= 4kt\ i^2\mathrm{erfc}\left(x/2(\alpha_{gas}\ t)^{\frac{1}{2}}\right) - 4kt\ i^2\mathrm{erfc}\left(x/2(\alpha_{glass}\ t)^{\frac{1}{2}}\right)$$

The maximum temperature difference is then sought:

$$\partial(\Delta T)/\partial x = -kt^{-\frac{1}{2}}((2/\alpha_{gas}^{\frac{1}{2}})\ \text{ierfc}\ (x/2(\alpha_{gas}\ t)^{\frac{1}{2}}) =$$

$$(2/\alpha_{glass})^{\frac{1}{2}}\ \text{ierfc}\ (x/2\alpha_{glass}\ t)^{\frac{1}{2}})) = 0$$

or, with $\phi = x/2(\alpha_{gas}\ t)^{\frac{1}{2}}$, ΔT has a maximum at that value of ϕ for which:

$$\frac{2\ \text{ierfc}\ (\phi\alpha_{gas}^{\frac{1}{2}}\ \alpha_{glass}^{-\frac{1}{2}})}{2\ \text{ierfc}\ \phi} = (\alpha_{glass}/\alpha_{gas})^{\frac{1}{2}}$$

$\alpha_{glass} = 0.50\ mm^2/sec \qquad \alpha_{gas} = 21\ mm^2/sec$

By trial and error solution, $\phi_{MAX} = 0.14$

$\therefore \Delta T_{MAX} = 0.64kt$

Now consider two of the observed cases: (1) The Thermocouple output reached 98 μv at ~ 100 sec, at which time, turbulence started; (II) The thermocouple output reached 102½ μv at ~330 sec, at which time turbulence started. The thermocouple is located at x≈8mm. Let ε be the thermocouple sensitivity.

Case I: $T_{gas} = 98\ \mu v\ \varepsilon^{o}/\mu v = 98\varepsilon^{o}$

$= kt\ 4i^2\ \text{erfc}\ x/2(\alpha_{gas}t)^{\frac{1}{2}}$

$= 100k\ 4i^2\ \text{erfc}\ 8/2(2100)^{\frac{1}{2}}$

$k = 1.2\ \varepsilon$

$\Delta T_{MAX} = (.64)\ (1.2)\ (\varepsilon)\ (100) = [76.8\ \varepsilon]^{o}$

Case II: $T_{gas} = 102\frac{1}{2}\ \mu v\ \varepsilon^{o}/\mu v = 102\frac{1}{2}\varepsilon^{o}$

$= kt\ 4i^2\ \text{erfc}\ x/2(\alpha_{glass}t)^{\frac{1}{2}}$

$= 330\ k\ 4i^2\ \text{erfc}\ 8/2(21 \times 330)^{\frac{1}{2}}$

$k = .349\ \varepsilon$

$\Delta T_{MAX} = (.64)\ (.349)\ (\varepsilon)\ (330) = [73.8\ \varepsilon]^{o}$

Thus for these two cases the maximum temperature differences are about the same although the heating rates differ from one another by a factor of three.

APPENDIX J

Vibration of Thermocouple Wire

The thermocouple wire is considered a circular section beam supported at each end. For such a structure, Kent (23) gives the natural frequency f_n as

$$f_n = 7.7(D/l^2)\ (E/w_l)^{\frac{1}{2}}$$

where: D = diameter, in.

l = length between end supports, in.

w_l = density, lb./in^3

E = modulus of elasticity, lb./in^2

For the case at hand: l = 1.0 in.

D = 0.001 in.

w_l = 0.31 lb./in^3 (Estimate)

E = 30 x 10^6 lb./in^2 (Estimate)

$\therefore$ f_n = 76 cps

APPENDIX K

Calibration of the Differential Thermocouple

The aim was to calibrate a differential copper-constantan thermocouple to read small temperature differences at 30-40°C. Each junction was wrapped to the bulb of a Beckmann Differential Thermometer and both thermometers placed in a small vessel containing a stirred liquid. This vessel was then placed in a large, well-stirred thermal bath held at about 40°C by a temperature controller. Thermocouple voltages were recorded and thermometer readings were made, both as a function of time, in order to:

1) Determine differences in reading between the two thermometers when both were at the same temperature
2) Determine the thermocouple voltage produced by the thermocouple when both junctions were at the same temperature.

The next step was to separate the two Beekmann Thermometers. Each thermometer, with its attached thermocouple junction, was placed in a small, liquid-filled vessel similar to that used above. Each vessel was then placed in a separate temperature-controlled thermal bath. The liquids in both the small vessels and the thermal baths were kept well-stirred. The set points of the bath controllers were manipulated so that a difference of several degrees existed between the temperatures of the two large baths. Once again, thermocouple voltages were recorded and thermometer readings were made, both a functions of time, in order to determine the thermocouple voltage caused by a known

temperature difference. A number of different temperature differences were used to generate the raw data for the calibration curve. The error in these temperature difference values was estimated as ±.04 C^{o}. It was necessary to record these data as a function of time because of the interplay of two factors: the impossibility of making simultaneous thermometer readings and the drift in temperature exhibited by the two temperature-controlled baths. Thus a particular voltage level could not be associated with a known temperature difference. It was necessary to go through several steps before the raw data could be converted into a calibration curve.

First, least-square lines were passed through the two sets of time-thermometer reading data obtained in each run. The same procedure was not required for the thermocouple voltage data, for these values showed little variation with time over intervals in excess of two hundred seconds. In addition, it was shown that the Allison LC filter did not affect the magnitude of these voltage signals when used as a low-pass filter attenuating at 2 cps. Supplementary experimental and analytical work were then performed to investigate time lags inherent in the system. It was found that the lags caused by both the Beckmann Thermometer and the LC filter present in the thermocouple circuit were small, when compared to the time intervals during which the thermocouple voltage did not fluctuate. Hence it was possible to associate this voltage with an average temperature difference; the latter value was obtained by averaging over the time interval during which the voltage held at a constant level.

A least-squares line was passed through the average temperature difference-voltage data. The equation was:

$$\text{Voltage } (\mu v) = 4.49 + 40.22\ (\overline{\Delta T}).$$

The work which led to this equation was performed at or near 40°C, i.e., about 10-15 C° above the level at which the thermocouple would eventually be used. It was thus necessary to correct the calibration equation for use at 25-30°C. The first step in this procedure was to determine the change in thermocouple output at zero temperature difference over a range of temperature levels. It was found that a change of 10 C° caused a decrease in thermocouple output of 1.82 μv. Hence the proper y-intercept for the calibration curve at 30 °C was estimated to be 2.67 μv. The slope of the line had also to be considered. A typical copper-constantan thermocouple shows a change of slope or sensitivity from 41 μv/C° at 30°C to 42 μv/C° at 40 °C, or a change of 2.4%. From this, it is estimated that the slope of the experimental calibration curve should be 39.26. Thus the calibration curve at 30 °C is estimated to be:

Thermocouple Voltage (μv) = 2.7 μv + 39 μv/C° $(\overline{\Delta T})$ C°

APPENDIX L

Peltier Battery Time Constant

The Peltier Battery consists of forty modified bismuth telluride elements sandwiched between two copper plates. The thickness of the complete assembly is given as (15.5 ± .5) mm. An attempt to analytically determine the response time of such a device when in contact at one face with a stagnant gas would be a formidable task. It is possible to estimate this quantity by proposing a simple model of the physical system, that of a 15.5 mm copper plate, insulated at one face. The response of such a plate to a step change in the temperature of the opposite face is available in the literature. According to Schneider (36), the temperature of the insulated face will have risen to 90% of the step change at a Fourier Number equal to 1.05. As the thermal diffusivity of copper is 111.4 mm^2/sec, the response time t_r is estimated as:

$$t_r = N_{Po}\ \delta^2/\alpha = (1.05)\ (15.5)^2/111.4 = 2.265 \text{ sec}$$

Hence the estimated upper bound on the frequency response is about ½ cps.

APPENDIX M

Equipment List

1) Thermal Diffusivity Cell

ITEM	MANUFACTURER/SUPPLIER	SIGNIFICANT CHARACTERISTICS
a) Inner Cylinder	Eck & Krebs, Inc. 27-09 40th Avenue Long Island City, N.Y.	Pyrex glass, 1½"O.D., 5½" long, 1/8" wall, finished ends.
b) Outer Cylinder	as above	Pyrex glass, 6"O.D., 6 3/4" long, 3/16" wall, finished ends.
c) Aluminum Plates	Whitehead Metals Products Company, 303 West 10 Street, N.Y., N.Y. 10014	Machined by Chemical Engineering Dept. Shop.
d) Peltier Battery	Ferroxcube Corporation of America, Saugerties, N.Y. 12477	Model PT 20/20 Optimum working current 20 A, at about 2 V when used for cooling.
e) Teflon O-rings	Stellar Plastics Co. Rochelle Park, N.J.	1½" I.D., .139" cross section 1½" I.D., .312" cross section
f) Teflon gaskets	Cadillac Plastic Co. 14-51 Broadway Long Island City, N.Y.	Machined by Chemical Engineering Dept. Shop.
g) "Swagelok" Connectors	Crawford Company, Cleveland, Ohio/R.S. Crum and Co., 1167 Globe Ave., Mountain-side, N.J.	O-seal straight thread connector 300-1-OR-BT. O-seal male adapter 401-A-4-OR

2) Peltier Battery - see item 1.

3) Peltier Battery Power Supply

a) Synchronous Motor	Bodine Electric Co./ Surplus	Type NSY-12, 115 VAC, single phase, 1800 rpm, 1/125 hp.

ITEM	MANUFACTURER/SUPPLIER	SIGNIFICANT CHARACTERISTICS
b) Step Function Speed Reductor Model 00142 (Gear Box)	Insco Corp., Groton, Mass./ B and B Motor & Control Corp., 96 Spring Street, N.Y., N.Y. 10012	1/1 - 10/1 in ten steps
c) Roller-actuated Switch	Unimax/Surplus	SS05B70, 15A, 110-125 VAC
d) DC Sources		Constructed from surplus parts.
e) Miniature Mercury Power Relay MR-14	Ebert Electronics Corp., 130 Jericho Trpe., Floral Park, N.Y. 11002	2 pole, 1 NO, 1 NC, 115VAC, 60 cps coil, contacts are 20A at 115VAC or 10A at 230 VAC, both 60 cps.

4) Thermocouple Probes

a) Thermocouples	Omega Engineering, Inc., Springdale, Connecticut	.001" Chromel-Alumel
b) Probes	as above	constructed to specifications

5) Electronic Apparatus

a) Analog Computer model TR-10	Electronic Associates Inc., West Long Branch, N.J.	
b) Operational Amplifiers SQ-10	Nexus Research Labs, 480 Neponset St., Canton Mass. 02021	

ITEM	MANUFACTURER/SUPPLIER	SIGNIFICANT CHARACTERISTICS
c) LC passive filter model 201	Allison Laboratories, Inc., 11301 East Ocean Ave., LaHabra, Calif.	One low cutoff filter (1 cps) & one high cutoff filter (2 cps); can be used independently or in tandem for bandpass.
d) Active Filter Model 330BR-4	Krohn-Hite Corp., 580 Massachusetts Ave., Cambridge, Mass. 02139	Bandpass filter only; cutoffs continuously variable .005-500 cps
e) RC passive filter	Surplus	Bandpass filter constructed from surplus
f) Strip Chart Recorder Mark 280	Brush Instruments Div. Clevite Corporation Cleveland, Ohio	Two 80 mm-wide channels, .05-200 mm/sec in 12 steps, .5mv/1-10mv/1 in 16 steps
g) Very High Gain Preamplifier	as above	DC suppression, -10 mv to +10 mv; 1μv/1 to 1 v/1 when used in usual manner with Mark 280
h) Power Supply Model 13-7304-00	as above	400 cps power supply & carrying case for preamplifiers
i) Strip Chart Recorder Mark II	as above	Two 40 mm-wide channels, 1-125 mm/sec in 4 steps; .01 -10 v/1 in 10 steps
j) Shielded Patch cord type 274-NL	General Radio Company 845 Broad Avenue Ridgefield, N.J.	3' shielded lead terminated in shielded double plugs.

ITEM	MANUFACTURER/SUPPLIER	SIGNIFICANT CHARACTERISTICS
k) Shielded Cable type 8451	Belden	2 wire shielded electronic cable
6) Optical Measurement Instrument		
a) Depth Measuring Stereomicroscope model ADM -2 with type S stand	Bausch & Lomb, Inc. Rochester, 2 N.Y.	Dial range 1" Least reading .001" repeatability ± .0004" total magnification 20X, field size .394", working distance 4"
b) Micro-lite Illuminator	as above	60 watt source with blue filter
7) Thermal Bath		
a) Pyrex Glass jar model 11-823-J	Fisher Scientific Co. 633 Greenwich Street New York, N.Y.	12" X 12" O.D.
b) Base, model 15-445-5	as above	
c) Support rods, model 15-445-10	as above	
d) Bi-metallic thermoregulator, model 15-445-25	as above	±.1°F sensitivity claimed
e) Electric Stirrer, model 14-503-V2	as above	
f) 75 watt heater unit, model 15-445-48V2	as above	
g) 300 watt heater unit model 15-445-50V2	as above	

ITEM	MANUFACTURER/SUPPLIER	SIGNIFICANT CHARACTERISTICS
h) 500 watt heater unit, model 15-445-55V2	Fisher Scientific Co. 633 Greenwich Street New York, N.Y.	
i) Powerstat-variable transformer, model 9-521-5V2	as above	7.5A, 0-135v output from 60 cps, 115 volt line
j) Thermometer, model 15-445-85	as above	-20 to 110°C, 1° subdivisions, 305 mm long
k) Copper cooling coil, model 15-445-65	as above	
l) Centrifugal Transfer Pump	Cole-Parmer Instrument and Equipment Co., 7330 N.Clark St., Chicago, Ill.	
m) "Temp-Tact" thermoregulator, model F	Chemical Rubber Company 2310 Superior Avenue Cleveland, Ohio 44114	0-300°C range, 300 mm stem length, ±.01°C sensitivity
n) "Circutemp" combination heater, controller, stirrer	as above	
8) Auxiliary Apparatus		
a) Vibration Damping Mount	Chemical Rubber Company 2310 Superior Avenue Cleveland, Ohio 44114	absorbs vibrations down to 9 cps from motorized devics
b) Bubble Leveler Model 12-000	Fisher Scientific Co., 633 Greenwich Street New York, N.Y.	
c) "Fiberglas" Building Insulation	Owens-Corning	

LITERATURE CITED

1. Abramowitz, M., Stegun, I.A., Editors, "Handbook of Mathematical Functions With Formula, Graphs, and Mathematical Tables", p. 1026, National Bureau of Standards, United States Department of Commerce, June, 1964.
2. Bannawitz., Ann. Physik 48, 577-92 (1915)
3. Bateman, J.S., "Proceedings of the Conference on Thermodynamic and Transport Properties of Fluids," Institute of Mechanical Engineers, London, 1957.
4. Brokaw, R.S., J. Chem. Phys. 32, 4, 1005-6 (1960)
5. Butler, J.N., Brokaw, R.S., J. Chem. Phys. 26, 6, 1636-43 (1957)
6. Carslaw, H.S., Jaeger, J.C., "Conduction of Heat in Solids," 2nd Edition, Oxford University Press, London, 1959.
7. Carslaw, H.S., Jaeger, J.C., "Operational Methods in Applied Mathematics," Dover Publications, Inc., New York, 1963.
8. Chandrasekhar, S. "Hydrodynamic and Hydromagnetic Stability," p. 43, Claredon Press, 1961.
9. Dickens, B.G., Proc. Roy. Soc. (London) A143, 517 (1934)
10. Egli, P.H., "Thermoelectricity", p. 23-24, John Wiley and Sons, Inc. New York, (1960).
11. Ferroxcube Corporation of America, "Ferroxcube Peltier Elements and Batteries", Bulletin 1500, Saugerties, New York.

12. Gregory, H., Archer, C.T., Phil. Mag. (7). 1, 593-606 (1926)

13. Gregory, H., Archer, C.T., Proc. Roy. Soc. (London) 110A, 91-122 (1926)

14. Harrison, W.B., Boteler, W.C., Spurlock, J.M., "Thermodynamic and Transport Properties of Gases, Liquids and Solids", p. 304-312, Mc-Graw Hill, New York, 1959.

15. Hawkins, G.A., Transactions of the ASME, A-168, 655-658 (1948)

16. Hirschfelder, J.O., J. Chem. Phys. 26, 274,282 (1957)

17. Hougen, O.A., Watson, K.M., "Chemical Process Principles", p. 101, John Wiley and Sons, New York 1947.

18. Jaeger, J.C., Australian Journal of Physics, 9, p. 167-179 (1956).

19. Jakob, M., "Heat Transfer", volume 1, John Wiley and Sons, New York, 1962.

20. Kaye, G.W.C., Higgins, W.F., Proc. Roy. Soc. (London) A117, 459-70 (1928)

21. Kannuluik, W.G., Martin, L.H., Proc. Roy. Soc. (London) A141, 144 (1933)

22. Kannuluik, W.G., Martin, L.H., Proc. Roy. Soc. (London) A144, 496 (1934).

23. Kent, R.T., "Kent's Mechanical Engineers Handbook - Design and Shop Practice," p. 16-04, John Wiley and Son, New York, 1938.

24. Kraussold, H., Forsch. Gebiete Ingenieurw, 5B, 186 (1934)

25. Lee, C.S., Bonilla, C.F., Preprint of paper "Thermal Conductivity of the Alkali Metal Vapors and Argon," presented at the Seventh Conference on Thermal Conductivity, National Bureau of Standards, Gaithersburg, Maryland (November 13-16, 1967)

26. Lenoir, J.M., "Thermal Conductivity of Gases at Atmospheric Pressure", Univ. of Arkansas Engr. Exp. Sta. Bull. No. 18, Fayetteville, Arkansas, 1953.

27. Liley, P.E., "Thermodynamic and Transport Properties of Gases, Liquids and Solids", p. 40-69, Mc-Graw Hill, New York, 1959.

28. Liley, P.E., TPRC Report 13, Thermophysical Properties Research Center of the School of Mech. Engr. of Purdue Univ., Lafayette, Indiana (1961).

29. Lion, K., "Instrumentation in Scientific Research-Electrical Input Transducers", p. 162, Mc-Graw Hill, New York, 1959.

30. Malkus, W.V.R., Proc. Roy. Soc. (London) A, 225, 185-95 (1954).

31. Mann, W.B., Dickins, B.G., Proc. Roy. Soc. (London) A134, 77-96 (1931)

32. Michels, A., Botzen, A., Physica 18, 605 (1952)

33. Neubert, H.K.P., "Instrument Transducers", p. 167, Oxford at Clarendon Press, 1963.

34. Peterson, J.R., Bonilla, C.F., Third Symposium on Thermophysical Properties, ASME, pp. 264-276 (March 22-25, 1965).

35. Perry, J.H., Editor, "Chemical Engineers' Handbook", 3rd Edition, McGraw Hill, New York, 1950.

36. Schneider, P.J., "Temperature Response Charts", p. 31, John Wiley and Sons, New York, 1963.

37. Sherman, M., Ostrach, S., J. Applied Mech., 34, p. 308-12, 1967.

38. Spangenberg, W.G., Rowland, W.R., The Physics of Fluids, 4, No. 6, p. 750 (1961).

39. Srivastava, B.N., Barua, A.K., Chakraborti, P.B., Trans. Faraday Soc., 59, 2522-7 (1963).

40. Taylor, W.J., Johnston, H.L., J. Chem. Phys. 14, 219 (1946).

41. Tsederberg, N.V., "Thermal Conductivity of Gases and Liquids" (English translation by Scripta Technica), The M.I.T. Press, Cambridge, Massachusetts, 1965.

42. Volk, W., "Applied Statistics for Engineers", p. 141, McGraw-Hill, 1958.

43. Westenberg, A.A., de Haas, N., Phys. Fluids 5, 266-73 (1962).

VITA

Arnold M. Goldstein attended The City College of New York and was graduated magna cum laude with a Bachelor of Chemical Engineering degree in January, 1963. He received the G. Edwin White Engineering Alumni Award in Chemical Engineering and the Hamilton Award. He was granted a Master of Engineering (Chemical) degree in June, 1965 by the City University of New York. During the period of his graduate study, the author was the recipient of a University Research Assistantship, a National Science Foundation Cooperative Fellowship, and a National Aeronautics and Space Administration Traineeship.

The author taught an undergraduate course in Chemical Engineering Thermodynamics during the Fall, 1966 semester. He was employed by the Lummus Company during the summers of 1962 and 1963 as a Process Engineer, and by Proctor and Gamble as a Research Engineer during the summer of 1964. He has accepted a full-time position with the Esso Research and Engineering Company.

He is an associate member of the American Institute of Chemical Engineers, and a member of Tau Beta Pi and Omega Chi Epsilon.